APPLICATION OF MICROWAVES IN PHARMACEUTICAL PROCESSES

LOH ZHI HUI

(B. Sc. (Pharm.) (Hons.), NUS)

A THESIS SUBMITTED

FOR THE DEGREE OF DOCTOR OF PHILOSOPHY

DEPARTMENT OF PHARMACY

NATIONAL UNIVERSITY OF SINGAPORE

2009

ACKNOWLEDGEMENTS

First and foremost, I wish to express my heartfelt gratitude to my supervisors, Associate Professor Paul Heng Wan Sia, Dr Celine Valeria Liew and Dr Lee Chin Chiat for their guidance and support during the course of my research. I am grateful for their constant encouragement, infinite patience and effort spent in going through my manuscripts. I am also grateful to Associate Professor Chan Lai Wah for her help and advice during my candidature. I would not have made it this far in my academic endeavors without them.

In addition, I wish also to thank the Head of the Department of Pharmacy, Associate Professor Chan Sui Yung for her constant motivation and invaluable advice on life throughout my years in NUS Pharmacy. I am indebted to NUS for the research scholarship awarded.

Special thanks to my dear friends in GEA-NUS, in particular, Sze Nam, Wai See, Lesley, Elaine, Emily, Constance, Dawn, Sook Mun, Stephanie, Wun Chyi and Christine for their companionship and for making my years as a research student so memorable! I wish to express my sincerest appreciation to Mrs Teresa Ang, Ms Wong Mei Yin and Mr Peter Leong for their invaluable technical assistance in the course of my work.

Last but not least, I wish to thank my family and Teck Choon for their love, understanding and unfailing support. Thank you!

Zhi Hui, 2009

TABLE OF CONTENTS

SUMMARY

The application of microwave technology in the manufacture of pharmaceutical products was studied via two processes, drying and melt granulation. Emphasis was placed on the significance of material dielectric properties in microwave-assisted processes and how they differed from conventional processing methods.

Dielectric properties of 13 common pharmaceutical materials were first evaluated at microwave frequencies 300 MHz, 1 GHz and 2.45 GHz with a focus on effects of density and moisture content on their dielectric responses. Although material dielectric responses increased with density and moisture content, the latter was primarily responsible for the differences in microwave dielectric properties of materials. Amongst them, anhydrous dicalcium phosphate and starch were found to interact more readily with microwaves.

Granulation and microwave-assisted drying of acetylsalicylic acid-loaded lactose 200M and 450M granules prepared using different powder loads (2.5–7.5 kg) and amounts of granulating liquid (8-14 %w/w) were investigated in a 25 L single pot high shear processor. Drying performance was investigated from the perspectives of granule size, porosity and moisture content. Powder load affected the pattern and extent of drying. As opposed to conventional drying, larger and wetter granules of higher porosities generally exhibited higher drying rates under microwave-assisted conditions, attributed to the volumetric heating and moisture-targeting properties of microwaves. Microwaves did not adversely affect drug stability. Acetylsalicylic acid

degradation (%) was correlated to the drying time of granules regardless of whether microwaves were employed for drying.

Microwave-induced melt granulation was accomplished in a 10 L single pot high shear processor with polyethylene glycol 3350 and a 1:1 anhydrous dicalcium phosphate-lactose 200M admixture as the binder and filler, respectively. Compared with conventional melt granulation performed by substituting microwaves with heat derived from the mixer bowl, the rates and uniformities at which the irradiated powders heated up were poorer. Thus, product temperature was less suitable for process monitoring in microwave-induced as compared to conventional melt granulation. Conversely, mixer power consumption signals were more suitable agglomeration markers in microwave-induced than conventional melt granulation. This was attributed to the slower rates of heating and its attendant effects on agglomerate growth patterns that rendered mixer power consumption signals more sensitive to granule size in microwave-induced melt granulation.

Disparities in heating capabilities and uniformities of powders in the 2 granulation processes affected the binder and moisture contents of resultant melt granules. Binder distribution was less efficient in microwave-induced melt granulation which resulted in greater intra- and inter-batch variations in the binder contents of granules. Content homogeneity was improved in conventional melt granulation. The longer massing durations and slower rates of agglomeration in microwave-induced melt granulation provided ample opportunities for evaporative moisture losses. As agglomeration was more spontaneous and occurred at a faster rate in the conventional process, more moisture was entrapped in the resultant granules. The compaction behavior of melt

granules were affected by their mean sizes, flow properties, porosities, binder and moisture contents. The last 2 factors affected granule compressibility and were responsible for the disparities in compaction behavior of melt granules produced in microwave-induced and conventional melt granulation.

LIST OF TABLES

LIST OF FIGURES

LIST OF SYMBOLS

A	Vertical intercept extrapolated from the best fit line of the linear portion of the Heckel plot
Alg	Sodium alginate
ASA	Acetylsalicylic acid
BD	Bulk density of melt granules
CI	Compressibility index of melt granules
CMG	Conventional melt granulation
C_p	Heat capacity of material
D	Relative density of a compact
D_A	Total densification of the granule bed in the die cavity before bond formation
DCP	Anhydrous dicalcium phosphate
Dp	Penetration depth of microwaves
D50	Mass median diameter of melt granules with reference to Figs. 34 and 35
D_{50}	Mass median diameter of dried granules or melt granules
$D_{50(p)}$	Mean particle diameter of starting materials
E	Electric field strength of microwaves
E_m	Post-melt specific energy consumption during melt granulation
f	Frequency of microwaves
HPLC	High performance liquid chromatography
HR	Hausner ratio of melt granules
i	Imaginary unit, $i^2 = -1$
k	Drying rate constant of granules

K	Slope of the linear portion of the Heckel plot obtained by regression
Lac	Lactose 200M
LF	Log frequency
M_c	Critical moisture content of material
MC	Moisture content of melt granules
MECH	Mechanical strength of compact formed under a compaction pressure of 102 MPa
MMG	Microwave-induced melt granulation
P	Compaction pressure
Para	Paracetamol
PAT	Process analytical technology
P_{av}	Average post-melt specific mixer power consumption during melt granulation
PC1, PC2	Principal components 1, 2
PEG	Binder content of melt granules
P_H	Mixer power consumption at the end of the high shear massing phase of melt granulation
P_L	Mixer power consumption at the end of the low shear massing phase of melt granulation
P_P	Peak mixer power consumption during the high shear massing phase of melt granulation
Pv	Microwave power absorbed per unit volume of material
PVP	Polyvinylpyrrolidone
PVP-VA	Polyvinylpyrrolidone-vinyl acetate
R_m	Maximum drying rate of granules
RSD	Relative standard deviation
Sta	Starch

$\tan\delta$	Loss tangent of material
TD	Tapped density of melt granules
Tf	Final temperature of material after microwave exposure at 2.45 GHz in a laboratory microwave oven
T_H	Product temperature at the end of the high shear massing phase of melt granulation
Ti	Initial temperature of material prior to microwave exposure at 2.45 GHz in a laboratory microwave oven
T_L	Product temperature at the end of the low shear massing phase of melt granulation
$T_{50\%}$	Time required for the removal of 50 % of the initial moisture content of granules
v_1, v_2	Volume fractions of air and material in a particulate system
ρ	Density of material
Єgr	Porosity of melt granules
Єcom	Porosity of compact formed under a compaction pressure of 102 MPa
ε	Complex dielectric constant or permittivity of material
ε_o	Permittivity of vacuum
ε'	Dielectric constant of material
ε''	Dielectric loss of material
ω	Angular frequency
λ_o	Free space wavelength
ΔT	Temperature rise experienced by material exposed to microwaves at 2.45 GHz in a laboratory microwave oven
ΔT/Δt	Rate of temperature rise experienced by material exposed to microwaves at 2.45 GHz in a laboratory microwave oven
%L, %Y	% lumps, % yield

1. INTRODUCTION

1.1. Microwave Processing of Pharmaceutical Materials and Products

Microwaves span the 300 MHz to 300 GHz frequency range of the electromagnetic spectrum (Schiffmann, 1995). The unique properties and superiority of microwaves over conventional sources of energy have generated immense interest in its use for industrial processing. Microwave technology has been widely embraced in the pharmaceutical field for various applications such as the extraction of natural products (Eskilsson and Björklund, 2000) and pharmaceutical actives (Hoang et al., 2007), organic syntheses of chemical compounds (De la Hoz et al., 2005), drying of pharmaceutical powders and granules, material modification as well as dosage form design. The last 2 applications have been recently detailed in a comprehensive review by Wong (2008).

When microwaves are directed towards a material, the energy may be reflected, transmitted or absorbed. The amenability of materials to microwave processing is dependent on their abilities to interact and absorb microwaves. The microwave energy dissipated or absorbed within a unit volume of irradiated material is governed by a complex interplay of material and equipment-related factors (Metaxas and Meredith, 1983):

$$Pv = \omega \varepsilon_o \varepsilon'' E^2 = 2\pi f \varepsilon_o \varepsilon' \tan\delta E^2 \quad (1)$$

Pv refers to the microwave power absorbed per unit volume of material (Wm^{-3}), ω is the angular frequency, E is the electric field strength (Vm^{-1}) and f is the frequency of the applied field (Hz). ε_o is the permittivity of vacuum. ε'', $\tan\delta$ and ε' refer to the

dielectric loss, loss tangent and dielectric constant of a material respectively. These 3 factors collectively describe the dielectric properties of a material.

1.2. Material Dielectric Properties

Dielectric properties are fundamental electrical characteristics of materials which govern their behavior when subjected to electromagnetic fields for purposes of heating, drying, material processing as well as process monitoring (Venkatesh and Raghavan, 2004; Gradinarsky et al., 2006). These properties largely determine the extent to which a material interacts with and absorbs microwaves. In the measurement of dielectric properties, the characteristic response of a material under the influence of an alternating electric field, referred to as the complex dielectric constant or permittivity ε, is measured over a wide frequency or temperature range (Craig, 1995). ε is governed by the following equation (Metaxas and Meredith, 1983):

$$\varepsilon = \varepsilon' - i\varepsilon'' \tag{2}$$

i is an imaginary unit and $i^2 = -1$. ε', the dielectric constant, reflects the polarizability of the material or its ability to store electrical charge. It affects the electric field developed internally within the irradiated material. The dielectric loss, as represented by ε'', is related to the ability of the material to absorb energy from the passing electric fields and conversion of that energy to heat. The loss tangent, $\tan\delta$, is defined as $\varepsilon''/\varepsilon'$ and represents the fraction of incoming energy that is dissipated as heat within the material. Dielectric properties are not unique qualities and are specific to a particular physicochemical state of the material. Thus, as materials undergo physicochemical changes during processing, their dielectric properties would similarly be altered. In the sections that follow, equipment and material-related factors

that affect the dielectric properties of materials and their interactions with microwaves is discussed with greater emphasis on those relevant to the pharmaceutical industry.

1.3. Factors Affecting Material-Microwave Interactions

Equipment-related factors are associated with specific physical aspects of microwaves such as their electric field strength and frequency. These inherent wave characteristics are often dictated by the source of microwaves and various technical aspects (e.g. dimension, shape) of the microwave cavity. Material-related factors refer to specific physicochemical characteristics of materials which affect the penetration of microwaves and its interaction with material molecules. These include the moisture content, chemical composition, state, density, size, geometry and thermal properties of materials.

1.3.1. Electric Field Strength of Microwaves

Microwaves are generated by a device known as a magnetron. From the source, the waves are conducted down a rectangular duct, also termed as a waveguide, and radiated through a transparent propylene window into an adjoining metal enclosure such as an oven or cavity containing the material to be irradiated (Aulton, 2007). Upon exposure to microwaves, a local electric field would be developed within the material. There are two main configurations of microwave cavities which can significantly affect the development of the local electric field. In a single-mode cavity, a standing wave pattern of microwaves is generated. At points where the material intercepts the waves at its maximum field intensity (peaks or troughs of the waves), the electric field strength evolved and subsequent heat dissipation within the material would be high. The heating effects experienced by the material or portions of it

located at the nodes of the waves would be negligible. In view of the non-uniform electric field intensity within the cavity, the physical location of the material in the cavity is vital for effective microwave processing and maximum energy utilization (Jia, 1993). Despite this limitation, single-mode oven configurations allow the focusing of microwaves on precise areas of the material load for targeted, selective heating. These ovens are more commonly encountered in organic chemistry applications where microwaves could be directed towards small-volume reaction vessels placed in a specific location in the microwave cavity.

Multi-mode microwave cavities, on the other hand, alleviate the problems associated with the non-homogeneous distribution of energy. In these configurations, microwaves, once introduced into the cavity, are reflected from the cavity walls back and forth continuously through the material. The reflection of microwaves off the cavity walls results in significant overlap and interference of the waves which disrupts any standing wave patterns established within the cavity. Under these circumstances, the microwave field becomes more homogeneous in all directions and the material can be irradiated and heated more uniformly regardless of its location in the cavity. Devices for stirring or mechanical agitation of the material load are often incorporated in the majority of microwave equipment to ensure that the load is exposed to a uniform dose of microwave energy throughout its volume. This is exemplified by the rotating Pyrex turntables seen in all domestic microwave ovens. By continuously rotating the material load, the turntable minimizes the effects of field variations within the microwave cavity. This ensures uniformity in microwave exposure of the material. In industrial processors such as the single pot high shear processor typically used for the microwave processing of pharmaceutical materials and products, the distribution

of microwave energy within the material load is enhanced by impeller and chopper action as well as equipment configurations that allow the mixer bowl to move in cradling motions. This provides mild agitation and continually exposes new surfaces of the material for microwave interrogation and interception. Uniform heating arises from the successive and gradual build up of microwave energy throughout the bulk volume of the material. In microwave-assisted fluidized-bed processors, such stirring devices are less crucial as the inherent particle dynamics facilitate energy distribution (Wang and Chen, 2000).

In the absence of stirring devices or under circumstances where mechanical agitation of the material load is not feasible, non-uniform irradiation and heating may occur. Microwave energy may be imparted to localized or superficial regions of the load. This situation may further be compounded by limitations in penetration depth of microwaves which is a common problem associated with the processing of materials and products at industrial capacities. The concept of microwave penetration depth is discussed in section 1.3.6.

1.3.2. Frequency of Microwaves

The effect of microwave frequency on the extent to which microwaves interact with a material is mediated through the innate dielectric characteristics of the material. Material dielectric properties vary considerably with the frequency of microwaves (İçier and Baysal, 2004). This frequency dependence of dielectric properties or dielectric dispersion as it is alternatively known, stems from the effects of polarization that arise from the orientational movements of dipolar molecules with the oscillating microwave field. This response is critically dependent on the relaxation times of the

dipolar molecules. Relaxation time refers to the time taken for the dipoles to revert to random orientation when the microwave field is terminated and is often influenced by the molecular weight or mobility of the dipolar molecules. The relaxation time affects the responsiveness of the dipolar molecules to the applied microwaves and governs the extent to which microwave energy can be effectively coupled into a material for heat production.

Classically, the frequency-dependent variation in dielectric constant and loss of a pure, polar material has been described mathematically by Debye (1929) (Fig. 1). For a pure polar liquid like water, there is no preferential direction of alignment of the polar molecules in the initial absence of an electric field. When an electric field is applied at low frequencies, the time interval taken for the field to reverse its polarity would presumably be longer than the relaxation times of the polar molecules. As a result, ample time is available for the molecules to respond and orientate in accordance to the direction of field changes. The partial neutralization of electrical charges imposed by the external field leads to charge storage by the polar molecules as evidenced by a high dielectric constant (region A).

As field frequency increases, the time interval between the next reversal in field polarity gradually becomes of a similar order to the relaxation times of the polar molecules. At this juncture, the molecules retain their ability to respond to the changing fields albeit with an increasing lag time. This causes the dielectric constant

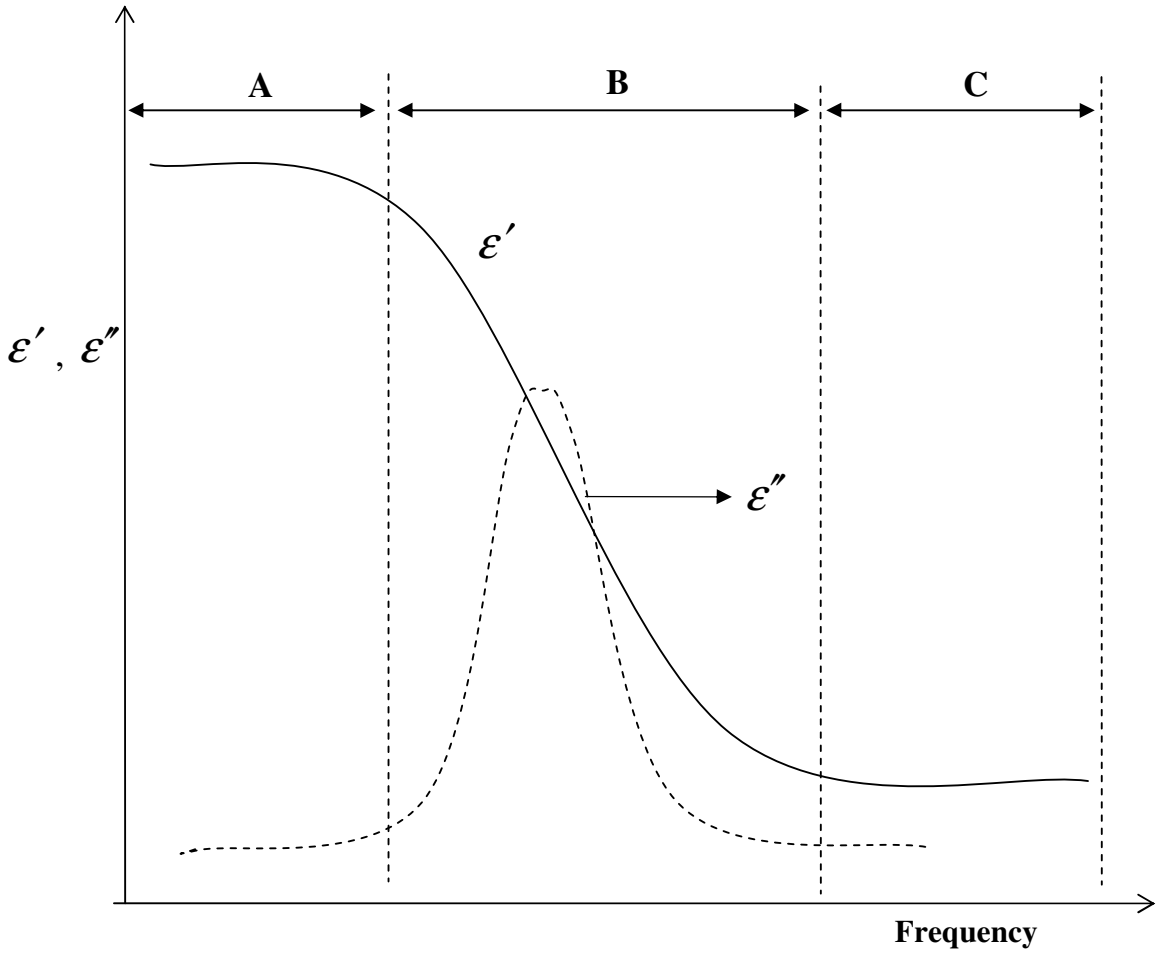

Fig. 1. Frequency dependence of the dielectric constant, ε', and loss, ε'', of a polar material.

to decline with the occurrence of a dielectric loss peak as a result of energy absorption and dissipation (region B). At very high frequencies, the time interval at which the field stays in the same direction is much shorter than the times required by the polar molecules to relax. These molecules will cease to respond and remain in their random, steady state orientations with minimal charge storage and energy dissipation (region C). Thus, when the applied field frequency is exceedingly high or low with respect to the relaxation frequencies of the polar molecules in a material, there is minimal energy absorption and the heating effects induced will be negligible. At intermediate frequencies, the heating effects are more pronounced with the most effective conversion of microwave energy to heat occurring at the frequency where the material exhibits its maximum dielectric loss.

As dielectric properties may be determined over a broad band frequency window (from 10^{-5} to 10^{11} Hz), different polarization mechanisms in materials may be investigated (Smith et al., 1995). At microwave frequencies, the main mechanism of polarization stems from the orientation of molecular dipoles. At far lower frequencies, the slow, hindered movements and vibrations of bulky macromolecules or polymers may be studied. Vibrations at the atomic or electronic level would match the higher infra-red and ultra-violet frequency regions of the electromagnetic spectrum. Hence, every material will display its own unique dielectric dispersion profile based on its innate physicochemical characteristics, field frequency and other related conditions of measurement.

1.3.3. Moisture Content of Material

The markedly higher dielectric constant of pure, liquid water (ε' ~ 78 at 1 GHz) (Metaxas and Meredith, 1983) relative to that of dry, organic materials (ε' ~ 2-5) at ambient conditions contributes to a heavy reliance of material dielectric properties on moisture content. In view of the hygroscopic nature of many common pharmaceutical materials, the effect of moisture content on their dielectric properties and thus microwave absorption capabilities cannot be overlooked. Materials containing higher moisture contents are generally more amenable to microwave processing, and as a result of their higher dielectric losses, heat more readily when irradiated.

The dielectric loss peak of pure liquid water in its unbound or 'free' state occurs approximately at 17 GHz at 20 ºC (Craig, 1995). Hence, the conversion of microwave energy to thermal energy for free water molecules would be most efficient at this frequency. However, in many materials of practical interest, water rarely exists in its free and unbound state. Often, it is physically absorbed in material capillaries and cavities or chemically bound to other molecules in a material. Furthermore, depending on the structural properties of a material, various forms of bound water exist which differ in their binding affinities (Nelson, 1994). Due to their restricted mobility, bound water molecules possess longer relaxation times and undergo dielectric dispersion at lower frequencies, with loss peaks occurring at frequencies ranging from 1 MHz-1 GHz (De Loor, 1968; Metaxas and Meredith, 1983; Schiffmann, 1995; İçier and Baysal, 2004). In practice however, the majority of industrial and domestic microwave appliances and equipment function at a much higher frequency of 2.45 GHz which is displaced from the frequencies at which both free and bound forms of water exhibit their maximum dielectric losses. This is because only selected frequency

bands of the electromagnetic spectrum are assigned for domestic, scientific and medical applications to avoid potential interferences with frequencies employed for telecommunication, defence and maritime applications (Schiffmann, 1995).

Regardless of frequency, the concentration and state of water absorbed in a material affect its dielectric loss and heating ability. The qualitative relationship between dielectric loss and moisture content of a material is shown in Fig. 2 (Metaxas and Meredith, 1983; Schiffmann, 1995). The distinct inflexion points in the profile demarcate the transition between the changing states of water in the material. At low moisture contents, the dielectric loss of the material is negligible as the moisture present exists primarily in bound form on the solid surface and possesses limited mobility in the presence of microwaves. As its moisture content increases and attains the critical level or critical moisture content (M_c), all the available binding sites in the material for water molecules become saturated. Further additions of water beyond this critical level result in a population of water molecules bound to a lesser extent and which couple more readily with microwaves due to their greater rotational mobility. As the fraction of mobile water molecules increases further, the dielectric loss of the material may increase proportionately or taper off as it approaches that of free, bulk water at moisture contents of 20-30 %.

1.3.4. Chemical Composition and State of Material

The chemical make-up of the molecular groups in a material affects its response to microwaves. Polar molecules comprise two chemically bonded atoms of markedly dissimilar electronegativities e.g. N-H, O-H, C-O, C-N, C-Cl. The different electron

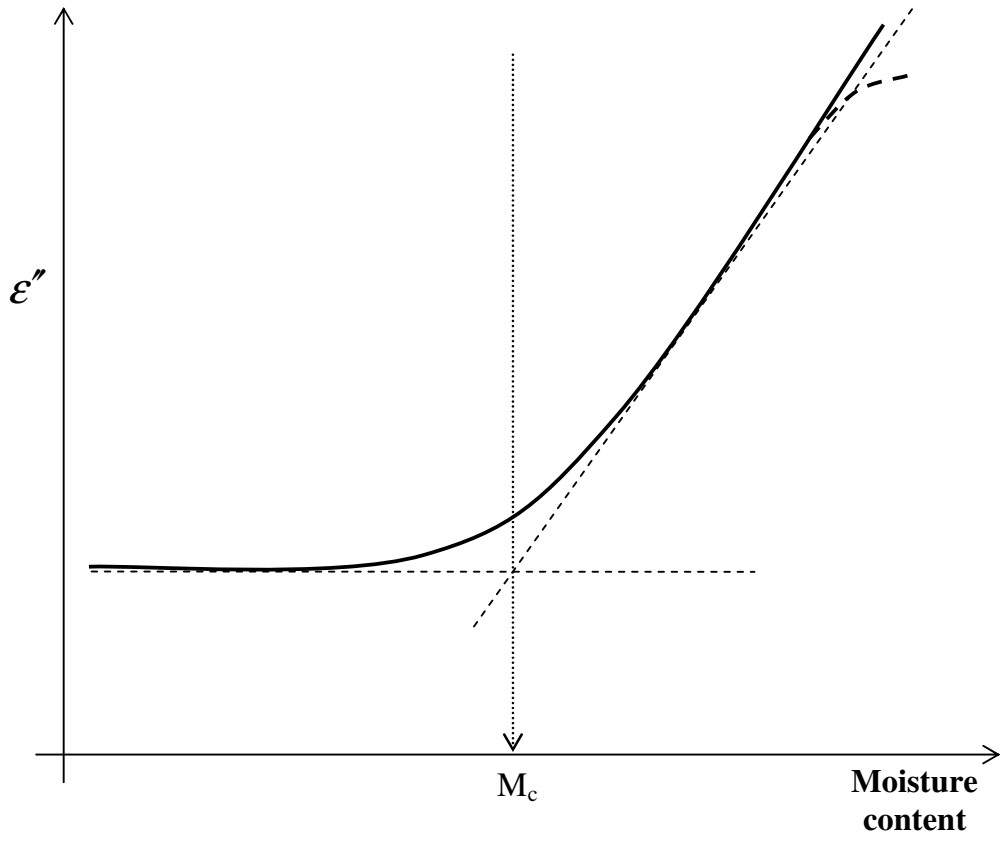

Fig. 2. Classical relationship between the moisture content and dielectric loss of a material. M_c refers to the critical moisture content of the material.

affinities of the bonded atoms result in the formation of positive and negative charge centers. These chemical moieties are more susceptible to microwave fields due to their polarizable nature. Non-polar molecules are formed when two atoms of similar electronegativities are bonded resulting in an equal sharing of electrons between them (e.g. C-H, C-C). For these non-polar moieties, the imposed microwave field may similarly induce the formation of transient positive and negative charge centers by causing temporary distortions of their electron clouds. The induced dipoles formed would likewise neutralize the effects of the external field and contribute to charge storage albeit to a lesser extent than polar molecules. Thus, non-polar molecules are generally less susceptible to the effects of microwaves as compared to polar molecules. The mobility of the charged molecular groups are in turn, affected by their surrounding physical environment. In a liquid system, these molecules rotate freely and respond most readily to the microwave field. Physical orientations of similar molecules are often restricted in the solid state due to extensive inter-molecular bonding interactions which impair their abilities to rotate or vibrate in response to the oscillating fields. This accounts for the greater dielectric susceptibility of liquids as compared to solids.

In reality, few materials of practical interest are like pure, polar liquids, comprising single, non-interacting dipoles that exhibit Debye behavior (Fig. 1). The chemical compositions of pharmaceutical materials are generally complex and comprise numerous different molecular groups which interact and mutually affect the electrical properties of each other. Such interactions are particularly notable in solids due to the physical proximity of the different molecular groups. In polymeric materials for instance, polarization is complex and spans over a wide frequency range. Depending

on the selected frequency, dielectric contributions may arise from the movements of small dipolar functional groups to side chains or even whole molecule motions. Mobility is affected by the presence of crystalline and amorphous regions within the main chain as well as the size of its pendant side groups and chains (Parker, 1972). On the other hand, due to their structural rigidity, crystalline materials tend to be non-polarizable or dielectrically inert at lower frequency ranges. Polarization in crystalline materials originates primarily from the displacement of electrons relative to the positive nuclei or the relative displacement of positive and negative charge centers with respect to each other. These are classified as electronic, ionic and molecular polarizations which typically occur at much higher ranges of frequencies corresponding to the infra-red and ultra-violet regions of the electromagnetic spectrum.

Macroscopically, the dielectric properties of solid materials originate from the cooperative motions of multiple, interacting dipolar groups under the influence of microwaves. Since each dipolar group possesses its own unique relaxation time and frequency, the dielectric dispersion profile of the material may display multiple overlapping loss peaks which result in the broadening of the dielectric spectra. Such non-Debye characteristics have been described by the Cole and Cole model (Cole and Cole, 1941) which has been shown to provide a more realistic and pragmatic description of the dielectric dispersion of solids (Goyette et al., 1990).

1.3.5. Density of Material

Density is an important factor that affects the dielectric properties of particulate materials. The effect of density is mediated through the interactions between

microwaves and a binary system of material particulates and air. In contrast to water, air possesses a very low dielectric constant and loss, 1 and 0, respectively (Schiffmann, 1986). Hence, compared to the true solid material, air inclusions in particulate forms of an identical material would dampen its dielectric response. Needless to say, the density variations and packing characteristics of particulate materials would influence their dielectric properties at the bulk level. Literature sources have consistently shown that materials with higher bulk densities and correspondingly smaller inter-particulate air volumes possess higher dielectric constants and losses (Schiffmann, 1986; Nelson, 1992a-b; Nelson, 1994; İçier and Baysal, 2004; Venkatesh and Raghavan, 2004).

The relationship between the dielectric properties of a true solid material and its air-particle mixture is described by two well known dielectric mixture equations as shown below (Nelson, 1992a-b; Nelson and Datta, 2001):

$$(\varepsilon)^{1/3} = v_1(\varepsilon_1)^{1/3} + v_2(\varepsilon_2)^{1/3} \tag{3}$$

$$(\varepsilon)^{1/2} = v_1(\varepsilon_1)^{1/2} + v_2(\varepsilon_2)^{1/2} \tag{4}$$

The Landau and Lifshitz (Landau and Lifshitz, 1960), Looyenga (Looyenga, 1965) dielectric mixture equation (equation 3) and complex refractive index dielectric mixture equation (Gladstone and Dale, 1863) (equation 4) allow the computation of the effective dielectric properties of an air-particle mixture based on the addition of the cube roots and square roots, respectively, of the dielectric properties of air and material of interest taken in proportion of their volume fractions. ε represents the complex permittivity of the air-particle mixture. ε_1 refers to the permittivity of the medium (air) in which particles of material with permittivity ε_2 are dispersed. v_1 and

v_2 are volume fractions of air and material respectively, where $v_1 + v_2 = 1$. Clearly, the resultant dielectric property of a mixture is skewed towards that of the component (air or material) occupying the larger fractional volume.

At the outset, these 2 equations were selected for discussion as out of several dielectric mixture equations identified in literature, they had been found to be most suitable for estimating the solid material permittivities of minerals, plastics and food substances based on measurements performed on particulate forms of these materials (Nelson, 1992a). Further derivation of these relationships leads to the expression of material dielectric properties as linear functions of their bulk densities which were useful in the food, agricultural and mining industries for the calculation of the dielectric properties of commercially relevant materials at different bulk densities (Nelson, 1983).

Since pharmaceutical processes such as granulation and tabletting involve changes in material density, understanding and quantifying the effects of these changes on the dielectric properties of pharmaceutical materials would be invaluable. As a start, it has been shown that dielectric mixture theories can be applied for the prediction of the overall dielectric properties of binary solid mixtures comprising two different pharmaceutical materials (McLoughlin et al., 2003a). These mixtures were composed of stearic acid, aspirin, paracetamol, citric and ascorbic acid mixed in varying proportions with starch or lactose. It was found that the contribution of each material to the overall dielectric response of the binary mixture was proportional to its fractional volume content. At this juncture however, more studies are needed to

extend the application of these equations to the complex and multi-component nature of typical pharmaceutical formulations.

1.3.6. Size, Geometry and Thermal Properties of Material

The physical dimensions of a material being processed is important in the way that it affects the extent to which microwaves can penetrate the material and enable bulk heating. For materials with dimensions smaller than or closely approximating the wavelength of microwaves at 2.45 GHz (12.2 cm), energy would be directed towards the core of the material where heating would occur at a higher rate as compared to its periphery. With continuous microwave exposure, rapid heat generation would occur volumetrically throughout the material. This typically occurs when materials or objects are exposed singly to microwaves. However, under circumstances where the dimensions of the materials or objects exceed the wavelength of microwaves such as that encountered during processing of large volume products, the energy dissipated within the product load would be less than that carried by the incident microwaves impinging on the surface of the load. This is because the ability of microwaves to traverse the entire load is dependent on its penetration depth in the load. Penetration depth is defined as the distance from the surface where the incident microwave power has decreased to 1/e or 37 % of its original value. It is computed from the wavelength of microwaves in free space and dielectric properties of the material load as shown in the equation below (Schiffmann, 1995):

$$Dp = \frac{\lambda_o \sqrt{2}}{2\pi}\left[\varepsilon'\left(\sqrt{1+(\varepsilon''/\varepsilon')^2}-1\right)\right]^{-1/2} \quad (5)$$

Dp is the penetration depth and λ_o is the free space wavelength. At the industrial microwave frequency of 2.45 GHz, λ_0 is 12.2 cm. ε' and ε'' are the dielectric constant and loss of the material load respectively. If ε'' is low, the equation may be simplified as:

$$Dp = \frac{\lambda_o \sqrt{\varepsilon'}}{2\pi\varepsilon''} \tag{6}$$

From equation 6, it can be observed that microwaves possess limited penetration depth when the material load possesses a high dielectric loss and absorbs microwaves readily. The absorption of microwaves as it traverses through the load leads to wave attenuation which results in microwaves being unable to completely traverse the entire depth of the load without a drop in its energy level. With microwave energy being delivered primarily to the superficial regions of the load, localized surface heating would predominate. The limited penetration depth of microwaves constitutes a major problem when materials and products are processed on a large scale. When bulk of the incident microwave energy is dissipated before reaching the core regions of the product load, uniform heating of the product can be challenging and time consuming as it then relies on the slow process of conductive heat transfer from the surface of the load to its core.

Apart from its physical dimensions, the geometrical shape of a material affects its ability to interact with microwaves. This factor is particularly relevant when materials or objects are exposed singly to microwaves. For objects with curved surfaces (e.g. spherical objects or cylinders), rapid internal heating would occur as their surface curvatures aid in the focusing of microwaves, resulting in the development of high,

localized electric fields in their cores (Chamchong and Datta, 1999). Regular and symmetrical objects heat more uniformly than irregularly-shaped objects (Schiffmann, 1986). For objects with sharp corners and edges, "edge-heating effects" may be experienced where microwave power concentrates along the corners and edges of objects resulting in the formation of localized hot spots (Chamchong and Datta, 1999). For instance, the sharp edges of a prism-shaped object have a higher tendency to overheat as compared to a cylinder with two flat bases and no distinct edges (Araszkiewicz et al., 2007). Both the phenomena of internal focusing and edge heating may be ascribed to microwave diffraction (Ryynanen, 1995).

Upon microwave exposure, the effects of polarization induced in the molecules of a dielectrically susceptible material would lead to molecular vibrations. The transmission of this vibrational energy throughout the material would result in heat generation. In addition to their dielectric properties, the heat capacities of materials also govern the ease at which materials heat up upon irradiation. The heat capacity of a material is defined as the amount of energy required to raise its temperature by 1 °C. Hence, heat would be generated at a maximum rate when the dielectric loss and heat capacity of the material is high and low respectively. Under circumstances where materials with relatively low dielectric losses are processed, microwave-induced heating may still occur if these materials possess sufficiently low heat capacities (Schiffmann, 1986). In fact, the heat capacity may, in exceptional situations, override the importance of dielectric loss in causing materials to heat on microwave exposure. For instance, despite their relatively non-polar nature as compared to water, oils warm considerably faster than water upon microwave exposure due to their significantly lower specific heat capacities (Prosetya and Datta, 1991; Taggard, 2004).

1.4. Measurement of Dielectric Properties and Dielectric Spectroscopy

In the measurement of dielectric properties, the characteristic response of a material under the influence of an alternating electric field is recorded. A wide array of dielectric measurement techniques can be employed, with the method of choice being dependent on the nature of material, level of accuracy, desired frequency range as well as the conditions under which measurements are desired (Venkatesh and Raghavan, 2005). The parallel-plate, coaxial probe, transmission line, free space and resonant cavity techniques of dielectric assessment are applicable to pharmaceutical solids and as their names suggest, differ primarily in the way the sample of interest is probed by the applied field. There is no single method available for characterizing material dielectric behavior over a broad band frequency window. The transmission line, free space and resonant cavity techniques allow measurements to be performed at frequencies greater than 1 GHz (Venkatesh and Raghavan, 2005). For lower frequency measurements, the parallel-plate methods and coaxial probes are preferred. Depending on the configuration and flexibility of the equipment set-up, measurements may be obtained over a selected frequency, time or temperature range.

For the majority of the techniques, the sample preparation step involves compacting the material of interest into a thin and smooth flat disc. In the parallel-plate method, the material compact is inserted between two parallel electrode plates to form a capacitor which is in turn, connected to an impedance analyzer. The impedance analyzer records the electrical signals transmitted or reflected from the material compact. The signals are then analyzed in conjunction with information on the geometrical properties of the compact to compute the relevant dielectric parameters of the material. Special precautionary measures have to be made to ensure proper contact

between the compact and the electrodes as air gaps present between the two would contribute to measurement inaccuracies. This problem can be avoided by fitting the electrodes with springs which allow slight pressure to be exerted on the compact thereby eliminating the air gap. Furthermore, the materials should be densely compacted to eliminate inter-particulate air spaces. This is particularly vital when the dielectric property of a true solid material is to be measured.

When a coaxial dielectric probe is used, material dielectric properties are measured simply by bringing the probe into contact with the flat surface of the material compact. An impedance analyzer would similarly analyze the transmitted and reflected electrical signals. Compared to the remaining techniques, the parallel-plate electrode and coaxial probe possess added flexibility in that they may be applied to liquid samples by simply immersing the electrode or probe into the liquid of interest during measurement. Transmission line methods of dielectric measurement are more challenging in terms of sample preparation. A transmission line acts similarly as a waveguide and provides a medium or space through which electric fields are propagated. Dielectric measurement is performed by incorporating the test material as part of a section of the transmission line. This is achieved by modifying the dimensions of the material compact such that it fits precisely into the cross-sectional area of the transmission line. The transmitted signals will be recorded at the receiving end of the transmission line and used to compute the dielectric properties of the material.

High frequency dielectric measurement techniques are less common due to cost issues. Both the free space and resonant cavity techniques offer the advantages of

ultra-high frequency and non-destructive methods of dielectric measurement. In the free space technique, a slab of the material is placed between two remote horn antennae, one of which focuses the electromagnetic waves at or through the material slab and the other being the receptor for the transmitted signals. The effect of the test material on the electromagnetic wave propagating in free space from one antenna to another is measured. This method has the advantage of being non-contacting which is useful in high temperature conditions or hostile environments. The resonant cavity technique, on the other hand, restricts dielectric measurements to a single frequency. The shift in resonance frequency of the cavity as a result of the introduction of the test material allows the calculation of the relevant dielectric properties.

A relatively simpler, more convenient and economical approach to the dielectric assessment of materials, particularly in the microwave frequency range, would be to evaluate their heating capabilities on microwave exposure in a laboratory microwave oven. The temperature rise experienced by a material following microwave exposure is governed by the following equation (Gabriel et al., 1998; McLoughlin et al., 2003a):

$$\Delta T/\Delta t = Pv / \rho C_p \qquad (7)$$

$\Delta T/\Delta t$ refers to the rate of temperature rise experienced by the material exposed to microwaves and Pv refers to the microwave power absorbed per unit volume of material (Wm^{-3}). ρ and C_p refer to the density (kgm^{-3}) and heat capacity ($Jkg^{-1}K^{-1}$) of the material respectively. $\Delta T/\Delta t$ is directly proportional to Pv, which as aforementioned in equation 1, is governed by the dielectric properties of the material, frequency and electric field strength of the applied microwave field. The microwave

oven method of dielectric assessment minimizes material handling, manipulation and more importantly, allows dielectric assessments to be performed on materials in their original, bulk states. When dielectric analyzers are inaccessible or when limited quantities of materials are available during the pre-formulation phases of product development, this mode of assessment provides preliminary information useful in guiding the selection of pharmaceutical materials amenable to microwave processing.

Low frequency dielectric spectroscopy of pharmaceutical systems, raw materials and finished products constitute a further aspect of dielectric measurement albeit with a different purpose. Instead of determining the electromagnetic properties of materials, the dielectric parameters obtained are used for elucidating the molecular and structural properties of the sample under test. Dielectric spectroscopy is rapid, non-invasive and eliminates the need for toxic solvents during sample preparation. It complements existing analytical techniques such as nuclear magnetic resonance and fourier transform infra-red techniques for the analysis and structural characterization of complex pharmaceutical systems such as gels (Craig and Tamburic, 1997), creams (Goggin et al., 1998), emulsions (Hill et al., 1990), solid dispersions and liposomes (Craig, 1992) as well as compacts (Labhasetwar and Dorle, 1988). It has shown promise in the assessment of the wettability of powders (Buckton et al., 1987) and was found to be more sensitive than routine tests such as X-ray diffraction, microscopy and flowability measurements in detecting the inter-batch or source variability of pharmaceutical excipients lecithin, cetostearyl alcohol (Rowe, 1997) and lactose (Craig et al., 1991).

Recently, a microwave spectroscopic technique was developed for characterizing the matrix properties of drug-loaded (chlorpheniramine and loratidine) hydroxypropylmethylcellulose films developed for transdermal applications (Anuar et al., 2007; Wong et al., 2007a). It was found that the microwave absorption and transmission characteristics of the films were sensitive to the state and extent of interaction between the polymer and drug molecules in the matrix which was postulated to affect the therapeutic effectiveness of the delivery system. Comprehensive summaries and reviews on the dielectric analysis of pharmaceutical systems have been provided by Smith et al. (1995) and Craig (1995).

1.5. Microwave Technology in Pharmaceutical Processing

The applications of microwave technology in pharmaceutical processing may be broadly classified into those that exploit the thermal and non-thermal effects of microwaves. Thermal applications of microwaves refer to those which utilize the heating effects produced by the waves. Non-thermal applications, on the other hand, take advantage of the specific interactions between microwaves and susceptible chemical moieties in the target material.

1.5.1. Thermal Effects of Microwaves

As an alternative source of heat, microwaves have been applied with remarkable success for drying both pharmaceutical raw materials and products. In numerous studies, microwave-assisted drying has out-performed conventional drying methods in terms of process efficiency and quality maintenance of high-value pharmaceutical materials and products.

1.5.1.1. Microwave-Assisted Drying

When water is exposed to microwaves, the polar molecules undergo intense rotational movements in an attempt to align themselves with the changing polarities of the field. The build-up of kinetic energy and collisions with neighboring molecules result in dielectric losses and frictional heat production which promote evaporation. This forms the basis of microwave-assisted drying.

Fundamentally, microwave-assisted drying differs from conventional drying in terms of the mode of heat generation and transfer. Conventional heat sources cause predominantly localized, surface heating and rely on the slow process of heat conduction from the hot surface of a material to its interior based on established thermal gradients. This often constitutes the rate limiting step in conventional drying processes. Microwaves, however, heat and dry in a unique manner. Microwave-induced heating occurs through direct interactions between the waves and molecules of the target material. This is mediated through the dielectric loss of the material which, as discussed above, is affected by its physicochemical properties. When materials possess favorable dielectric properties and are of physical dimensions smaller than the wavelength of microwaves (12.2 cm), the penetrative and volumetric heating nature of microwaves allow for instant and rapid internal heat generation. Therefore, a faster and more efficient rate of heating and drying can be anticipated under microwave-assisted conditions (Kardum et al., 2001).

The selectivity of microwaves is a further advantage. When conventional energy sources are employed, heat generation tends to be indiscriminate and depend largely on the heat capacities and other related thermal properties of the material.

Microwaves, on the other hand, couple and interact selectively with materials possessing favorable dielectric properties. In the context of drying, this would mean that microwaves interact preferentially with the strongly dipolar water molecules in the moistened material. This targeted and selective heating property of microwaves improves the energy efficiency of drying. The energy efficiency of a dryer indicates the fraction of available energy used for the evaporation of water and is expressed as a ratio of the energy used for the evaporation of water to the total energy supplied to the dryer (Kudra, 2004). With microwaves being preferentially absorbed by water molecules, bulk of the energy supply is diverted to moisture removal. This improves energy utilization and brings about significant cost savings.

Microwave-assisted drying is dynamic and its efficiency changes to suit the immediate needs of the product. The characteristic phases of a microwave-assisted drying process can similarly be described by Fig. 2. At the outset, this profile provides an indication of the moisture content required in a material before effective microwave-induced heating and drying can take place. Above the M_c of the material, drying proceeds at a rapid rate due to the enhanced thermal properties of unbound moisture. The wetter regions of the material will experience improved heating and drying rates by virtue of their higher dielectric losses (Jones and Rowley, 1996; Sanga et al., 2000). This is advantageous as moisture is rarely uniformly distributed within a material undergoing drying and higher localized rates of drying in the wetter regions will aid overall moisture-leveling and improve the uniformity of drying early in the process.

As drying proceeds, the gradual decrease in moisture content and proportion of free moisture in the material results in a corresponding decrease in dielectric loss and rate of moisture removal. When the moisture content of the material attains a sufficiently low level where it becomes predominantly bound in nature, the rate of drying becomes retarded due to diminished interactions between microwaves and bound moisture. This typically marks the end point of drying. In conventional drying processes, the temperature of the material increases at this point due to the accumulation of excessive heat energy. However, when microwaves are employed, the rate of heating falls to a low level at the end of the process following its reduced coupling with microwaves at low moisture levels. Therefore, microwave-assisted drying auto-regulates both the moisture and thermal profiles of a material undergoing drying. With accelerated moisture removal and minimal exposure of a product to excessively high drying temperatures, the stability of both moisture and heat-labile constituents are guaranteed (Jansen and Van der Wekken, 1991).

Over the past decade, the perceived benefits and superiority of microwave-assisted drying has spurred new developments of novel, hybrid dryers designed to incorporate the elements of microwave heating into traditional drying set-ups e.g. vacuum, tray and fluidized-bed dryers. In these hybrid systems, the unique penetrative and volumetric heating capabilities of microwaves are exploited as an ideal complement to conventional modes of drying typically reliant on surface heating and the slow process of conductive heat transfer. Most notably, the incorporation of microwave heating elements into high shear granulators (Poska, 1991; Stahl and Van Vaerenbergh, 2005; Giry et al., 2006) has generated immense interest in the use of microwaves for processing and drying pharmaceutical products. These high shear

granulator-dryers, alternatively known as single pot processors, feature integrated granulation and drying capabilities in a single unit and allow powder mixing, granulation and drying to occur in a seamless and continuous fashion *in-situ*. Apart from the minimization of dust and cross-contamination, a key feature of these processors lies in the myriad of choices available for drying. There are options for microwave, vacuum, conduction and gas-assisted drying. By combining microwaves with any of the available modes of drying, the drying process can be specifically tailored to the needs of the product. This confers tremendous flexibility and offers customized solutions for drying pharmaceutical products. Today, single pot technology has become synonymous with the microwave processing of pharmaceutical products. It fulfills the criteria of modern-day dryers with strict conformance to current good manufacturing practice standards, validated processing as well as real-time process monitoring and control.

1.5.1.2. Comparisons between Microwave-Assisted and Conventional Drying Processes

To understand how the aforementioned features of microwave energy can impact the outcomes of drying, many studies have embarked on comparative evaluations of microwave-assisted and conventional drying of pharmaceutical granules or pellets in terms of process efficiencies and end product quality. These studies were performed either in single equipment furnished with various modes of drying (e.g. single pot processors or fluidized-bed processors equipped with microwave drying functions) or in different types of dryers. For valid comparisons, the granules or pellets were manufactured by an identical method, typically by high shear granulation or

extrusion-spheronization, before being subjected to the various drying methods of interest.

In the work of Doelling and Nash (1992) and Doelling et al. (1992), a fluidized-bed processor was structurally modified to enable microwave-assisted fluidized-bed drying. Four representative wet pharmaceutical granulations manufactured using low shear granulation in a planetary mixer were subjected to fluidized-bed drying with and without microwave input. It was found that the disadvantages of slow initial drying rates and non-uniform moisture distribution typically associated with fluidized-bed drying were eliminated through microwave assistance. The introduction of microwaves as a supplementary energy source exerted negligible effects on the size, flow, morphology and compressibility of resultant granules. These findings were echoed in a subsequent study by Mandal (1995) who provided further evidence that supplementing existing drying media with microwaves resulted in minimal modifications to critical properties of granules such as their bulk and tapped densities, compressibility, morphology, hardness and dissolution profiles.

However, several studies have also shown otherwise, with measurable physical differences being detected in the size, bulk/tapped density, friability, porosity, hardness, shape, surface property, compressibility and compactibility of granules subjected to microwave-assisted and conventional methods of drying (e.g. fluidized-bed, vacuum and tray drying). Chatrath and Staniforth (1990) evaluated the effects of several drying techniques such as pulsed microwave-vacuum, fluid-bed, ambient, tray, vacuum, radio-frequency and freeze drying for high shear wet-granulated microcrystalline cellulose and compared the compaction characteristics of the dried

granules. It was found that granules subjected to different drying methods possessed different compaction characteristics as reflected by the tensile strengths and work of failure of resultant tablets. In a study by Bataille et al. (1993), spheroids comprising lactose and microcrystalline cellulose were manufactured by extrusion-spheronization and dried either in a microwave or hot air oven. Although drying was accelerated by greater than 20 times in the microwave oven, resultant spheroids possessed greater surface irregularities and were more porous and deformable than their counterparts dried in the traditional hot air oven. Recently, Hegedűs and Pintye-Hódi (2007) evaluated the microwave-vacuum and fluidized-bed drying of wet granules prepared in a single pot high shear granulator. The granules comprised predominantly corn starch and an unidentified active ingredient. Granules dried under the influence of both microwaves and vacuum were larger and more spherical. Due to their lower porosities, they were less susceptible to deformation and required higher compaction pressures to form tablets. The higher attrition rates experienced in the fluidized-bed dryer resulted in smaller and rougher granules which were irregularly-shaped and more porous. This rendered them more deformable.

Fewer studies compared the influence of microwave-assisted and conventional methods of drying on drug stability. In a study by Chee et al. (2005), moist granules containing a moisture-sensitive drug, acetylsalicylic acid, were subjected to static and dynamic microwave drying with the aim of evaluating the extent of drug degradation during the drying process. Dynamic microwave drying was performed using a single pot high shear granulator equipped with a bowl swinging function which provided mild agitation to the granules and aided the uniform distribution of microwave energy during drying. The static mode of microwave drying was performed in a laboratory-

scale microwave oven. The comparators were taken to be dynamic fluidized-bed and static hot air oven drying without microwave input. Interestingly, it was found that the introduction of microwaves and its power level did not exert an adverse effect on drug stability. The extent of drug degradation was directly related to the efficiency at which moisture was removed in the various drying processes. Regardless of whether microwaves were used, dynamic modes of drying generally brought about decreased extents of drug degradation through improved dissipation of heat and moisture during the process. The reverse was observed for static modes of drying involving both hot air and microwave oven drying where a greater extent of drug degradation was observed due to the lower efficiencies of moisture removal.

1.5.1.3. Unique Features and Mechanisms of Microwave-Assisted Drying

In studies where significant differences were detected between the qualities of products subjected to microwave-assisted and conventional methods of drying, it may be erroneous to conclude that the observed disparities were attributed specifically to the effects of microwaves. This is because as different dryers were used to compare conventional and microwave-assisted drying, the observed differences in product qualities might have stemmed from specific equipment features such as the presence of agitative forces, vacuum, energy efficiency and consumption of the dryer rather than the effects of microwaves *per se*. Moreover, as microwaves become less efficient when the residual moisture content of a product falls below its M_c, supplementary energy sources, gas-assisted or vacuum drying are often introduced to assist in the final leg of the drying process. Hence, microwaves are rarely used alone and without appropriately designed controls, it remains difficult to assess the true effects of microwaves on product quality.

Despite extensive studies carried out to compare the outcomes of microwave-assisted and conventional modes of drying, few studies in the pharmaceutical field go in-depth into the kinetics and mechanisms of moisture removal under the influence of microwaves. Studies that perform mechanistic investigations on microwave-assisted drying have been centered primarily on non-pharmaceutically related materials. These included glass beads, gypsum and concrete spheres, porous granular materials of specific shapes and sizes (cylinders, slabs and spheres), ceramics, as well as selected food materials e.g. potato (Stammer and Schlünder, 1993; Adu and Otten, 1996; Remmen et al., 1996; Ratanadecho et al., 2001; Ratanadecho et al., 2002; Araszkiewicz et al., 2004; Araszkiewicz et al., 2006; Araszkiewicz et al., 2007). With microwave-assisted drying being a largely material-dependent process, these studies focused specifically on the effects of the starting physicochemical and dielectric properties of the materials on their interactions with microwaves during drying. Material samples of various sizes, initial moisture contents and shapes were treated with microwaves and their interactions with microwaves were investigated by tracking the changes in their thermal and moisture distribution profiles. Thermal profiling studies were performed using thermocouples, fiber-optic probes or infra-red imaging techniques. The moisture distribution profiles were obtained with the aid of moisture analyzers, gravimetric analyses or gamma-ray attenuation techniques. These studies were conducted at a microscopic level where a single material sample or a small collection of them were irradiated.

The results showed that variations in sizes, shapes and initial moisture contents of the samples influenced their dielectric properties which in turn affected the degree of microwave penetration, absorption and heating. The findings were in accordance to

theory. For material samples physically smaller than the wavelength of microwaves (12.2 cm at 2.45 GHz), microwaves could traverse the entire sample volume without attenuation. However, the heat distribution within this category of materials tended to be non-uniform with greater heat accumulation within their core regions. This effect was most pronounced in samples which were spherical as their curved surfaces were able to direct and focus the microwaves centrally, causing the central regions to heat up far more rapidly than their surfaces (Dolande and Datta, 1993). Due to the minimization of heat loss, greater heat accumulation was also observed in physically larger samples. With regards to the effect of moisture content, it was found that the intensity of heat generation, total internal pressures developed, as well as mass transfer within an irradiated, wet porous material was proportional not just to their moisture contents, but how the moisture apportioned into free and bound fractions. Free water absorbed significantly higher amounts of microwave energy and heated more readily than their bound counterparts (Perkin, 1979).

These results have obvious implications on the microwave-assisted drying of pharmaceutical granules and pellets. From the viewpoint of an agglomerate, the concentration of microwave energy within the interior of each agglomerate during drying creates strong pressure gradients which provide the impetus for the diffusion of liquid and vapor entrapped within the core out to its surface. With thermal and moisture diffusion now proceeding in a unidirectional manner from inside out, the moisture content of the agglomerate would be expected to increase with distance from its core. This distinctive feature of microwave-assisted drying opposes what is typically observed during conventional drying where moisture typically increases from the surfaces to the cores of the agglomerates as they are dried in the opposite

direction. Thus, unlike conventional drying methods where the efficiencies of heating and drying are governed by the conditions of the external drying medium, thermal properties and in particular, the exposed surface area of the wet material (Stahl and Van Vaerenbergh, 2005), the performance of microwave-assisted drying hinges on critical material attributes that govern their dielectric properties and internal moisture movement. Such paradigm shifts call for a need to re-evaluate the factors affecting drying. With further research, a whole new array of material attributes may potentially surface as performance indicators of microwave-assisted drying.

However, as the aforementioned studies were usually conducted on a small scale involving microwave exposure of a single material object or a small collection of them, it remained disputable if the results were relevant to the microwave-assisted drying of powders, granules or pellets on a larger, macroscopic scale. The main difference between a microscopic (single particle) and a macroscopic (bed of particles) viewpoint lies in the sample to wavelength ratio (Araszkiewicz et al., 2007). At the macroscopic level where incident microwaves impinge on a collection of particles forming a static bed, the extent of microwave absorption and internal heat generation relies on a delicate balance between the dielectric property of the particulate material and penetration depth of microwaves which is in turn, affected by the dimensions of the bed (section 1.3.6). McMinn et al. (2004, 2006) studied the microwave drying of wetted powder beds comprising both active pharmaceutical ingredients and excipients in a laboratory microwave oven. During the process, the center temperatures of the powder beds were monitored using thermocouples inserted at various depths of the bed. It was shown that the temperature profiles of the powder beds were dependent on the dielectric, physical and thermal properties of the wetting

solvent and powder, with heat being distributed non-uniformly across the cross-sections of the beds. Like single particles or objects subjected to microwave heating, the surface temperatures of the beds remained lower than their centers throughout microwave exposure. Clearly, the penetration depth of microwaves in this case did not limit the extent of heating. Although the powders were treated in their bulk states, the powder layers formed were thin (3–30 mm) due to the small quantities (≤ 100 g) tested. Under these circumstances, microwaves could permeate the entire powder bed without significant attenuation.

The effects of penetration depth became more apparent when larger quantities of powders or granules were subjected to microwave-assisted heating and drying. This was clearly illustrated in a study by Vromans (1994) in which 500 g of lactose and starch powders moistened to varying extents were subjected to static microwave-vacuum drying in a self-assembled drying apparatus comprising a 1 L round bottom flask, magnetron and condenser with a vacuum outlet. Based on preliminary dielectric measurements performed using a cavity perturbation technique, it was found that starch and lactose differed considerably in their dielectric properties with the former possessing a significantly higher dielectric loss even in its dry state. However, the higher dielectric loss of starch was found to be unfavorable during drying as it decreased the penetration depth of microwaves into the powder bed, resulting in localized surface overheating and non-uniform drying of the moistened starch powders. Complete heating of starch relied on the slow process of conductive heat transfer from its surfaces. On the other hand, drying was more uniform for the moistened lactose powders as microwaves could penetrate deeper into the powder bed, eliminating the need for continuous mixing. It was concluded that for starch-

based products or products comprising materials of similar dielectric properties, mixing or agitation of the product was mandatory during microwave exposure to ensure greater uniformity in heat dissipation and the preservation of product quality.

Ironically, as microwaves are being promoted as a new medium for volumetric and bulk heating which could potentially ease the scale-up of pharmaceutical drying processes, the mode of propagation of microwaves within a dielectric medium may, under certain circumstances, limit the extent of microwave penetration and subsequent energy dissipation within the material. As clearly demonstrated in the cited study, despite the fact that dielectrically susceptible materials are more amenable to microwave processing, the effects of up-scaling may be more pronounced when these materials are processed due to the limitations in penetration depth of microwaves. Thus, to fully reap the volumetric and bulk heating capabilities of microwaves, a fine balance has to be achieved between the dielectric properties and physical dimensions of the material load such that effective microwave processing is not hampered by limitations in its depth of penetration.

1.5.1.4. Process Monitoring and Problems Related to Microwave-Assisted Drying

Process analytical technology (PAT) has become the recent catchphrase in pharmaceutical processing. The ability to control and monitor pharmaceutical processes on-line, in-line or at-line has turned the emerging concept of ‘quality by design’ into a reality. Since the implementation of PAT, significant improvements in pharmaceutical process control and capability have diminished the reliance on sampling techniques for quality assurance. This facilitates process up-scaling and provides the key to the manufacture of high quality pharmaceutical products.

To date, many state-of-the-art microwave processors are furnished with tools for real-time process monitoring. Typically, microwave dryers are equipped with electrical sensors which enable the monitoring of the incident and reflected microwave power as well as the electric field distribution within the cavity during drying. The temporal evolution of these electrical signals provides reliable information useful for monitoring or analyzing the ongoing process. For instance, by subtracting the reflected microwave power from the incident or output power recorded during the process, the microwave energy absorbed by the wet product for the evaporation of water, together with the energy and drying efficiencies of the process may be quantified (Berteli et al., 2007).

Alternatively, the microwave energy absorbed by a wet product may be inferred from the strength of the electric field in the cavity. In microwave-assisted drying, a product ceases to absorb microwave energy once a low residual moisture content has been attained. The unabsorbed microwaves cause the electric field strength in the cavity to rise. Arc detectors or electric field sensors detect this build-up in radiation field intensity and automatically down-regulate or deactivate the microwave system completely. Apart from providing an accurate control of the final moisture content of the product, such devices prevent excessive accumulation and reflection of unabsorbed microwaves in the cavity which serve to protect the product, magnetron and user from any unwarranted exposure to microwave radiation.

The temporal evolution of electric field strength was used for monitoring the dynamic microwave-assisted drying of moistened corn starch and lactose in a 75 L single pot high shear processor (Duschler et al., 1995). For a material with a high dielectric loss

like starch, microwave absorption was not solely dependent on its moisture content and occurred even in its dry state. Thus, the strength of the evolved electric field remained relatively consistent throughout the drying process. The situation was different for a low loss material such as lactose which ceased to absorb microwaves once no residual moisture was left to evaporate. The accumulation of unabsorbed microwaves caused the electric field strength to peak which served as a useful marker of the end point of drying. However, the authors also cautioned that such measures for drying end point detection should be employed with due discretion as the interpretation of electric field patterns became more complicated when the powders were granulated. Under circumstances where lumps or accumulation of wall material occurred during granulation, continuous microwave absorption by these localized wet masses resulted in the persistence of a constant electric field strength in the microwave cavity even though the majority of the well-formed granules had been adequately dried. In these situations, overheating might occur and this posed considerable risks to product quality. Hence, the use of electric field and arc detection sensors should be reserved in cases where optimal conditions exist for uniform agglomeration and microwave absorption. In the absence of these sensors, a more theoretical approach may be applied. Péré et al. (2001) developed semi-empirical equations to compute the microwave power absorbed by the irradiated materials as functions of their dielectric properties, moisture contents and temperatures.

Dielectric properties are dynamic qualities and changes in the physicochemical characteristics of materials in the course of processing are likely to cause corresponding changes to their dielectric properties. As materials and products are often exposed to challenging temperature regimes during processing, it is not

uncommon for their temperatures to rise in the process. The phenomenon of thermal runaway occurs when the dielectric loss of a material increases with temperature or upon attaining a critical temperature limit (Metaxas and Meredith, 1983). As drying ensues with the material heating up and absorbing incremental amounts of microwave energy, a thermal avalanche may be triggered causing local rises in its temperature. Unless there is sufficient thermal conductivity in the material to dissipate local heat, the hot spots generated may cause quality deterioration not only in terms of the chemical degradation of thermolabile active constituents but also material rupture. The latter occurs when the high internal temperatures and pressures developed within the material core causes entrapped moisture to evaporate or vaporize at a rate exceeding that at which diffusion can occur through the structure of the material. Under these circumstances, the electric field sensors possess diminished sensitivity towards the moisture content of the material and process monitoring can be challenging.

Thus, in addition to electric field sensing methods, thermal imaging techniques have been developed to map, visualize and obtain real time information on the macroscopic and volumetric distribution of heat in different pharmaceutical materials exposed to microwaves. In the work of Kelen et al. (2006a-c), moistened powder loads of microcrystalline cellulose, corn starch, calcium hydrogen phosphate, mannitol, lactose and calcium carbonate each weighing 6.3 kg were dried under the influence of microwaves in a 25 L single pot high shear processor. The powder loads were evenly sectioned into 6 layers each measuring 2 cm thick by means of dielectrically inert polytetrafluoroethylene dividers. The cross-sectional surface temperatures of the powders after a fixed duration of microwave exposure were captured with infra-red

cameras and the images obtained used to quantify and characterize the heating pattern of each powder layer.

The results showed a progressive reduction in temperature as bed depth increased. This was consistent with the concepts of penetration depth as large volumes of powders were heated in this study. For multi-component powder formulations comprising materials of vastly different dielectric properties, it was found that the temperature disparity between a 'hotspot' and its immediate surroundings could exceed 100 °C. Interestingly, the results also revealed that apart from their innate dielectric behavior, the temperature distribution within the powder loads were affected by a multitude of equipment variables. The shape of the microwave cavity, location of the microwave inlet window and the presence of metallic protrusions (mixer, chopper, spray nozzles, temperature sensors) influenced the electric field and heat distribution within the load. The hottest area of the powder load was found to be situated directly under the microwave inlet window due to localized field concentrations at the power feed point.

Compared to electric field sensing, thermal mapping techniques provide a more direct way of monitoring a drying process. The temperature distribution profiles obtained for the different materials could be used as a basis for the selection of diluents most appropriate for the formulation of thermo-labile actives. It was postulated that when pharmaceutical actives possess lower critical temperature limits, excipients with higher dielectric losses are preferred as they would then be preferentially heated by microwaves during the process. If subsequent drying proceeded at a sufficiently fast rate, the risk of dielectric heating of the active compound would be minimized.

To circumvent the problems of non-uniform or over-heating typically associated with microwave processing, pulsed microwave drying techniques may be adopted. This involves exposing the product intermittently to microwaves in a time-varying fashion. Microwaves are periodically switched on and off according to pre-determined time intervals. Such temporal variations in energy input allow for temperature and moisture equilibration. During the cycle 'off' times, the hotter areas are cooled by heat diffusion to the cooler, surrounding material, allowing for the redistribution of heat and moisture within the product undergoing drying. It has been reported that intermittent microwave heating mitigate drying-induced stresses by minimizing the build up of heat and hotspots, thereby contributing to significant improvements in product quality (Zhang and Mujumdar, 1992; McLoughlin et al., 2003b). Apart from quality enhancements, there have been other purported advantages of pulsed or intermittent microwave heating. In numerous drying studies involving bio-products, the intermittent application of microwave energy was shown to be more favorable than continuous microwave drying in terms of drying kinetics (Chen et al., 2001), energy efficiency (García and Bueno, 1998; Gunasekaran, 1999) and cost savings (Chua et al., 2003). Few studies however, have been conducted on the pulsed microwave heating and drying of pharmaceutical materials and products.

1.5.2. Non-Thermal Effects of Microwaves

Apart from heating and drying applications, microwave technology provides new approaches for processing materials that are not amenable to conventional methods of processing (Ku et al., 2002). Specifically, microwaves offer an avenue for the enhancement and modification of the physicochemical properties of materials via specific material-microwave interactions which are non-thermal in nature. These

interactions have been exploited primarily for the design of controlled-release dosage forms.

1.5.2.1. Dosage Form Design

Microwaves have been utilized as a tool for the design of controlled-release dosage forms based on natural polymers such as alginate, chitosan and pectin (Wong et al., 2002; Nurjaya and Wong, 2005; Wong et al., 2005b). In these studies, polymer beads and microspheres were prepared and exposed to microwaves in a laboratory microwave oven both continuously and intermittently. Aged polymer beads were subjected to similar treatment. Using differential scanning calorimetry and fourier transform infra-red analysis, it was found that microwave radiation induced the formation of cross-linkages and enhanced polymer-polymer as well as drug-polymer interaction (complexation) in these matrices. The release of encapsulated small molecule drugs such as sulphathiazole and sodium diclofenac were effectively retarded without any compromises on their chemical stabilities. Furthermore, the microwave-treated polymer matrices possessed excellent *in-vitro* and *in-vivo* biocompatibility and biodegradability. By substituting the use of noxious chemical cross-linking agents with microwave technology, the enviromental impact of material processing was greatly minimized.

However, varying degrees of success were achieved with different polymers. Microwaves exerted minimal effects on chitosan matrices. Although both alginate and pectin were more responsive, the effects of microwaves on drug release from these matrices were at odds. The rate and extent of drug release from microwave-treated alginate matrices was decreased under selected irradiation conditions whereas the

applied waves actually enhanced drug release from pectinate matrices. It appeared that the molecular arrangement of the polymer chains affected the responses of the polymer matrices to microwaves and that a combination of polymers was more favorable for effective drug release retardation. For instance, alginate-chitosan or pectin-chitosan matrices were preferred over single polymer systems for retarding drug release. Complexation of alginate or pectin with chitosan improved the retention capabilities of the matrices and prevented the leakage of encapsulated drugs which would have otherwise occurred in the porous, pure alginate or pectin matrices. Under the influence of microwaves, the decrease in rate and extent of drug release from the combined matrices was mediated through enhancements in polymer-polymer interaction, drug-polymer interaction and polymer cross-linking. It was also noteworthy that aged polymer matrices responded differently to microwaves as compared to freshly prepared ones. An example could be seen in the study by Bodek and Bak (1999) where thermally-aged chitosan-sodium diclofenac matrices possessed substantially reduced dielectric losses and polarizability attributed to the effects of cross-linking, loss of moisture, and other structural changes related to aging. These matrices thus required a different pattern of microwave exposure to achieve controlled drug release.

In the hope of achieving better results and greater consistencies in drug release outcomes, the potential of poly(methyl vinyl ether-*co*-maleic acid) was explored. Poly(methyl vinyl ether-*co*-maleic acid) and its analogs are widely used as thickening agents, encapsulating agents, denture adhesives and adjuvants for transdermal drug delivery systems (Matsuya et al., 1996; Arbós et al., 2002; Arbós et al., 2003; Luppi et al., 2003; Kockisch et al., 2005; Owens et al., 2005; Salman et al., 2005). Unlike

alginates or pectin, its potential in controlling the release of small molecule drugs from oral dosage forms has not been scrutinized.

Poly(methyl vinyl ether-*co*-maleic acid) matrices previously cross-linked with Ca^{2+} and Zn^{2+} ions were exposed to microwaves to evaluate its effects on the release of encapsulated sodium diclofenac in the colon (Wong et al., 2007b; Wong et al., 2008). It was hypothesized that by microwave processing, drug release from the polymer matrix could be sustained further downstream in the gastrointestinal tract. The results indicated that the extent of drug release retardation was controlled by the state of polymer-polymer interaction and polymer-drug interaction in the matrices. Interestingly, for matrices cross-linked by Ca^{2+}, microwaves were found to both promote and impede drug release, depending on the intensity of radiation applied. The loss in drug release retardation capability of the Ca^{2+} cross-linked matrices was attributed to the loss of polymer-polymer interaction. Greater success rates were achieved with corresponding matrices cross-linked by Zn^{2+} where drug release retardation was observed regardless of radiation intensity. At fixed radiation intensities, the extent of drug release retardation from matrices cross-linked by Zn^{2+} was proportional to the duration of microwave exposure. Similar effects on drug release were achieved in microwave-treated starch (Malafaya et al., 2001) and gelatin-based (Vandelli et al., 2004) matrices encapsulating non-steroidal anti-inflammatory drugs.

Many pharmaceutical actives possess poor bioavailability and solubility enhancements of these drugs constitute a key area of interest in pharmaceutical research. Microwaves have been employed as an effective tool for enhancing the

solubility and bioavailability of poorly aqueous soluble drugs via the formation of solid dispersions and nanocomposite materials. In a study by Kerč et al. (1998), results obtained from differential scanning calorimetry and X-ray diffraction revealed that the microwave treatment of binary solid mixtures comprising felodipine and inert carriers like amorphous silicon dioxide or crystalline sodium chloride caused the conversion of crystalline felodipine to its amorphous or microcrystalline state. Expectedly, the duration of microwave exposure exerted an important bearing on the amorphous state of the drug and its resultant dissolution properties.

A similar technique was used to prepare solid dispersions comprising ibuprofen and hydrophilic carriers such as polyvinylpyrrolidone-vinyl acetate copolymer and hydroxypropyl-β-cyclodextrin (Moneghini et al., 2008). Microwave treatment resulted in the conversion of crystalline ibuprofen to its amorphous form. Coupled with the hydrophilicity of the carriers, a remarkable enhancement in the *in-vitro* dissolution rate of ibuprofen was achieved in the microwave-treated solid dispersions as compared to the pure drug. Bergese et al. (2003) employed microwaves for the preparation of activated drug-matrix nanocomposites. The nanocomposites comprised matrix microparticles of crospovidone or beta-cyclodextrin in which both nanocrystals and molecular clusters of ibuprofen, nimesulide or nifedipine were embedded. Microwave treatment of the original physical mixtures of drug and matrix particles had caused significant transformations of the drug molecules from their microcrystalline state to matrix-embedded molecular clusters characterized by a residual crystallinity of less than 30 %.

Recently, solid dispersions of a poorly water-soluble drug, tibolone, in a polyethylene glycol matrix were prepared by both conventional and microwave-induced melt mixing (Papadimitriou et al., 2008). Using high performance liquid chromatography, the stability of tibolone was found to be unaffected by microwaves used at lower power outputs. Compared to conventional heat application, microwaves led to significantly shorter preparation times. This was attributed to its penetrative and volumetric heating capabilities which minimized the reliance on thermal gradients for heat transfer. Furthermore, it was found that the use of microwaves enhanced the diffusion of drug in the liquid polymer melt and this led to a finer distribution of drug in the melt matrix. Scanning electron micrographs of the irradiated dispersions provided evidence of the reduction in crystal size of tibolone. These factors were believed to have caused an elevated dissolution rate of tibolone in melt dispersions prepared using the microwave technique.

In a bid to address the pH-dependent bioavailability of loratadine, microwaves have been successfully applied for the preparation of loratadine-dimethyl-β-cyclodextrin inclusion complexes (Nacsa et al., 2008). Physical mixtures of the drug and cyclodextrin were suspended in 50 % alcohol and treated in a laboratory microwave oven. Although dissolution studies revealed that the improvement in solubility and rate of dissolution of loratadine from complexes prepared using microwaves was comparable to that prepared using the conventional kneading method, the preparation process was significantly hastened with microwave treatment. Furthermore, results obtained thermal analytical studies and fourier transform infra-red analysis revealed that microwaves did not cause any chemical changes to the loratadine molecule.

1.5.2.2. Physical Transformations Induced by Microwaves

From the above examples, it is clear that microwave technology provides a novel approach for purposeful material design and modification. Prior knowledge of electromagnetic theory, dielectric properties of pharmaceutical materials and their amenabilities to microwave processing would generate greater technical know-how and interest amongst the scientific community on these lesser known uses of microwaves.

However, the specific mechanisms of material-microwave interactions have continued to intrigue scientists to this day. In microwave-assisted drying for instance, the microwave energy imparted to the product may not result exclusively in heat generation and solvent evaporation. The microwaves may interact non-thermally with specific chemical moieties or molecular groups that may inadvertently result in physical transformations to the product or its intermediates. More often than not, the insidious nature of these interactions go undetected till they manifest as altered physical properties of the products, or at a more microscopic level, transformations in the solid state structure, phase and surface areas of active constituents or excipients (Dávid et al., 2000).

Drawing from the aforementioned examples on microwave-induced cross-linking of natural polymers, subjecting pharmaceutical formulations comprising these polymeric materials to microwave processing or drying may precipitate similar reactions which may impair the functional roles of these excipients and affect the therapeutic efficacies of the final dosage forms. Indeed, some studies have demonstrated that changes to the crystallinity of starch occurred following microwave exposure (Szepes

et al., 2005). The extents of these changes were dependent on the botanical origins of the starch samples. It appeared that potato and maize starches possessed different microwave susceptibilities due to their structural differences (Szepes and Szabó-Révész, 2007). Whilst the crystallinity, water retention capability, swelling power and capacity of maize starch remain unaltered following microwave exposure, the corresponding characteristics of potato starch were modified significantly following similar treatment. Hence, maize starch was preferred over potato starch in the formulation of pharmaceutical products subjected to microwave-assisted drying as its dielectrically inert character conferred a certain level of protection against potential changes caused by microwave-induced heating. On the flip side, these results unveiled further opportunities for the use of microwaves as a suitable, selective and non-conventional method for purposeful physicochemical modification of potato starch.

Preliminary evidence of microwave-induced solid state changes to active pharmaceutical ingredients have also surfaced (Killeen, 1999). When granules containing acetaminophen were subjected to microwave-vacuum drying in a 75 L high speed vertical granulator, it was found that the applied microwaves caused modifications to the crystallite structure of the drug. This resulted in changes to the compressibility and compaction properties of the dried granules which were postulated to affect its *in-vivo* performance. Supplementary work on the dielectric properties of acetaminophen could potentially justify these findings.

1.5.3. Microwave Technology for Moisture-Sensing Applications

Apart from its use as a medium for processing pharmaceutical materials and products, microwaves may indirectly be employed for sensing or detecting the quality characteristics of pharmaceutical products and their intermediates during processing. This is based on the principle that since dielectric properties are unique to a specific physicochemical state of a material, the physicochemical changes that it undergoes in the course of processing would inevitably bring about corresponding changes in its dielectric properties which may readily be monitored.

Microwave technology has established a strong foothold for moisture analysis of food and agricultural products due to the high dielectric susceptibility of water. In response to the PAT initiative of the U.S. Food and Drug Administration, this has led to rising interest in the development of microwave sensors for the remote, on-line moisture-sensing of pharmaceutical intermediates and products during processing. Compared to near-infrared waves which are sensitive primarily to surface moisture, the lower frequencies and thus higher penetration depths of microwaves are more advantageous for it allows the detection and quantification of moisture entrapped or embedded within a product (Buschmüller et al., 2007).

In two recent studies, microwave sensors were used for *in-situ* moisture determination of wetted powders and granules during high shear granulation (Gradinarsky et al., 2006) and fluidized-bed drying (Buschmüller et al., 2007), respectively. In high shear granulation, an open-ended coaxial probe affixed at the base of the mixer bowl was used to monitor the changing dielectric properties of microcrystalline cellulose powders as they underwent initial wetting and subsequent agglomeration. Water

existed primarily in its bulk or free state when it was first mixed with the powders. As granulation proceeded with the particles agglomerating, the water molecules became increasingly bound to the solid particles resulting in a decreased proportion of free water. This reduced availability of free water molecules lowered the dielectric response of the agglomerating powders. By monitoring the changes in contents and states of water in the wetted microcrystalline cellulose powders via the temporal evolution of their dielectric properties, the end point of granulation was predicted. A similar principle was applied to the fluidized-bed drying of granules. Instead of water addition, the dielectric responses of the wet granules now decreased with water being removed as a result of drying. With the evolved dielectric profiles closely mirroring the characteristic phases of drying, the residual bound and unbound concentrations of water in the granules as well as the end point of drying were established.

However, the action of high speed impellers and air fluidization created dynamic material density patterns in the vessel which affected their interactions with the microwave sensor. In high shear granulation, changes to the impeller speed generated varying material density patterns in the mixer. The agglomeration of particles inevitably reduced the effective area of contact between the probe and powders with the consequence of diminished probe sensitivity. Particle fluidization in a fluidized-bed dryer also created complex and rapidly shifting material density patterns which affected dielectric property measurements. These confounding effects of density led to compromises on the accuracies of moisture measurement. Based on previous studies on the dielectric moisture measurement of food and agricultural products (Kraszewski and Nelson, 1992), it was noted that the effects produced by variations in the bulk densities of the products were similar in magnitude to those caused by

changes in their moisture contents. In other words, for products containing the same moisture content but different bulk densities, the dielectric sensing device would interpret the higher bulk density as additional moisture content, thereby introducing errors in moisture measurement.

To circumvent this problem, measures have been adopted to compensate or eliminate the effects of density by the development of density-independent functions which depend exclusively on material moisture content under standard temperature conditions (Meyer and Schilz, 1980; Kent and Meyer, 1982; Powell et al., 1988; Kraszewski et al., 1998; Trabelsi and Nelson, 1998). Density-independent functions may comprise 1 or 2 dielectric parameters (ε' and ε'') determined at different frequencies. More commonly, both variables ε' and ε'' are measured simultaneously at a fixed frequency and combined in a single expression. Two variable density-independent functions are purported to possess universal character and are applicable at microwave frequencies regardless of the dielectric measurement technique (Trabelsi and Nelson, 1998). The following 6 density-independent functions have been proposed by various authors (Kraszewski et al., 1998; Trabelsi and Nelson, 1998):

$$F1 = \frac{\varepsilon''}{\varepsilon' - 1} \quad (8)$$

$$F2 = \frac{\sqrt{\varepsilon''}}{\sqrt[3]{\varepsilon'} - 1} \quad (11)$$

$$F3 = \frac{\varepsilon''}{\sqrt{\varepsilon'} - 1} \quad (9)$$

$$F4 = \frac{\sqrt{\varepsilon''}}{\sqrt{\varepsilon'} - 1} \quad (12)$$

$$F5 = \frac{3}{40} \frac{\varepsilon''}{\sqrt{\varepsilon'}\left(\sqrt{\varepsilon'} - 1\right)} \quad (10)$$

$$F6 = \frac{1}{2} \frac{\sqrt{\varepsilon'} + 1}{\sqrt{\varepsilon'}} \frac{\varepsilon''}{\varepsilon' - 1} \quad (13)$$

These equations nullify the effects of density and relate directly to the moisture content of the materials. In the study by Gradinarsky et al. (2006) on the high shear wet granulation of microcrystalline cellulose as cited earlier, a density-independent function of similar form was adopted with reasonable success to relate the extent of wetting of the microcrystalline cellulose powders directly to its dielectric properties during granulation. Comprehensive summaries on these functions have been provided by Berbert and Stenning (1996) as well as Shrestha et al. (2005).

1.6. Current Knowledge Gap on Dielectric Properties of Pharmaceutical Materials and Potential Applications of Microwave Technology

The prevalence of microwave technology for household use has not been followed as readily by the pharmaceutical industry. This stems from genuine concerns with regards to the potential long term effects of microwave-induced heating on pharmaceutical materials and products. To alleviate these concerns, an in-depth knowledge of the dielectric properties of common pharmaceutical materials and how these translate to their interactions with microwaves is necessary. Such information is also useful for the quick identification and selection of materials with dielectric responses suitable for the intended application of microwave technology. An adequate understanding of the mechanisms of material-microwave interactions would allow such interactions to be optimized to facilitate and further enhance the outcomes of microwave processing. In the long run, these would promote greater acceptance of microwaves as an alternative energy source for pharmaceutical processing.

To date, there is a paucity of information on the fundamental dielectric properties of primary pharmaceutical materials. Some pioneering work was performed over recent

years by McLoughlin and co-workers (McLoughlin et al., 2003a-b; McMinn et al., 2004, 2006). They investigated the dielectric heating capabilities of several important pharmaceutical actives and excipients such as acetylsalicylic acid, paracetamol, lactose, starch, benzoic acid, stearic acid, ascorbic acid, citric acid, ammonium acetate and sodium benzoic acid using a simple laboratory microwave oven. It was found that the rank order of their dielectric heating responses corresponded to the magnitudes of their dielectric properties determined using a low frequency (10^3 Hz) dielectric spectrometer. Furthermore, the microwave drying patterns of the materials were found to be closely associated to their dielectric heating capabilities.

Despite the promise shown by these results, there remains a need for information on the dielectric properties of pharmaceutical materials at higher frequencies since they are of greater significance in microwave processing. The microwave frequency most commonly encountered for food or pharmaceutical processing is 2.45 GHz and dielectric measurements at these higher frequency ranges are often plagued by technical difficulties and high costs of instrumentation (Smith et al., 1995). These factors have greatly reduced the accessibility and availability of information pertaining to the high frequency dielectric behavior of pharmaceutical materials.

The quest for knowledge on the dielectric properties of pharmaceutical materials is faced with several impeding challenges. Despite the availability of a wide array of dielectric analyzers, the relevance of the data obtained to an actual processing situation is disputable as typically, particulate, rather than compacted forms of materials are subjected to microwave processing. This problem is further exacerbated by the physicochemical transformations that materials undergo in the course of

processing. Granulation and size enlargement, particle densification, moisture loss, morphological, structural and chemical alterations of materials result in dynamically changing dielectric properties which are complex and difficult to predict. Thus, in addition to the dielectric assessment of primary pharmaceutical materials, the effects of the physicochemical and bulk properties of these materials on their dielectric responses should be evaluated. Last but not least, although it has been postulated that dielectric mixture equations (equations 3 and 4) allow the prediction and computation of the dielectric properties of solid mixtures that comprise more than one single constituent, their validity to complex, multi-component pharmaceutical formulations remains to be tested.

Within the current realm of use, some of the reported benefits of microwave technology include improved drying performance and energy utilization, significant energy savings, accelerated product development, reduced incidences of adverse effects and the offerings of more unique and environmentally friendly approaches for the design of materials and dosage forms with specialized therapeutic features. As drying constitutes an indispensable part of pharmaceutical processing, further research on microwave-assisted drying is warranted. With knowledge gained on the dielectric properties of pharmaceutical materials, more studies could be directed from a material or formulation perspective to shift the current focus away from a predominantly equipment-centered approach. This would build a more holistic picture of the microwave-assisted drying process.

Despite its apparent simplicity, the potential of microwaves as an energy source for granulation processes, e.g. melt granulation, has not been demonstrated. It is

envisaged that with a prudent choice of excipients, the unique volumetric and targeted heating characteristics of microwaves could facilitate selective and rapid bulk heating of powders. This could potentially shorten processing times, ease temperature build-ups and minimize the exposure of thermo-labile constituents of a formulation to temperatures beyond limits critical to their stabilities. Hence, microwave-induced melt granulation represents yet another exciting field where microwave energy could be put to good use in pharmaceutical processing.

2. HYPOTHESES AND OBJECTIVES

The proposed study aimed to investigate the significance and impact of material dielectric properties in microwave-assisted pharmaceutical processes as well as explore potential process applications of microwaves. The research work was undertaken to prove the following hypotheses:

A. The dielectric properties of pharmaceutical materials would affect their amenability to microwaves and outcomes of microwave-assisted processes. These processes would encompass both the current, well-established drying practices as well as future microwave applications in the field of melt granulation.
B. Microwave-assisted pharmaceutical processes would differ from those driven by conventional energy sources in terms of process control and product quality.

To test the aforementioned hypotheses, studies were carried out to accomplish the following objectives:

1. To evaluate the dielectric properties of common pharmaceutical materials.

Limited information is currently available on the high frequency dielectric properties of primary pharmaceutical materials despite its relevance to microwave processing. The high frequency dielectric properties of selected pharmaceutical excipients and actives, together with the effects of field frequency, moisture content and density of materials on these properties would be investigated. In addition, the potential of a density-independent function for dielectric moisture analyses of pharmaceutical materials would be evaluated.

2. **To investigate the effect of formulation variables on microwave-assisted drying and drug stability.**

In view of the material dependency of microwave-assisted drying, there is an underlying need to examine the process in greater depth particularly from a material- or product-oriented viewpoint. The formulation employed for a wet granulation process in a single pot high shear processor would be varied with the aim of investigating the effects of the physicochemical characteristics of resultant wet granules on their microwave-assisted drying rates *in situ*. Comparisons would be drawn with conventional drying performed in the same equipment. The impact of microwave-assisted drying on the stability of a moisture-sensitive drug, acetylsalicylic acid, would also be examined.

3. **To demonstrate the feasibility of microwave-induced melt granulation.**

The use of microwaves for melt granulation has not been documented in literature. As many common pharmaceutical materials are dielectrically inert in dry form, a prudent choice of materials during pre-formulation is necessary for microwave-induced melt granulation to be viable. The feasibility of microwave-induced melt granulation would be demonstrated in a single pot high shear processor using a known, dielectrically active formulation. Comparisons would be drawn with conventional melt granulation performed in the same equipment. The effects of the modes of heating and massing time on agglomerate growth and yield of melt granules manufactured using the two methods would be assessed. Their process monitoring and control capabilities would be compared based on the evolved mixer power consumption and product temperature profiles.

4. **To evaluate the physicochemical properties and compaction behavior of melt granules produced in microwave-induced and conventional melt granulation.**

The different heating strategies employed in microwave-induced and conventional melt granulation may influence the distribution of molten binder material during granulation and consequently, affect the physicochemical properties of resultant melt granules. The size and size distribution, binder distribution patterns, moisture contents, flow properties and porosities of melt granules produced using the two granulation methods would be compared. The relative influences of these granule properties on their compaction behavior and compressibility would also be evaluated.

The results and discussion specific to these objectives are presented in Chapter 4, sections A-D.

3. MATERIALS AND METHODS

3.1. Materials

For the determination of dielectric properties, a range of pharmaceutical materials commonly employed as fillers, binders and disintegrants in pharmaceutical dosage forms as well as selected active pharmaceutical ingredients were used. The fillers included α-lactose monohydrate (Pharmatose 200M, DMV, the Netherlands), starch (National 78-1551, Pregelatinized corn starch NF, National Starch and Chemical, USA) and anhydrous dicalcium phosphate (Rhodia, USA). Polyvinylpyrrolidone (PVP) C15, K25, K29/32 and K90D (Plasdones C15, K25, K29/32 and K90D, ISP, USA) are long chain synthetic water-soluble homopolymers of N-vinyl-2-pyrrolidone differing in their molecular weights and polymer chain lengths. Polyvinylpyrrolidone-vinyl acetate (PVP-VA) S630 copolymer (Plasdone S630, ISP, USA) is a synthetic, linear 6:4 random copolymer of N-vinyl-2-pyrrolidone and vinyl acetate. Sodium alginate (Manucol LB, ISP, USA) is a naturally-occurring polymer derived from brown algae. The PVP polymers and sodium alginate are typically employed as binding agents. Cross-linked polyvinylpyrrolidones (cross-linked PVP) XL and XL10 (Polyplasdones XL and XL10, ISP, USA) represented the tablet disintegrants used in this study. Paracetamol (Kangle, Wenzhou Pharm Factory, China) and acetylsalicylic acid (Sintor, Romania) are the model drugs evaluated.

Subsequently, selected materials were employed for the wet granulation-drying as well as melt granulation experiments. For the wet granulation-drying experiments, granules were prepared from α-lactose monohydrate of two different particle sizes (Pharmatose 200M and 450M, DMV, the Netherlands), together with cross-linked PVP XL10, PVP-VA S630 copolymer and acetylsalicylic acid as the diluent,

disintegrant, binder and moisture-sensitive drug, respectively. Prior to use, both types of lactose were pre-sieved with a 1 mm aperture size sieve to remove existing lumps. Similarly, acetylsalicylic acid was pre-sieved with a 355 μm aperture size sieve and the undersize fraction was used for granulation. Deionized water was employed as the granulating liquid to moisten the powders and activate the binder to facilitate agglomeration. For drug stability analyses by high performance liquid chromatography (HPLC), acetonitrile (HPLC grade, Merck, Germany) and phosphate buffer (pH 2.8), prepared using 85 % ortho-phosphoric acid (Merck, Germany) and potassium dihydrogen phosphate (Merck, Germany), were used to constitute the mobile phase.

For the melt granulation studies, admixtures of α-lactose monohydrate (Pharmatose 200M) and anhydrous dicalcium phosphate were employed as carriers. They were granulated using polyethylene glycol 3350 (Clariant, Germany) which served as the meltable binder material. Analytical grade chloroform (Merck, Germany) was used for the analysis of the binder contents of the melt granules formed. The Karl Fischer method was employed for the determination of the moisture contents of melt granules. Hydranal Composite-2 (Riedel-de Haën, Germany) was used as the titrant. The working solvent comprised anhydrous methanol (Panreac Quimica Sa, Spain) and formamide (Hydranal Formamid Dry, Riedel-de Haën, Germany). Magnesium stearate (Riedel-de Haën, Germany) was used as a lubricant for studies on the compaction behavior and compressibility of melt granules.

3.2. Methods

3.2.1. Determination of Moisture Contents and Physical Characteristics of Starting Materials

3.2.1.1. Determination of Moisture Content

Moisture content was determined by thermo-gravimetric analysis (DTG 60H, Shimadzu, Japan). An aluminium pan was filled with a thin layer of material and heated from 28-105 ºC at a rate of 5 ºC/min under a nitrogen environment. Depending on bulk density, the quantity of material used each time ranged from 6-10 mg. Moisture content (%w/w wet basis) was calculated from the loss in weight of the material upon heating and drying.

3.2.1.2. Determination of Particle Size

Particle size as represented by the mean particle diameter, $D_{50(p)}$, was determined by laser diffraction (LS230 with dry powder feeder, Coulter, USA).

3.2.1.3. Determination of True and Bulk Densities

True density was estimated using a pycnometer (Pentapycnometer, Quantachrome, USA). Apart from acetylsalicylic acid and polyethylene glycol 3350, materials were first dried for 2 hours in a convection oven (Model 600, Memmert, Germany) pre-heated at 95 ºC then cooled overnight prior to the test. For acetylsalicylic acid, drying was conducted overnight in a vacuum oven (Gallenkamp, UK) set at 450 mbar and 60 ºC. A lower temperature was chosen to prevent any heat-induced degradation of acetylsalicylic acid. The same oven was used for drying polyethylene glycol 3350. As the melting point of polyethylene glycol 3350 was approximately 55 °C, it was dried at a lower temperature but greater extent of vacuum than acetylsalicylic acid (50 ºC

and 550 mbar). Upon cooling, the dried materials were packed into the measurement cells for the estimations of their true densities under helium purge.

Bulk density was determined by sieving the material through a 1 mm aperture size sieve such that it flowed freely, with the aid of a glass funnel, into a graduated cylinder cut exactly at the 25 ml mark. The weight of material occupying 25 ml was determined. Bulk density was defined as the weight of material divided by its volume.

A minimum of 3 replicated experiments was conducted for each of the tests aforementioned. The functions, moisture contents, particle sizes, true and bulk densities of all the starting materials are presented in Table 1.

3.2.2. Dielectric Analysis

3.2.2.1. Preparation of Material Compacts (Untreated Materials)

All materials were compacted prior to dielectric analysis. An accurately weighed sample of material was filled into a cylindrical stainless steel die of a universal testing machine (Autograph AG-100kNE, Shimadzu, Japan) and compacted between 2 flat-faced punches (14.93 mm in diameter) with the upper punch approaching the stationary lower punch at 2 mm/min. Each material was compacted under a range of pressures to produce compacts of different densities. Due to the inherent differences in their compactibility characteristics, the amounts of materials used and pressures applied ranged from 0.127-0.878 g and 6.9-542.6 MPa, respectively. These values were chosen such that compacts formed were mechanically strong and did not chip or break upon handling. After each compaction cycle, the lower punch was removed and

Table 1. Moisture contents and physical characteristics of the starting materials.

Material	Function	Moisture content[a] (%w/w)	$D_{50(p)}$[a] (µm)	True density (g/ml)	Bulk density[a] (g/ml)
Lactose 200M	Filler	0.236 (0.046)	36.83 (1.19)	1.535	0.425 (0.010)
Lactose 450M		0.234 (0.075)	27.15 (0.53)	1.531	0.327 (0.001)
Anhydrous dicalcium phosphate		0.225 (0.064)	15.84 (3.91)	2.842	0.701 (0.004)
Starch		9.402 (0.354)	74.31 (3.24)	1.483	0.478 (0.009)
Sodium alginate	Binder	9.744 (0.176)	164.03 (8.26)	1.720	0.867 (0.015)
Polyvinylpyrrolidone					
C15		6.866 (0.375)	53.82 (0.85)	1.196	0.449 (0.002)
K25		6.766 (0.475)	73.09 (4.29)	1.179	0.387 (0.002)
K29/32		8.492 (0.080)	121.10 (5.84)	1.140	0.333 (0.002)
K90D		17.113 (1.067)	380.55 (64.52)	1.200	0.349 (0.003)
Polyvinylpyrrolidone-vinyl acetate S630 copolymer		4.675 (0.123)	58.12 (5.03)	1.197	0.245 (0.001)
Polyethylene glycol 3350		0.596 (0.169)	255.18 (7.59)	1.218	0.586 (0.014)
Cross-linked polyvinylpyrrolidone	Disintegrant				
XL		11.727 (0.037)	121.33 (0.78)	1.197	0.215 (0.002)
XL10		13.302 (0.669)	31.97 (0.51)	1.196	0.264 (0.008)
Paracetamol	Drug	0.221 (0.136)	41.68 (3.34)	1.301	0.271 (0.002)
Acetylsalicylic acid		0.156 (0.041)	185.74 (7.13)	1.392	0.587 (0.020)

$D_{50(p)}$ refers to the mean particle diameter.
[a] Standard deviations are indicated in parentheses.

the formed compact gently ejected from the die. Each compact was individually sealed in bags and allowed to recover for a minimum of 3 days prior to use.

3.2.2.2. Preparation of Material Compacts (Dried Materials)

Materials containing higher moisture contents, namely, starch, sodium alginate, the PVP binders and disintegrants, were dried to constant weight in a convection oven (Model 600, Memmert, Germany) pre-heated to 95 °C. Upon cooling, the dried materials were compacted following the procedure described in section 3.2.2.1. Drying adversely affected the compactibility characteristics of the materials as negligible amounts of moisture remained to facilitate inter-particulate bond formation. Therefore, significantly higher pressures were required for the preparation of mechanically strong compacts as compared to those applied for the untreated materials. Resultant compacts were stored and equilibrated over silica gel for 3 days prior to use. As dried sodium alginate could not be compacted within the allowable limits of the equipment load cell, it was excluded from the study. For all untreated and dried materials, five replicated compacts were prepared each time.

Starch is a popular excipient in pharmaceutical dosage forms as it performs multi-functional roles. This material was selected to test the effectiveness and sensitivity of a density-independent function to moisture variation. A 2-4 g sample of starch was spread thinly on a petri-dish and several of these were first accurately weighed then subjected to drying in a convection oven (Model 600, Memmert, Germany) pre-heated to 90 °C. The drying profile of starch was determined gravimetrically by monitoring the weight loss of 5 samples of starch at pre-determined time points of 1.5, 3, 4, 8, 12, 15 and 30 min into the drying process. At these selected time points,

samples of starch were also retrieved from the remaining petri-dishes and stored in tightly sealed amber bottles. After a total of 90 min, drying was terminated and all the starch samples were cooled and equilibrated over silica gel for 24 hours. The end point of drying was set at 90 min as it was found from preliminary trials that moisture loss from starch became negligible after 1 hour. The dried and cooled starch samples were re-weighed and the values used for the computation of the initial moisture content (%w/w wet basis) of starch. The starch samples previously obtained and stored in sealed amber bottles at the different time points of drying were compacted in an identical manner as described in section 3.2.2.1.

3.2.2.3. Measurement of Compact Density

After recovery, all the compacts produced were accurately weighed using a 3 decimal place electronic balance (CP423S, Sartorius, Germany). Thickness measurements were performed with a micrometer screw gauge (Mitutoyo, Japan) at 3 pre-defined locations diametrically across each compact and averaged to obtain the mean thickness of each compact. The density of each compact was computed by dividing its weight by volume.

3.2.2.4. Measurement of Dielectric Properties

Material dielectric properties were determined over a frequency range of 1 MHz–1 GHz at 23 ± 1 °C using a parallel-electrode sample holder (16453A Dielectric material test fixture, Agilent, USA) connected to an impedance analyzer (E4991A RF Impedance/material analyzer, Agilent, USA) as shown in Fig. 3. Prior to the measurements, the equipment was calibrated using polytetrafluoroethylene discs.

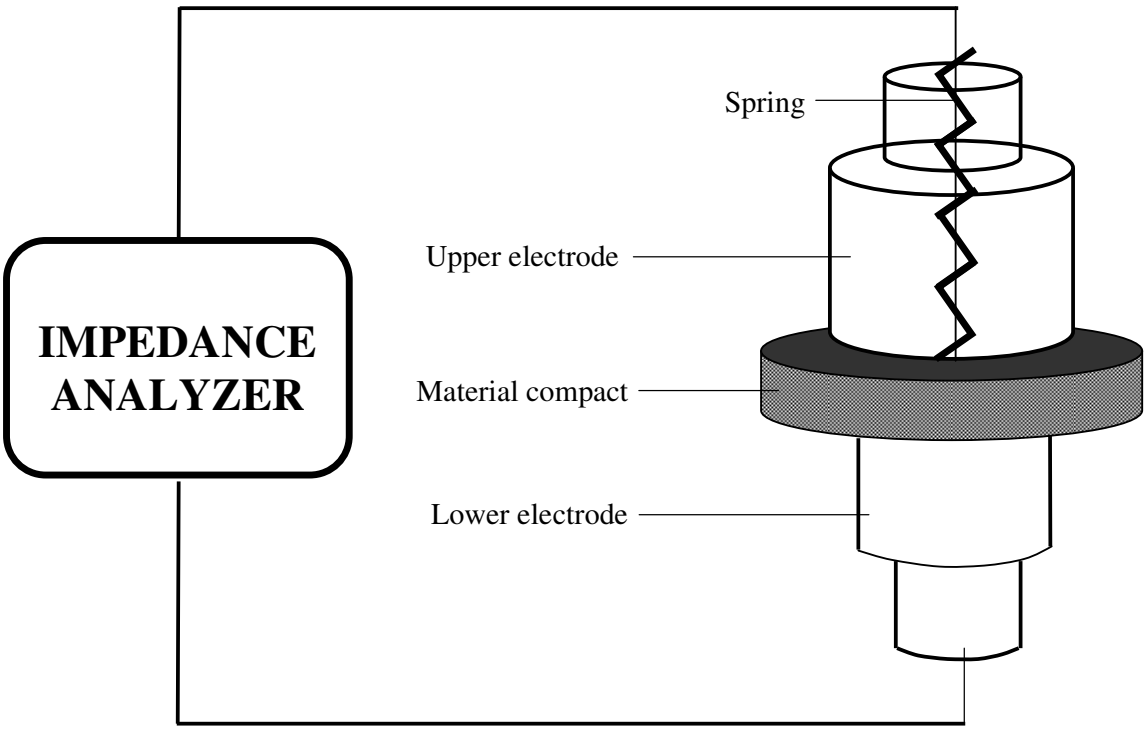

Fig. 3. Schematic diagram of the dielectric measurement system (not to scale).

Polytetrafluoroethylene is non-polar and possesses a dielectric constant of 2 over the range of frequencies investigated in this study (Kinney, 1957; Mathes, 1988).

For the actual measurements, each material compact was inserted between the plates of the parallel-electrode sample holder. The upper electrode had an internal spring which allowed the compact to be fastened between the electrodes thereby ensuring intimate contact between the surfaces of the compact and electrodes. This minimized any air gaps existing between the sample and the electrodes which may act as a further capacitor in series (Craig, 1995). As an oscillating electric field of increasing frequency was applied to each material compact, the alternating positive and negative charges on the electrode plates resulted in polarization of the polar molecules/functional groups in the material and storage of electrical charge. From the mean thickness of each compact, the capacitance of the material at a particular frequency was calculated and corresponding dielectric constant (ε') and loss (ε'') derived. Resultant dielectric constant and loss spectra were obtained by scanning each compact repeatedly over the frequency range of interest. A minimum of 3 compacts was analyzed for each untreated and dried material.

3.2.3. Determination of Microwave-Induced Heating Capabilities of Materials in a Laboratory Microwave Oven

The microwave-induced heating capabilities of materials were determined using a laboratory microwave oven (NN-MX21WF, Panasonic, Japan). Prior to the test, the initial temperature of a material, Ti (°C), was measured by means of a platinum resistance thermometer connected to a temperature controller with a digital display (Model 89810-10, Cole-Parmer Instrument Co., USA). The material was then gently

sieved through a 1 mm aperture size sieve such that it packed uniformly, with the aid of a glass funnel, into a 10 ml measuring glass. The weight of each material occupying a fixed 10 ml volume was recorded and used for the computation of its density during the heating experiment.

With minimum disturbance, each material was then placed on the center of the microwave oven turntable and exposed to a microwave power output of 800 W for 60 s. The turntable minimized the effect of field variations within the oven thereby ensuring uniformity in microwave exposure of the material. The final temperature of the material after microwave exposure, Tf (°C), was measured immediately after irradiation. The thermometer was fully inserted into the material each time its temperature was taken. The microwave-induced heating capability of the material was evaluated based on its temperature rise, ΔT (ºC), obtained by calculating (Tf-Ti). All experiments were conducted at ambient conditions of ~ 24 ºC. A minimum of 4 replicated experiments was performed for each material.

3.2.4. Wet Granulation and Drying of Granules in a Single Pot High Shear Processor

Wet granulation and drying were carried out in a 25 L single pot high shear processor (UltimaPro^{TM}25, Collette, Belgium). The processor was equipped with multiple drying functions allowing the use of microwaves, bowl-jacketed heating, gas assistance (Transflo^{TM}) and vacuum for drying. These are depicted in a schematic in Fig. 4.

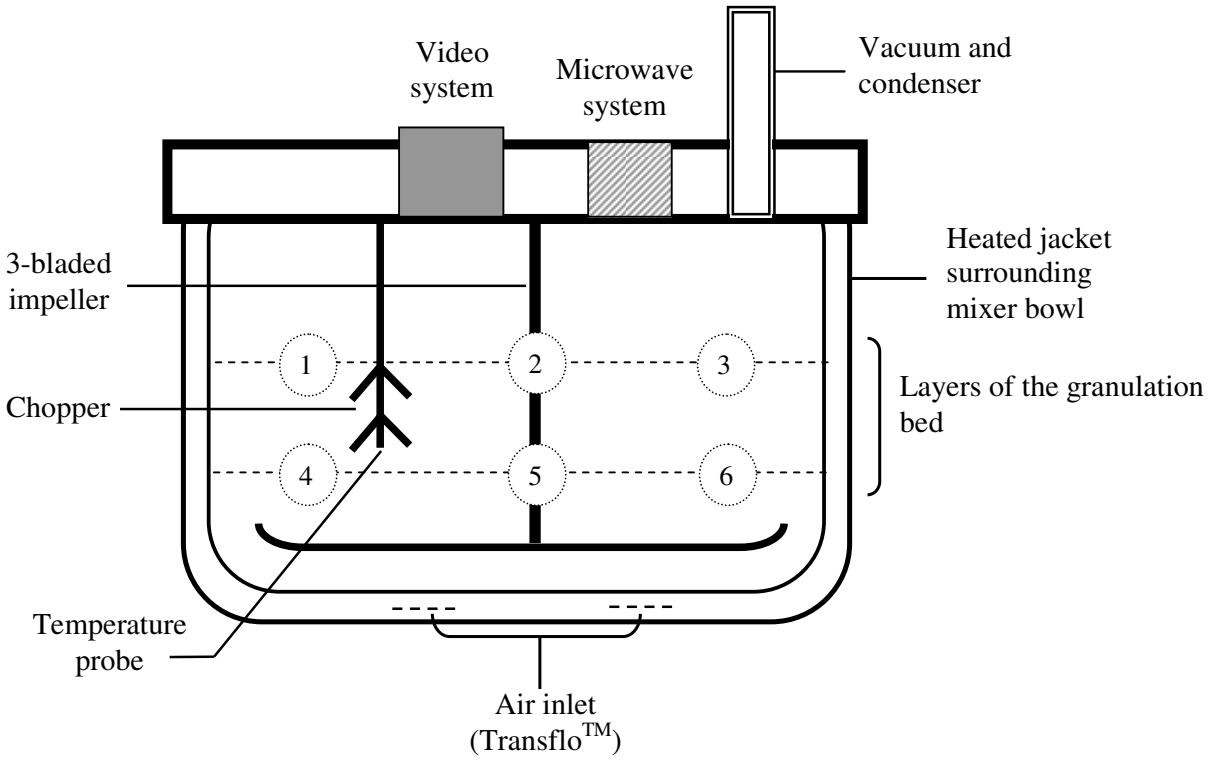

Fig. 4. Schematic of the cross-section of the single pot high shear processor (not to scale). 1-6 refer to the 6 sampling locations for the determination of the residual moisture contents of granules during drying.

The different formulations used for wet granulation are shown in Table 2. Based on preliminary trials conducted, the amount of granulating liquid employed for each lactose type was different. Lactose 200M granules were prepared with 8 and 11 %w/w of granulating liquid whereas lactose 450M granules were prepared with 11 and 14 %w/w of granulating liquid. The different liquid requirements arose from disparities in specific surface areas of the powders (Kibbe and Weller, 2005). Four different batch sizes of lactose 200M and 450M granules were prepared using powder loads of 2.5, 4, 6.5 and 7.5 kg.

Table 2. Formulation of lactose 200M and 450M granules.

Material	**Lactose 200M granules**	**Lactose 450M granules**
Lactose 200M	88 %	-
Lactose 450M	-	88 %
Cross-linked polyvinyl pyrrolidone XL10	2 %	2 %
Polyvinylpyrrolidone-vinyl acetate S630 copolymer	5 %	5 %
Acetylsalicylic acid	5 %	5 %
Total dry weight of powder (kg)	2.5, 4, 6.5, 7.5	2.5, 4, 6.5, 7.5
Granulating liquid (%w/w)[a]	8, 11	11, 14

[a] Deionized water expressed as a % of the total dry weight of powder.

3.2.4.1. Wet Granulation

Wet granulation was carried out at ambient conditions. Accurately-weighed quantities of powders were first dry mixed for 5 min using a 3-bladed impeller operating at a speed of 280 rpm. Thereafter, the required amount of granulating liquid was pumped into the mixer bowl with the aid of a pressurized vessel set at 0.4 bar. The same

pressure was used for all experiments to ensure that the rate of liquid addition was consistent. During liquid addition, the impeller speed was maintained with the addition of the chopper operating at a speed of 600 rpm. After the desired quantity of liquid has been added, subsequent massing and granulation was carried out for a total of 14 min at an impeller speed of 425 rpm for 10 min and 180 rpm for the remaining 4 min. The speed of the chopper was set at 2870 rpm throughout the entire granulation phase.

3.2.4.2. Microwave-Assisted Drying of Granules

For granules dried under microwave-assisted conditions, a microwave power output of 300 W, together with a jacketed bowl maintained at 55 ºC provided the main sources of thermal energy for drying. A vacuum was created in the mixer bowl by lowering the internal bowl pressure to 50 mbar. This was based on manufacturer specifications which had restricted the use of microwaves to a bowl pressure range of 30-100 mbar (Chapter 2, Operating manual for UltimaPro^{TM}25, Machine serial no. 02V0025010, Collette, Belgium, 2004). A small stream of purified air introduced at the base of the mixer bowl (Transflo^{TM}) minimized product adhesion and facilitated the transport of moisture from the interior of the granulation bed to its surface during drying.

To prevent the formation of hotspots as a result of non-uniformity in electric field distribution, intermittent agitation of the granulation bed was effected during drying with the impeller and chopper operating at the lowest speed of 44 rpm. This was performed only for the first 15 min of drying when the granules were still wet. Wetter granules have been found to be more resilient to attrition and breakage than their drier

counterparts in the presence of shearing stress (Nieuwmeyer et al., 2007). This was because there was a greater tendency for granule growth than breakage or attrition when the moisture contents of granules were still high, resulting in a net size increase at higher moisture contents. A bowl swinging function which caused the mixer bowl to tilt to an inclination of 75 º was also activated during drying, providing mild agitation to the granules. Due to its ability to encourage a gentle mixing action, the swinging function was maintained throughout the entire duration of drying. This greatly minimized the attrition and sticking of granules undergoing the end stages of drying.

The process settings during dry mixing, granulation and microwave-assisted drying were kept constant for all the formulations tested. Each run was repeated at least twice.

3.2.4.3. Conventional Drying of Granules

Additional batches of lactose 200M and 450M granules were prepared using powder loads of 7.5 kg and 11 %w/w of granulating liquid. These were dried under conditions as described above but without microwave assistance and represented the control batches of granules.

3.2.4.4. Charting the Drying Profiles of Granules

The drying profiles of granules were charted by determining the residual moisture contents of granules sampled at 0, 5, 10, 15, 25, 35, 45 and 60 min into the drying process. Due to the likelihood of non-uniform moisture distribution in the granulation bed during drying, samples of granules, each weighing 6-10 g, were retrieved from six

different locations in the mixer bowl at each sampling time point (Fig. 4). The mean residual moisture contents of these 6 samples of granules provided a more accurate representation of the moisture present in the whole batch of granules. If granules were deemed insufficiently dried at the end of 60 min, further drying and sampling were carried out at 15 min intervals.

The weights of the freshly-retrieved granules were accurately determined with a 4 decimal place electronic balance (A200S, Sartorius, Germany). Subsequently, they were dried for 1 h in a convection oven (Model 600, Memmert, Germany) maintained at 105 ºC. The residual moisture contents of granules were calculated by subtracting the final weights of the dried and cooled granules from their initial weights and expressing this difference as a percentage of the final dry weight of granules. The drying profiles were obtained by plotting the mean residual moisture contents of granules (%w/w dry basis) against drying time (min).

3.2.4.5. Computation of Drying Parameters

The drying profiles were subjected to regression analysis (SigmaPlot® 8.0, Systat Software Inc., USA). Goodness-of-fit of the experimental curves to model equations were assessed by R^2 values. Drying rate parameters were derived from the first derivatives of the model equations and used to evaluate the drying performances of the various batches of granules.

3.2.4.6. Physical Characterization of Granules

3.2.4.6.1. Size Analyses of Wet Granules

A sample of wet granules was retrieved immediately after each granulation run was completed. These were observed under a stereomicroscope (Olympus, SZH, Japan) and sized using image analysis software (Micro Image, Media Cybernetics, USA). One hundred and twenty wet granules were sized and their mean equivalent circle diameters computed. This refers to the diameter of a circle with the same area as that of the granule observed perpendicular to the surface on which the granule rests.

3.2.4.6.2. Size Analyses of Dried Granules

After drying was completed, the granules harvested were sieved through a 4 mm aperture size sieve (Endecotts Ltd., UK) to remove the lumps formed. The proportion of lumps was calculated by expressing the weight of the oversize fraction ($\geq$ 4 mm) of granules as a percentage of the total weight of granules harvested. The undersize fraction of granules (< 4 mm) was divided by means of a spinning riffler (PT, Retsch, Germany) to obtain representative samples for subsequent size analyses.

One hundred grams of granules < 4 mm were sieved through a stack of sieves (Endecotts Ltd., UK) with aperture sizes ranging from 90 to 2800 µm arranged in a $\sqrt{2}$ progression. Sieving was carried out for 10 min at an amplitude of 1 mm using a vibratory mechanical sieve shaker (Endecotts Ltd., UK) and the weight of granules retained on each sieve was recorded. The mass median diameter, D_{50}, referred to the size of granules at the 50^{th} percentile of the cumulative undersize plot. The modal fraction represented the size fraction in which the majority of the granules from each

batch were found. At least 3 replicated experiments were conducted and the results averaged.

3.2.4.6.3. Determination of Bulk Densities of Granules

Bulk density determinations were carried out by allowing representative samples of granules from each batch to flow freely, with the aid of a funnel, into a graduated cylinder cut at the 100 ml mark. The weight of granules occupying 100 ml was determined. Bulk density was computed by dividing the weight of granules by its volume. Four replicated experiments were conducted and the results averaged.

3.2.4.6.4. Determination of Crushing Strengths and Friability Studies of Granules

The mechanical strengths of all lactose 200M and 450M granules prepared using 11 %w/w granulating liquid were determined by crushing and friability tests. Representative samples of granules from each batch were sieved through a nest of sieves with aperture sizes ranging from 355 to 1000 μm arranged in a √2 progression. Those that were retained exactly within the apertures of 500, 710 and 1000 μm sieves were retrieved and individually crushed by a platen moving at a velocity of 5 mm/min (EZ Tester-100N, Shimadzu, Japan). The maximum load (mN) required to crush each individual granule was recorded. A minimum of 25 granules was crushed for each size fraction and the results averaged to represent their crushing strengths.

Granules 355–500 μm in size were subjected to friability tests as they were physically too small to be crushed. Accurately weighed 7 g samples of these granules together with 25 steel balls, each weighing 0.88 g and measuring 6 mm in diameter, were

subjected to 100 revolutions in a friabilator (TA20, Erweka, Germany). The steel balls acted as attrition agents during the test. Fine particles produced as a result of attrition were sieved through a 250 µm aperture size sieve (Endecotts Ltd., UK) and the weight of granules retained on the sieve was recorded. Each experiment was repeated thrice and the results averaged. Friability index was calculated in the following manner:

$$\text{Friability index (\%)} = \frac{\text{Initial weight of granules (g)} - \text{Weight of granules retained on 250 µm sieve (g)}}{\text{Initial weight of granules (g)}} \times 100 \quad (14)$$

3.2.4.7. Determination of Volume of Granules in Mixer Bowl during Drying

The volume of granules in the mixer bowl was derived from their bulk densities as determined in section 3.2.4.6.3:

$$\text{Volume of granules (ml)} = \text{Dry powder weight (g)} / \text{Bulk density of granules (g/ml)} \quad (15)$$

3.2.4.8. Determination of Percent Degradation of Acetylsalicylic Acid

The percent degradation of acetylsalicylic acid during granulation and drying was determined by HPLC (LC 2010A, Shimadzu, Japan) in accordance to a method previously established (Chee et al., 2005). For all formulations, analyses were carried out on the powder mixtures after the dry mixing stage, wet granules prior to drying and final dried granules prepared from 2.5 and 7.5 kg powder loads. These were annotated by ‘powder’, ‘wet’ and ‘dried’, respectively. The percent degradation of

acetylsalicylic acid obtained for 'powder' was largely the amount of drug degradation during storage, prior to its use for granulation. It was taken as the baseline for the amount of acetylsalicylic acid degraded.

A reversed phase C-18 column (Hypersil® BDS-C18, 5 µm, 4.6 mm x 150 mm, Agilent, USA) was employed as the stationary phase whereas the mobile phase consisted of phosphate buffer (pH 2.8) and acetonitrile in a ratio of 4:1. The powders and granules were pulverized before analyses. An accurately weighed amount of the pulverized material (approximately 150 mg) was dissolved and made up to a final volume of 20 ml with the mobile phase. The suspension was then ultrasonicated (LC60H, Fisher Scientific, Germany) for 10 min before being filtered through a 0.45 µm membrane filter (RC, Sartorius, Germany). Ten µL of the filtrate were used for the assay. The column was maintained at 40 ºC throughout the analyses, and the detection wavelength employed was 254 nm.

The areas under the curves of the degradation product, salicylic acid, and remaining acetylsalicylic acid were determined and their corresponding concentrations calculated according to standard calibration curves. Four replicated assays were carried out. The percent degradation of acetylsalicylic acid was calculated in the following manner:

$$\text{Degradation of acetylsalicylic acid (\%)} = \frac{\text{Concentration (g/ml) of degraded acetylsalicylic acid}}{\text{Concentration (g/ml) of degraded acetylsalicylic acid + Concentration (g/ml) of remaining acetylsalicylic acid}} \times 100 \quad (16)$$

3.2.5. Melt Granulation in a Single Pot High Shear Processor

3.2.5.1. Microwave-Induced Melt Granulation

A 10 L single pot high shear processor (UltimaPro^{TM}10, Collette, Belgium) was used to carry out the melt granulation experiments. The equipment is a scaled-down version of that shown earlier in Fig. 4. The processor is equipped with a water-jacketed mixer bowl and microwave-emitting device capable of generating microwaves ranging from 0-900 W in power output. Instead of a three-bladed impeller, a six-bladed version with speeds adjustable up to 630 rpm was employed for granulation.

Accurately weighed powders amounting to a total of 1000 g of a 1:1 admixture of lactose 200M and anhydrous dicalcium phosphate, together with 20 %w/w (expressed as a percentage of the dry weight of admixture) polyethylene glycol 3350, were first mixed geometrically in a bag. The powder mixture was then transferred to the mixer bowl that was pre-heated to 50 ºC. Further mixing was carried out in the bowl at an impeller speed of 400 rpm until the powders have equilibrated with the bowl temperature. Product temperature measurements were performed with a platinum thermocouple that was in constant contact with the contents of the bowl. By pre-heating and equilibration, the starting temperatures of the powder masses were consistent at the start of each granulation run (Betz et al., 2004).

Upon equilibration, the powders were exposed to a microwave power output of 900 W and subjected to high shear massing at the maximum impeller speed of 630 rpm. Concurrently, the temperature of the mixer bowl was programmed at an offset of -1 ºC. This controlled its temperature such that it constantly remained 1 ºC lower than its

contents, providing the assurance that subsequent rises in temperature of the powder masses beyond 50 ºC was attributed solely to microwave energy and frictional heat produced from the shearing action of the impeller. The bowl also served as an insulator minimizing heat loss from the irradiated powders. In accordance to manufacturer specifications (Chapter 2, Operating manual for UltimaPro^{TM}10, Machine serial no. 04V0010005, Collette, Belgium, 2005), the pressure within the mixer bowl was reduced to 80 mbar when microwaves were activated.

High shear massing at 630 rpm was carried out until the powders were heated to the melting point of polyethylene glycol 3350. The melting point was determined from the temperature at which a sharp rise in mixer power consumption, suggesting an increased consistency of the powder mass at the onset of binder melting, was observed. This was confirmed to be 55 ºC based on preliminary trials. Massing was continued for further 10, 14, 16 and 18 min after the onset of melting of polyethylene glycol 3350. After the appropriate massing time had elapsed, microwaves were deactivated and the impeller speed reduced to 500 rpm for another 4 min. During this low shear massing phase, the bowl was ventilated to atmospheric pressure. The mixer bowl temperature was maintained at its -1 °C offset.

3.2.5.2. Conventional Melt Granulation

To ensure comparability with microwave-induced melt granulation, the procedure adopted for conventional melt granulation was identical to that described above with the exception that microwave energy was substituted by heat derived from the water-jacketed mixer bowl maintained at 60 ºC. All other processing parameters were kept

constant. As overgrowth was encountered at massing times of 14, 16 and 18 min, additional batches of granules were prepared at 6, 8 and 12 min.

Outputs of mixer power consumption and product temperature were continuously recorded during microwave-induced and conventional melt granulation (TrendManager Pro V5, Honeywell, USA). All experiments were repeated at least thrice.

3.2.5.3. Comparisons between Microwave-Induced and Conventional Melt Granulation

From the product temperature profiles, the heating capabilities of the agglomerating powder masses during microwave-induced and conventional melt granulation were compared. Various parameters were extracted from the mixer power consumption and product temperature profiles. These included: peak mixer power consumption (P_P) during high shear massing as well as the mixer power consumption and product temperature at the end of the high shear (P_H, T_H) and low shear massing phases (P_L, T_L).

Mixer power consumption measurements have also induced energy input considerations. The post-melt specific energy consumption, E_m, and average post-melt specific mixer power consumption, P_{av}, was derived from the mixer power consumption versus massing time curve. E_m was computed by integrating the mixer power consumption over the time of high shear massing after the onset of melting of polyethylene glycol 3350, and dividing the answer by the weight of powder used. It reflected the energy supplied per kg of powder for the formation of granules. P_{av} was

calculated by dividing E_m by the time of high shear massing after the onset of melting of polyethylene glycol 3350. P_{av} reflected the overall work involved in the transformation of 1 kg of powder into melt granules (Heng et al., 1999). The significance of these parameters in the depiction of agglomerate growth during microwave-induced and conventional melt granulation was compared.

3.2.5.4. Determination of Baseline Mixer Power Consumption

The baseline mixer power consumption referred to the power consumed when an empty mixer was run under the stipulated conditions (Mort, 2005). It provided an indication of the level of 'noise' that was contributing to the actual gross power consumption signal measured during the actual granulation process. For mixer power consumption signals to be adequately sensitive towards the agglomeration process *per se*, a high signal to noise ratio is desirable.

The main aim of this experiment was to assess the effect of mixer bowl temperature on the baseline mixer power consumption. This was carried out by operating the empty processor under different regimes in which the mixer bowl temperature was ramped up from ambient temperature to 50 ºC and 60 ºC, then back to ambient temperature again. Both 50 ºC and 60 ºC were temperature set points of the mixer bowl during the actual granulation experiments. The temperature of the mixer bowl was held for 15 min at each set point. It was necessary to reduce the bowl temperature back to ambient conditions to verify that any observed variation in the baseline mixer power consumption was not attributed to prolonged usage of the processor. The impeller speed and bowl pressure were maintained at 630 rpm and 80 mbar, respectively, both of which were set points employed during microwave-induced and

conventional melt granulation. The mixer power consumption and bowl temperature were continuously monitored throughout the process.

3.2.5.5. Evaluation of Physicochemical Properties of Melt Granules Produced in Microwave-Induced and Conventional Melt Granulation

3.2.5.5.1. Yield and Size Analyses of Melt Granules

Melt granules harvested from each run were sieved immediately through a 2.80 mm aperture size sieve (Endecotts Ltd, UK). Both the oversize and undersize granules were subsequently cooled to ambient temperature by spreading them in thin layers on trays. The oversize granules (≥ 2.80 mm) were regarded as lumps and their proportion (% lumps) was calculated by expressing the weight of granules retained on the 2.80 mm aperture size sieve as a percentage of the weight of melt granules harvested. Percent yield was in turn, calculated by expressing the weight of melt granules harvested as a percentage of the total weight of starting materials. The extent of mass adhesion to the bowl wall and impeller was inferred from the difference between the weight of the starting materials and the yield.

The undersize granules (< 2.80 mm) constituted the usable melt granules obtained from each product batch. The proportion of usable granules (% usable) referred to the total weight of melt granules < 2.80 mm expressed as a percentage of the total weight of the starting materials. The usable granules were sub-divided using a spinning riffler (PT, Retsch, Germany) into representative samples for subsequent characterizations. Their size distribution was determined in accordance to the method described in section 3.2.4.6.2. Likewise, the mass median diameter (D_{50}) of melt granules referred to the size of granules at the 50^{th} percentile of the cumulative undersize plot. The span

of melt granules was obtained by subtracting the size of granules at the 10^{th} percentile of the cumulative undersize plot from that at the 90^{th} percentile and dividing the result by D_{50}. The proportion of fines (% fines) referred to the weight of granules finer than 90 μm expressed as a percentage of the weight of granules subjected to sieving. Three replicated experiments were carried out each time and the results averaged.

3.2.5.5.2. Determination of Binder Contents of Melt Granules

Based on an established method (Wong et al., 1999), the binder contents of melt granules were determined using a near infra-red spectrophotometer (UV-3600 Spectrophotometer, Shimadzu, Japan). Following size analyses, an accurately weighed quantity of melt granules was obtained from each sieved fraction and dispersed in a known volume of chloroform. Chloroform dissolves polyethylene glycols and thus served as an extracting agent for the binder material in the melt granules. Coarser granules ≥ 1.00 mm were first dispersed in chloroform then ultrasonicated in a water bath for 30 s to improve extraction efficiency. The remnant granule materials, lactose and anhydrous dicalcium phosphate, being insoluble in chloroform, were removed by membrane filtration (Regenerated cellulose, 0.45 μm, Sartorius, Germany). The filtrate obtained was analyzed for its content of polyethylene glycol 3350 at 2488 nm. Preliminary experiments performed on physical mixtures of the 3 formulation constituents showed minimal interferences from both lactose 200M and anhydrous dicalcium phosphate on the absorbance measurements of polyethylene glycol 3350 at the wavelength of interest. Three replicated experiments were carried out each time and the results averaged.

3.2.5.5.3. Determination of Moisture Contents of Melt Granules

The moisture contents of melt granules were determined using a Karl Fischer apparatus (701 KF Titrino, Metrohm Ion Analysis, Switzerland). Representative samples (~ 25 g) of melt granules were obtained from each product batch and milled for 8 s using a small laboratory grinder. Coarser granules were subjected to an additional 5 s of milling. An accurately weighed quantity (~ 0.5 g) of milled granules was then introduced to the working solvent comprising a 1:1 ratio of anhydrous methanol and formamide. Prior to its use, the solvent was subjected to a pre-titration step for the removal of traces of residual moisture. This ensured that subsequent volumes of Karl Fischer reagent dispensed during the actual titration were attributed to moisture present in the milled granules *per se*. Three replicated experiments were carried out each time and the results averaged.

3.2.5.5.4. Determination of Flow Properties of Melt Granules

The bulk densities of melt granules were first determined according to the method described in section 3.2.4.6.3. The granules were then subjected to tapping (Stamfpvolumeter Stav 2003, JEL, Germany) until they have attained a constant volume. Tapped density was computed by dividing the weight of granules by its final, unchanged volume after tapping. A minimum of 3 replicated experiments was carried out each time and the results averaged. Hausner ratios and compressibility indices of the granules were calculated from the following formulae (Newman, 1995):

$$\text{Hausner ratio} = \text{Tapped density}/\text{Bulk density} \quad (17)$$

$$\text{Compressibility index (\%)} = [(\text{Tapped density} - \text{Bulk density})/\text{Tapped density}] \times 100 \quad (18)$$

3.2.5.5.5. Estimation of True Densities of Melt Granules

Melt granules that were previously milled were employed for the estimations of their true densities. Prior to the test, the milled granules from each product batch were spread thinly on trays and dried overnight at 50 ºC in a vacuum oven set at 550 mbar (Gallenkamp, UK). Upon cooling, the dried, milled granules were packed into the measurement cells for the estimations of their true densities under helium purge (Pentapycnometer, Quantachrome, USA). Five replicated measurements were performed each time and the results averaged.

3.2.5.5.6. Determination of Porosities of Melt Granules

The porosities of melt granules were estimated from their tapped and true densities according to the following formula (Kumar et al., 2002):

$$\text{Granule porosity (\%)} = [1 - (\text{Tapped density}/\text{True density})] \times 100 \quad (19)$$

3.2.5.6. Evaluation of Compaction Behavior of Melt Granules Produced in Microwave-Induced and Conventional Melt Granulation

3.2.5.6.1. Compaction of Melt Granules

A universal testing machine (Autograph AG-100kNE, Shimadzu, Japan) equipped with a 10 mm diameter flat-faced punch and die set was used for the compaction of melt granules. The granules were first dry mixed with 1 %w/w magnesium stearate as a lubricant. An accurately weighed 0.5 g sample of lubricated melt granules was transferred to the die cavity and compacted under a fixed pressure of 102 MPa. The rate of compaction was set at 5 mm/min. Compacts formed were gently ejected from

the die and allowed to recover in an enclosed chamber for a minimum of 24 hours prior to characterization. Eight compacts were prepared each time.

3.2.5.6.2. Determination of Mechanical Strengths and Porosities of Compacts

The mechanical strengths and porosities of the compacts were used to describe the compaction behavior of melt granules. Upon recovery, all the compacts produced were accurately weighed using a 3 decimal place electronic balance (CP423S, Sartorius, Germany). Thickness measurements were performed with a micrometer screw gauge (Mitutoyo, Japan) at 5 pre-defined locations of each compact and averaged to obtain the mean thickness of the compact. Compact porosity was estimated using the following formula (Larhrib and Wells, 1997a):

$$\text{Compact porosity } (\%) = (1\text{-}D) \times 100 \qquad (20)$$

D refers to the relative density of the compact calculated from the ratio of its apparent density (quotient of compact weight and volume) to the true density of its constituent melt granules as determined in section 3.2.5.5.5.

The mechanical strengths of compacts were assessed using a hardness tester (HT1, Sotax, Switzerland). The average force (N) required to crush 5 compacts was determined.

3.2.5.7. Evaluation of Compressibility of Melt Granules

The compressibility of selected batches of melt granules, namely, melt granules prepared at 6 and 10 min in conventional melt granulation as well as 18 min in microwave-induced melt granulation were also evaluated. An identical procedure as

described in section 3.2.5.6.1 was applied, with the exception that both the die wall and lower punch were pre-lubricated with an alcoholic suspension of magnesium stearate prior to granule filling. The die and punches were cleaned and re-lubricated after each compaction cycle. Eight compacts were prepared at each of the compaction pressures of 13, 25, 38, 51, 63, 102, 152, 203, 253 and 304 MPa. The change in density of the granule bed as a function of the applied pressure was plotted and analyzed off-line using the Heckel equation (Heckel, 1961):

$$\ln\left(\frac{1}{1-D}\right) = KP + A \qquad (21)$$

D refers to the relative density of the compact formed at a particular pressure P (MPa) and is calculated from the ratio of the apparent density of the compact (quotient of compact weight and volume) to the true density of its constituent melt granules. K and A are constants derived from the linear portion of the Heckel plot. K refers to the slope of the best fit line obtained from linear regression and its reciprocal represents the yield pressure of melt granules. Yield pressure provides a measure of the degree of plasticity and compressibility of the granules. A refers to the extrapolated intercept of the best fit line on the vertical axis. From this vertical intercept, D_A can be calculated based on the following formula:

$$D_A = 1 - e^{-A} \qquad (22)$$

D_A reflects the total densification of the granule bed in the die cavity as a result of granule filling, rearrangement and movement, before the formation of bonds amongst the granules or its constituent particles.

3.2.6. Statistical Analysis

Using SPSS version 11.0 (SPSS Inc., USA), one-way analysis of variance (ANOVA) was used to compare 2 or more sample means with post-hoc testing (Scheffe or Tukey) when significant differences were detected amongst the means. The independent samples t-test was performed to compare 2 sample means. Sample means were significantly different if $p < 0.05$. The Pearson correlation test was used to test for significant correlations ($p < 0.05$) between 2 independent sets of data.

3.2.6.1. Multivariate Data Analysis

When a property of interest is affected by the simultaneous contributions of several different variables, multivariate data analysis provides a useful tool for uncovering hidden or latent trends amongst them. Compared to univariate approaches, multivariate data analysis provides a more pragmatic and holistic approach to data analysis as it allows all pertinent inter-variable relationships present in a data set to be investigated simultaneously (Esbensen, 2001). By doing so, the most important factor(s) affecting the property of interest may be identified. Principal component analysis constitutes the workhorse of multivariate data analysis. It was employed to evaluate the "cause and effect" relationships amongst the process control and product quality aspects of the melt granulation processes.

3.2.6.1.1. Significance of Mixer Power Consumption and Product Temperature in Process Monitoring of Melt Granulation

Principal component analysis (The Unscrambler®, Camo Software AS., Norway) was carried out to compare the relative significance of the various mixer power consumption and product temperature parameters in the depiction of agglomerate

growth during microwave-induced and conventional melt granulation. The melt granulation experiments constituted the samples, whereas the variables included the mixer power consumption and product temperature parameters as well as the mean granule size, percent lumps and yield for the different granulation experiments carried out. Upon entering the samples and variables, an output known as a loading plot was generated by the software. The loading plot provided a projection view of the existing inter-variable relationships (Esbensen, 2001).

3.2.6.1.2. Influences of Physicochemical Properties of Melt Granules on Compaction Behavior

Principal component analysis (The Unscrambler®, Camo Software AS., Norway) was also performed to compare the relative influences of the various physicochemical properties of melt granules on their compaction behavior. Likewise, the melt granulation experiments constituted the samples, whereas the list of variables included the mean size, span, percent fines, bulk and tapped densities, Hausner ratios, compressiblity indices, porosities, moisture and binder contents of melt granules as well as the mechanical strengths and porosities of resultant compacts produced under a compaction pressure of 102 MPa. Similarly, the results were analyzed based on the loading plot generated which provided a projection view of the inter-variable relationships amongst the parameters of interest.

4. RESULTS AND DISCUSSION

Part A. Dielectric Properties of Pharmaceutical Materials

The dielectric properties of pharmaceutical materials were assessed based on their dielectric constants and losses determined over a frequency range of 1 MHz–1 GHz using a dielectric analyzer as well as their microwave-induced heating capabilities, ΔT, in a laboratory microwave oven. The former technique required materials to be compacted whereas the latter method involved testing the materials in their bulk forms. For dielectric properties determined using the dielectric analyzer, the effects of field frequency on material dielectric constants and losses were first evaluated. Dielectric measurements were also performed on dried forms of the materials that contained high initial moisture contents, namely, starch, PVP C15, K25, K29/32, K90D, PVP-VA S630, cross-linked PVP XL and XL10.

At specific frequencies within the microwave frequency range of 300 MHz-1 GHz, the effect of material density was investigated by measuring the dielectric properties of material compacts prepared under different compaction pressures. The effect of moisture content was evaluated by examining the relationship between the moisture contents and microwave dielectric losses of the different materials in their true solid states, where confounding density influences could be eliminated.

The applicability and sensitivity of a single frequency density-independent function $\sqrt{\varepsilon''}/\left(\sqrt[3]{\varepsilon'}-1\right)$ to moisture variation of a model material, starch, was explored. Since the dielectric analyzer and laboratory microwave oven differed in their modes of dielectric assessment, test frequency ranges and physical properties of the test samples, the results derived from the two techniques were compared. Attempts were

made to discuss the relevance of the data obtained to pharmaceutical processes that involve microwave assistance. Specific examples of these applications would be detailed in parts B (microwave-assisted drying) and C (microwave-induced melt granulation) of the study.

A.1. Effect of Field Frequency on Material Dielectric Properties

The variations in dielectric constants and losses of all materials plotted as functions of frequency expressed on a logarithmic scale are shown in Figs. 5 and 6. Expectedly, linear relationships were observed between material dielectric constants and field frequency (Fig. 5). Apart from lactose, acetylsalicylic acid and paracetamol whose dielectric constants remained relatively constant at 2.6-2.7 across the whole frequency range, the dielectric constants of the remaining materials declined gradually as frequency increased. This indicated that the frequency range of 1 MHz-1 GHz fell within the region of dielectric dispersion of the test materials and the decrease in their dielectric constants stemmed from the decreasing polarizabilities of the molecules at increased field frequency.

As the differences in density between the untreated and corresponding dried forms of materials were marginal (~0.002-0.034 g/ml), direct comparisons were made between them. The decreases in dielectric constants of the untreated materials were visibly more pronounced when the spectra of both untreated and dried forms of the materials were plotted on the same scale. This indicated that the dielectric dispersions of the untreated materials were attributed partly to water molecules inherent in their structures.

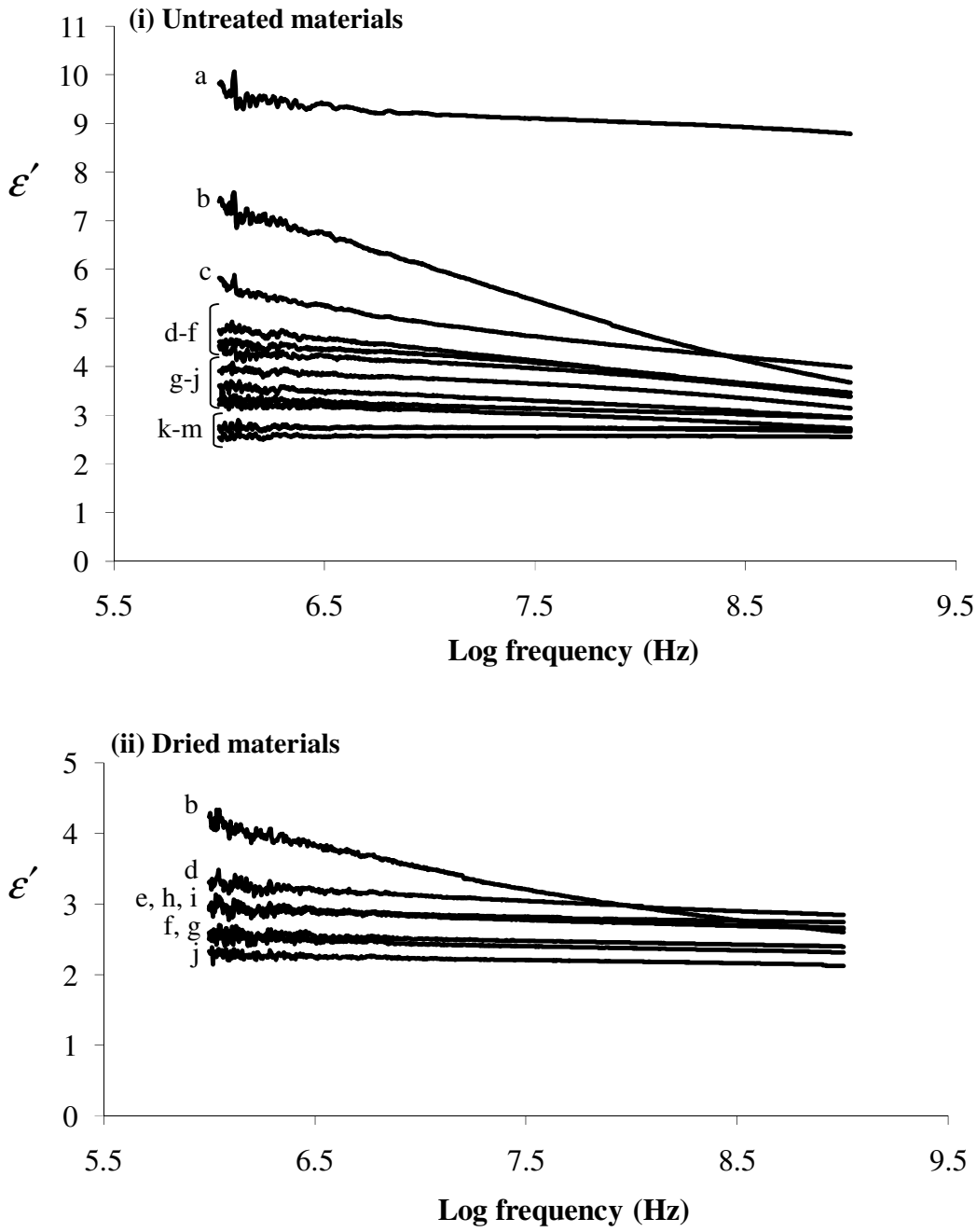

Fig. 5. Frequency dependence of the dielectric constants of a: anhydrous dicalcium phosphate, b: starch, c: sodium alginate, d: PVP C15, e: PVP K29/32, f: PVP K90D, g: cross-linked PVP XL10, h: PVP K25, i: PVP-VA S630, j: cross-linked PVP XL, k, l: lactose, acetylsalicylic acid and m: paracetamol.

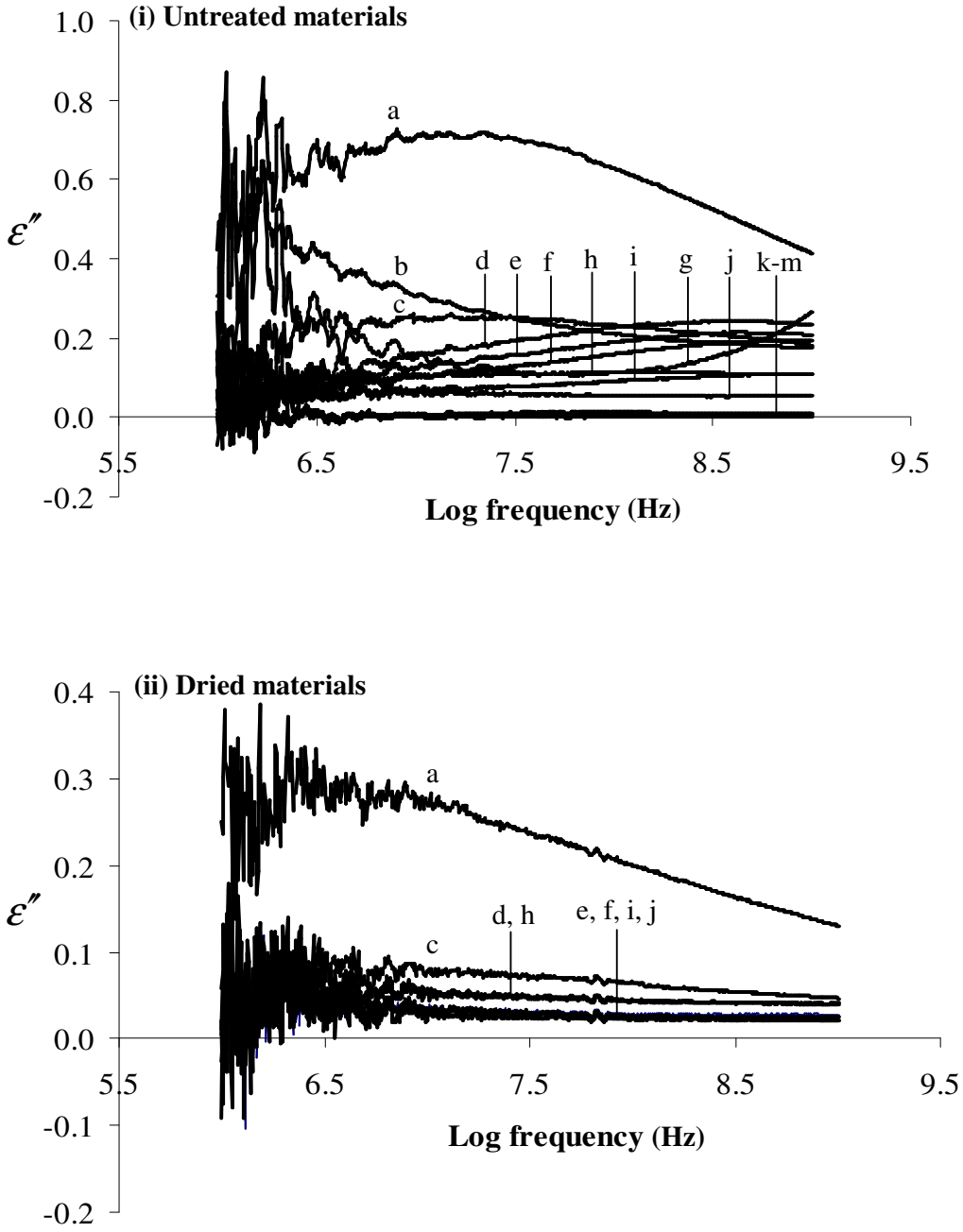

Fig. 6 Frequency dependence of the dielectric losses of a: starch, b: sodium alginate, c: PVP C15, d: PVP K29/32, e: PVP K90D, f: cross-linked PVP XL10, g: anhydrous dicalcium phosphate, h: PVP K25, i: cross-linked PVP XL, j: PVP-VA S630, k, l and m: lactose, acetylsalicylic acid and paracetamol.

At the frequency range studied, dielectric contributions originating from the bulky polysaccharide and polymer chains *per se* were outweighed by the effects of water molecules. Energy dissipation of the water molecules contributed to the peaks observable in the dielectric loss spectra of materials that contained higher moisture contents such as the PVP binders (K90D and K29/32), disintegrants (XL and XL10) and starch (Fig. 6i). On the other hand, materials containing negligible amounts of moisture like paracetamol, acetylsalicylic acid and lactose as well as those subjected to drying (Fig. 6ii) possessed unvarying and minimal losses at all frequencies.

By virtue of their increased dielectric losses, untreated materials were likely to heat better on exposure to electromagnetic waves as compared to their dried counterparts, with the most effective conversion of electromagnetic energy to heat occurring at frequency bands at which the materials exhibited their maximum dielectric losses. However, the electromagnetic frequencies available for industrial processing are displaced from these maxima. Although microwaves span a wide frequency range of 300 MHz to 300 GHz, 2.45 GHz has been designated for industrial uses to avoid potential interferences with frequencies employed for telecommunication, defense and maritime applications.

This study aimed to evaluate the dielectric responses of pharmaceutical materials under typical conditions of microwave processing. Since the maximum microwave frequency afforded by the equipment is 1 GHz, the closest compromise was reached by determining the dielectric properties of materials within the range of microwave frequencies available and correlating them to their heating responses under the influence of microwaves at 2.45 GHz in a laboratory microwave oven. Hence,

subsequent discussions on the effects of material density and moisture content would focus on the dielectric properties of materials at the lower and upper limits of the range of microwave frequencies (300 MHz-1 GHz) employed in this study.

A.2. Effect of Material Density on Dielectric Properties

To investigate the effects of material density, values were first extracted, at specific logarithmic frequencies (LF) of 8.5 and 9, from the dielectric spectra of the untreated materials compacted to different densities. These were then plotted against their respective material densities as shown in Figs. 7 and 8. The two figures corresponded respectively, to material dielectric properties at the lower (~300 MHz, LF 8.5) and upper limit (1 GHz, LF 9) of the microwave frequency range examined.

It could be observed that the dielectric constants and losses of the majority of the materials increased significantly with density at both microwave frequencies. The effects of density were less pronounced for lactose, acetylsalicylic acid and paracetamol whose dielectric constants and losses remained low at all density levels. Taking the dielectric constant and loss of air (density = 0 g/ml) to be 1 (Hedrick et al., 1998) and 0 (Schiffmann, 1995), respectively, linear relationships were observed between cube root functions of the dielectric parameters ($\sqrt[3]{\varepsilon'}$ and $\sqrt[3]{\varepsilon''}$) and density for all materials apart from PVP-VA S630 copolymer. For the latter, a linear relationship was observed directly between its dielectric parameters (ε' and ε'') and density.

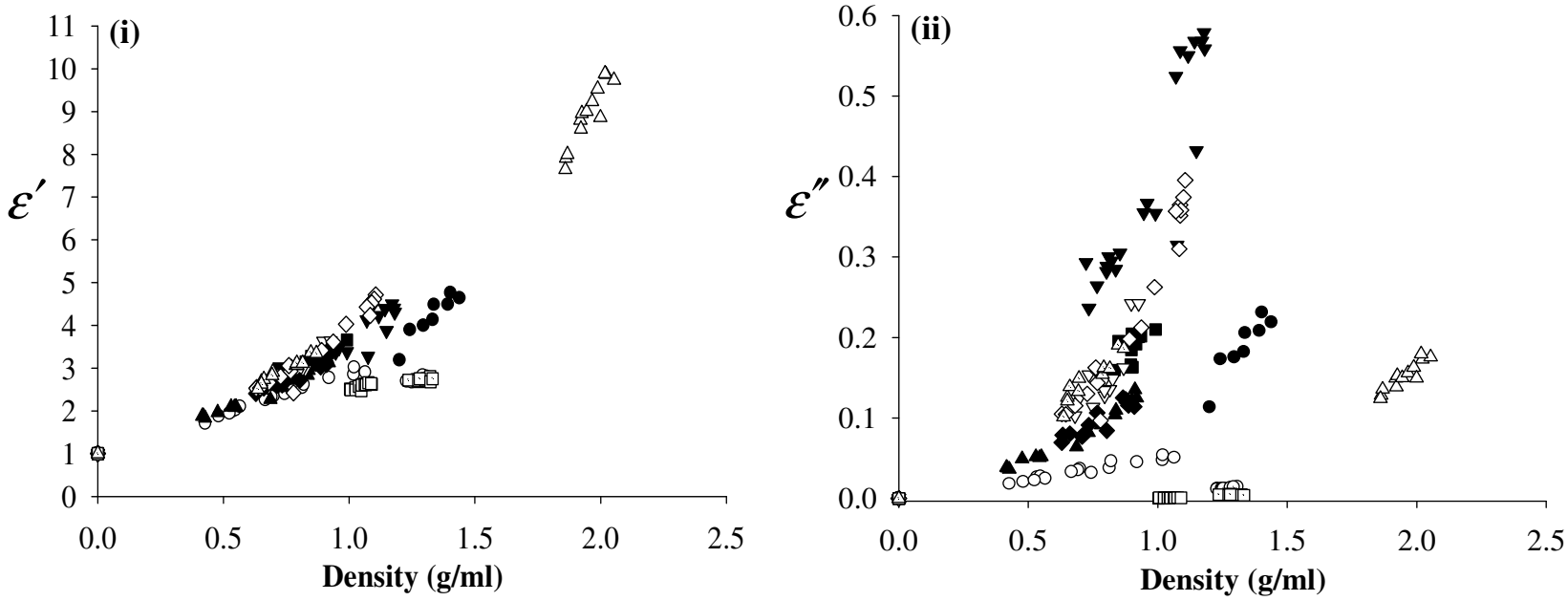

Fig. 7. Density dependence of the (i) dielectric constants and (ii) losses of (⊙) lactose, (Δ) anhydrous dicalcium phosphate, (▼) starch, (●) sodium alginate, (■) PVP C15, (♦) PVP K25, (▽) PVP K29/32, (◊) PVP K90D, (○) PVP-VA S630, (▲) cross-linked PVP XL, (◬) cross-linked PVP XL10, (□) paracetamol and (⊡) acetylsalicylic acid at LF 8.5 (~ 300 MHz).

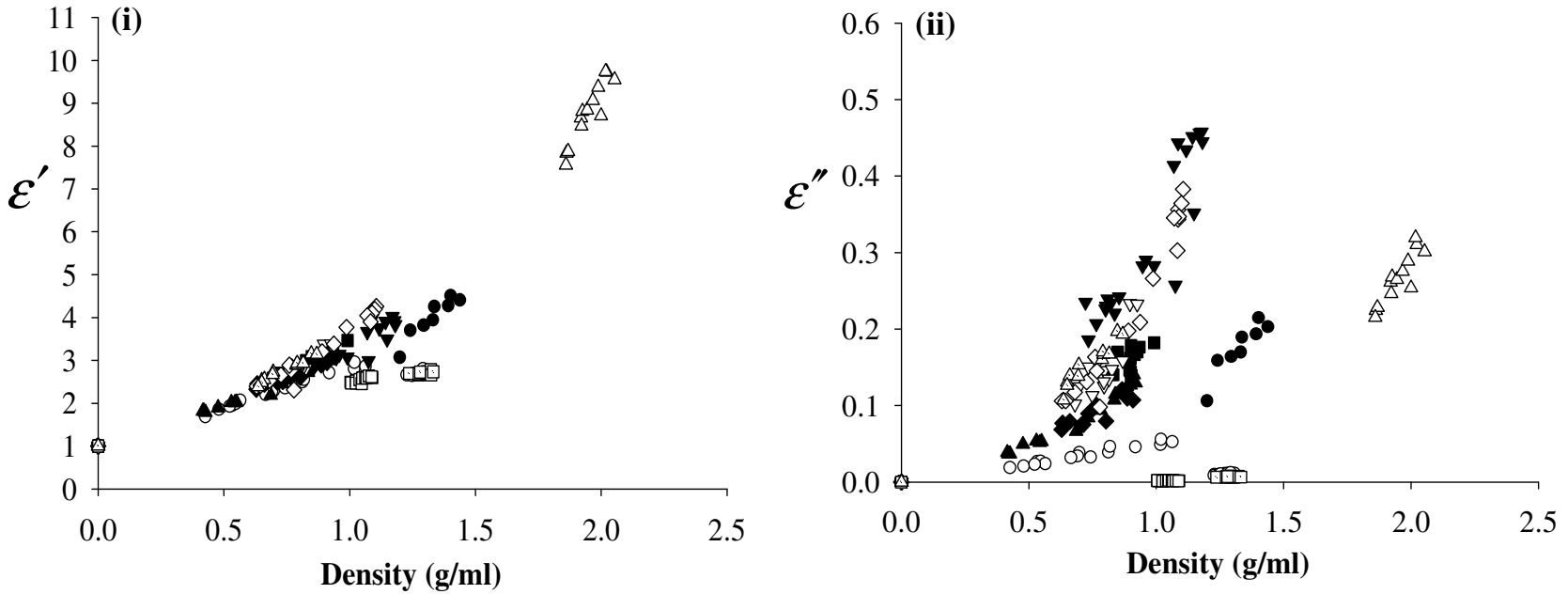

Fig. 8. Density dependence of the (i) dielectric constants and (ii) losses of (⊙) lactose, (Δ) anhydrous dicalcium phosphate, (▼) starch, (●) sodium alginate, (■) PVP C15, (♦) PVP K25, (▽) PVP K29/32, (◊) PVP K90D, (○) PVP-VA S630, (▲) cross-linked PVP XL, (◬) cross-linked PVP XL10, (□) paracetamol and (⊡) acetylsalicylic acid at LF 9 (1 GHz).

The cubic relationships observed between the dielectric properties of the majority of materials and their densities were consistent with the Landau and Lifshitz (Landau and Lifshitz, 1960), Looyenga (Looyenga, 1965) dielectric mixture equation (equation 3, section 1.3.5). As shown earlier, this equation describes the effective dielectric properties of solid mixtures as the addition of the cube roots of the dielectric properties of its constituents taken in proportion of their volume fractions. Attempts were also made in this study to fit the experimental data to the next commonly encountered complex refractive index mixture equation (Gladstone and Dale, 1863) (equation 4, section 1.3.5) which expresses the dielectric parameters of materials as quadratic functions of their densities. However, based on the goodness-of-fit (R^2) of the experimental data obtained, it appeared that the majority of the materials in this study conformed preferentially to the Landau and Lifshitz, Looyenga dielectric mixture equation. Unlike the complex refractive index mixture equation which was found to be inappropriate for selected materials due to poorer fitting, the Landau and Lifshitz, Looyenga equation was applicable to the entire range of materials studied. The linear relationships and R^2 values are summarized in Table 3.

A.2.1. Microwave-Induced Heating Capabilities of Materials in a Laboratory Microwave Oven

To determine the relevance of the measured dielectric properties of materials to their responses to microwaves at 2.45 GHz, the equations in Table 3 were used to compute the microwave dielectric losses of materials at densities equivalent to those in the heating experiments performed using the laboratory microwave oven. Results obtained from the heating experiments and dielectric measurements were compared.

Table 3. Equations governing the relationships between the microwave dielectric properties and densities of materials.

Material	Eqn (LF 8.5)	R^2	Eqn (LF 8.5)	R^2	Eqn (LF 9)	R^2	Eqn (LF 9)	R^2
Lactose	$\sqrt[3]{\varepsilon'} = 0.313\rho + 1$	0.999	$\sqrt[3]{\varepsilon''} = 0.180\rho$	0.993	$\sqrt[3]{\varepsilon'} = 0.308\rho + 1$	0.999	$\sqrt[3]{\varepsilon''} = 0.167\rho$	0.993
Anhydrous dicalcium phosphate	$\sqrt[3]{\varepsilon'} = 0.551\rho + 1$	0.991	$\sqrt[3]{\varepsilon''} = 0.273\rho$	0.997	$\sqrt[3]{\varepsilon'} = 0.545\rho + 1$	0.992	$\sqrt[3]{\varepsilon''} = 0.329\rho$	0.996
Starch	$\sqrt[3]{\varepsilon'} = 0.542\rho + 1$	0.947	$\sqrt[3]{\varepsilon''} = 0.745\rho$	0.876	$\sqrt[3]{\varepsilon'} = 0.489\rho + 1$	0.951	$\sqrt[3]{\varepsilon''} = 0.690\rho$	0.882
Sodium alginate	$\sqrt[3]{\varepsilon'} = 0.459\rho + 1$	0.974	$\sqrt[3]{\varepsilon''} = 0.428\rho$	0.993	$\sqrt[3]{\varepsilon'} = 0.439\rho + 1$	0.975	$\sqrt[3]{\varepsilon''} = 0.418\rho$	0.993
Polyvinylpyrrolidone								
C15	$\sqrt[3]{\varepsilon'} = 0.543\rho + 1$	0.992	$\sqrt[3]{\varepsilon''} = 0.631\rho$	0.982	$\sqrt[3]{\varepsilon'} = 0.513\rho + 1$	0.992	$\sqrt[3]{\varepsilon''} = 0.603\rho$	0.981
K25	$\sqrt[3]{\varepsilon'} = 0.524\rho + 1$	0.982	$\sqrt[3]{\varepsilon''} = 0.586\rho$	0.934	$\sqrt[3]{\varepsilon'} = 0.500\rho + 1$	0.981	$\sqrt[3]{\varepsilon''} = 0.579\rho$	0.927
K29/32	$\sqrt[3]{\varepsilon'} = 0.553\rho + 1$	0.980	$\sqrt[3]{\varepsilon''} = 0.664\rho$	0.972	$\sqrt[3]{\varepsilon'} = 0.520\rho + 1$	0.983	$\sqrt[3]{\varepsilon''} = 0.660\rho$	0.973
K90D	$\sqrt[3]{\varepsilon'} = 0.583\rho + 1$	0.967	$\sqrt[3]{\varepsilon''} = 0.663\rho$	0.969	$\sqrt[3]{\varepsilon'} = 0.542\rho + 1$	0.971	$\sqrt[3]{\varepsilon''} = 0.660\rho$	0.965
Polyvinylpyrrolidone-vinyl acetate copolymer S630	$\varepsilon' = 1.869\rho + 1$	0.989	$\varepsilon'' = 0.048\rho$	0.955	$\varepsilon' = 1.801\rho + 1$	0.990	$\varepsilon'' = 0.048\rho$	0.952
Cross-linked polyvinylpyrrolidone								
XL	$\sqrt[3]{\varepsilon'} = 0.511\rho + 1$	0.989	$\sqrt[3]{\varepsilon''} = 0.599\rho$	0.815	$\sqrt[3]{\varepsilon'} = 0.485\rho + 1$	0.990	$\sqrt[3]{\varepsilon''} = 0.605\rho$	0.828
XL10	$\sqrt[3]{\varepsilon'} = 0.583\rho + 1$	0.993	$\sqrt[3]{\varepsilon''} = 0.708\rho$	0.956	$\sqrt[3]{\varepsilon'} = 0.545\rho + 1$	0.994	$\sqrt[3]{\varepsilon''} = 0.717\rho$	0.958
Paracetamol	$\sqrt[3]{\varepsilon'} = 0.354\rho + 1$	0.996	$\sqrt[3]{\varepsilon''} = 0.079\rho$	0.620	$\sqrt[3]{\varepsilon'} = 0.350\rho + 1$	0.996	$\sqrt[3]{\varepsilon''} = 0.115\rho$	0.935
Acetylsalicylic acid	$\sqrt[3]{\varepsilon'} = 0.307\rho + 1$	0.995	$\sqrt[3]{\varepsilon''} = 0.128\rho$	0.981	$\sqrt[3]{\varepsilon'} = 0.304\rho + 1$	0.995	$\sqrt[3]{\varepsilon''} = 0.147\rho$	0.989

ε', ε'' and ρ refer to the dielectric constant, loss and density (g/ml) of the materials, respectively.

The microwave-induced heating capabilities of the materials in the laboratory microwave oven are presented in Fig. 9.

At their respective densities during testing, the microwave-induced heating capabilities of the materials differed significantly with starch and PVP K90D exhibiting the highest heating responses of 48 and 34 ºC respectively. These were followed by sodium alginate, cross-linked PVP XL10, PVP K29/32 and cross-linked PVP XL with relatively high ΔT values in the range of 17.8-26.9 ºC. The microwave-induced heating capabilities of PVP C15, anhydrous dicalcium phosphate, PVP K25 and PVP-VA S630 were in the lower range of 10.5-14.9 ºC. Lactose, paracetamol and acetylsalicylic acid heated at the slowest rates, with mere temperature increments of 4.1-7.7 ºC.

The high dielectric susceptibility of starch as reflected by its ΔT value and dielectric profile as shown earlier suggested an increased likelihood of microwave-starch interaction. Indeed, physicochemical modifications to starch following microwave irradiation, as exemplified by changes in their solubilities, crystalline structures, swelling characteristics and morphologies, have been documented quite extensively (Lewandowicz et al., 1997; Lewandowicz et al., 2000; Szepes et al., 2005; Szepes and Szabó-Révész, 2007).

Practically, materials should possess dielectric losses > 0.01 for effective heating under the influence of microwaves (Metaxas and Meredith, 1983; Orfeuil, 1987). It was apparent from Figs. 7(ii) and 8(ii) that lactose, paracetamol and acetylsalicylic acid barely fulfilled this criteria at all density levels and this could possibly account

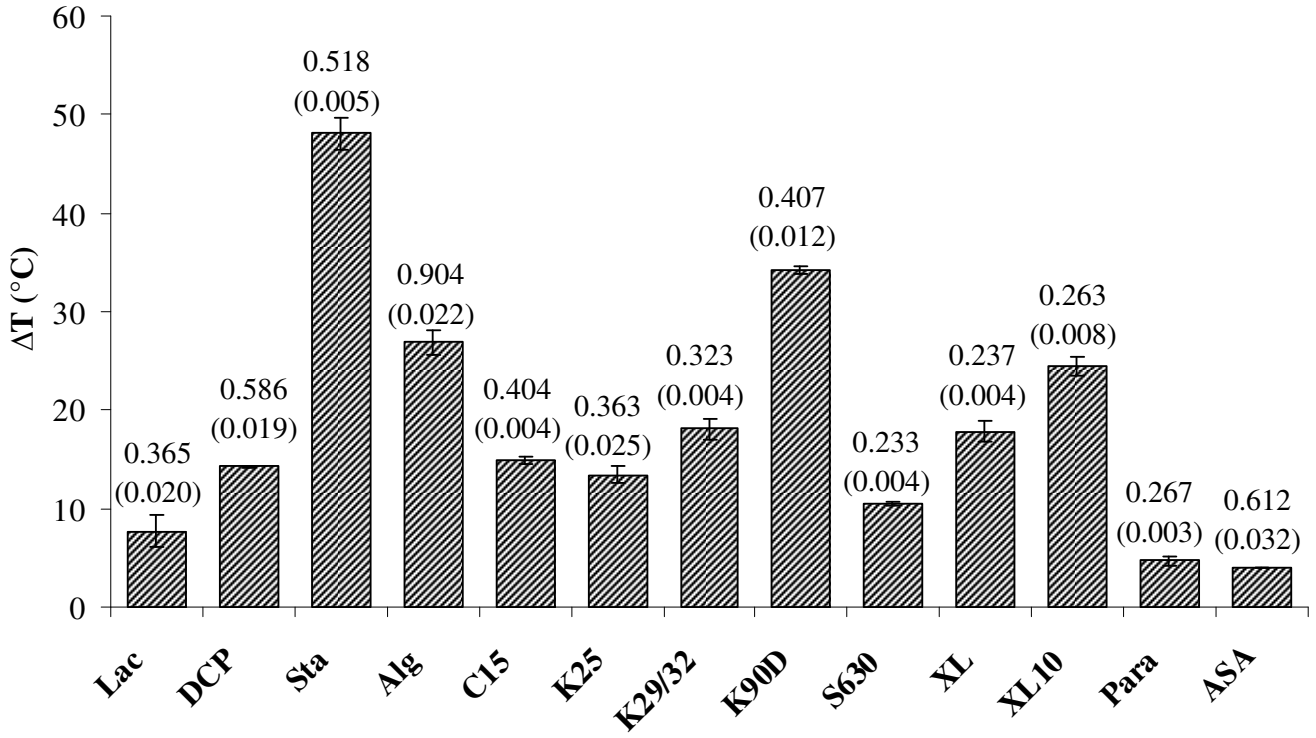

Fig. 9. Microwave-induced heating capabilities (ΔT) of materials at their respective densities during testing (standard deviations are parenthesized). Lac: lactose, DCP: anhydrous dicalcium phosphate, Sta: starch, Alg: sodium alginate, C15: PVP C15, K25: PVP K25, K29/32: PVP K29/32, K90D: PVP K90D, S630: PVP-VA S630, XL: cross-linked PVP XL, XL10: cross-linked PVP XL10, Para: paracetamol and ASA: acetylsalicylic acid.

for their low microwave-induced heating capabilities relative to the remaining materials. These results echoed earlier observations of several authors. The dielectrically inert character of lactose had been reported by Kudra et al. (1992) as well as McLoughlin et al. (2003a) and was believed to contribute to its physical stability during microwave-assisted processing. This was verified in a recent study by Szepes et al. (2007) in which 20 min of continuous microwave irradiation of α-lactose monohydrate was found not to cause any significant alterations to its crystallinity, thermal properties and particle size. The low dielectric susceptibilities of acetylsalicylic acid and paracetamol had also been documented by McLoughlin et al. (2003a). Based on a similar argument, these active ingredients may potentially be safeguarded against possible microwave-induced transformations during processing.

The microwave-induced heating capabilities and calculated microwave dielectric losses of the materials correlated significantly with each other (Pearson correlation coefficient, $R = 0.782$ and 0.761 at LF 8.5 and 9, respectively, $p < 0.01$), implying a reasonable association between the two modes of dielectric assessment. It could be inferred from these results that the capacitance-based measurement of dielectric properties in which compacted forms of materials were exposed to rapidly alternating electric fields within the confines of 2 charged parallel electrodes may be likened to the microwave processing of material particulates in a cavity or enclosure. The latter functioned similarly as a pair of electrodes by providing boundaries for the electric field in which materials were interrogated or processed. Under circumstances where the high costs of instrumentation preclude the use of high frequency dielectric measurements, the laboratory microwave oven provides a reliable alternative for assessing the susceptibilities of materials to microwave energy.

A.3. Relationship between Moisture Contents and Dielectric Properties of Materials

The influence of moisture content was analyzed with respect to the microwave dielectric losses of the test materials as this relationship provides the fundamental basis of microwave-assisted drying. As the dielectric losses measured in this study were affected by simultaneous variations in the densities and moisture contents of materials, the effect of moisture content was investigated by examining the relationship between the moisture contents and microwave dielectric losses of the different materials in their true solid states, where the effects of intra- and inter-particulate air inclusions on dielectric properties could be eliminated.

The relationship between the moisture contents and microwave dielectric losses of the different materials extrapolated to their respective true densities is shown in Fig. 10. In spite of the diverse compositions, structures and moisture-binding affinities of the materials, the effect of moisture content on their microwave dielectric properties were apparent in that materials with higher moisture contents generally exhibited higher dielectric losses at both microwave frequencies. Materials with inherently low moisture contents such as lactose, paracetamol and acetylsalicylic acid possessed minimal dielectric losses close to 0. The subsequent increase in microwave dielectric losses assumed by the different materials with increasingly higher moisture contents followed a somewhat sigmoidal profile (indicated by dotted lines) similar to that shown earlier in Fig. 2 (section 1.3.3). Two distinct outliers, namely, anhydrous dicalcium phosphate and starch could be observed at the outset. They possessed unexpectedly higher dielectric losses than predicted based on their moisture contents.

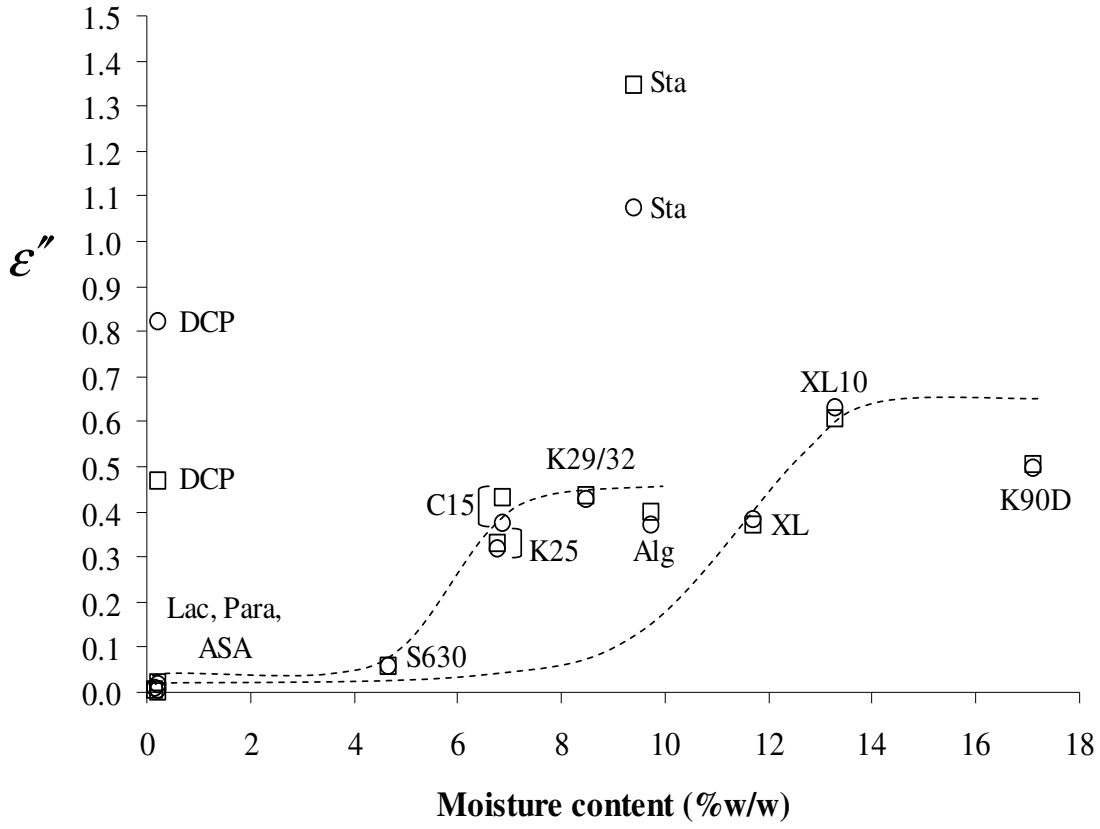

Fig. 10. Relationship between the moisture contents and dielectric losses of the materials at their respective true densities at LF (□) 8.5 and (○) 9. Lac: lactose, DCP: anhydrous dicalcium phosphate, Sta: starch, Alg: sodium alginate, C15: PVP C15, K25: PVP K25, K29/32: PVP K29/32, K90D: PVP K90D, S630: PVP-VA S630, XL: cross-linked PVP XL, XL10: cross-linked PVP XL10, Para: paracetamol and ASA: acetylsalicylic acid.

As discussed in section 1.3.3, the critical moisture content (M_c) of a material is the moisture content which saturates the available binding sites of the material. Further additions of water beyond the M_c value results in the occurrence of water molecules which are free and unbound in nature. Bound and unbound water molecules exhibit vastly different dielectric properties. As M_c represents the transition point between the bound and unbound states of water in a material, it may be deduced from the inflexion point of the dielectric loss versus moisture content profile of the respective material as depicted in Fig. 2. Based on this approach, two groups of materials with different M_c values could be distinguished from Fig. 10. The M_c values of PVP-VA S630, PVP K25, C15, K29/32 and sodium alginate were similar and approximated at 4-5 %w/w. For materials with higher moisture contents such as the cross-linked PVP(s) XL, XL10 and PVP K90D, their M_c values were higher and ranged from 9-10 %w/w.

At this point, it may seem invalid to categorize and analyze materials of differing identities collectively. However, further experimental evidence provided the necessary justification for this approach. It had been previously shown in Fig. 6(ii) that as field frequency increased to the microwave range (LF 8.5-9), the dielectric losses of the dried materials, namely, PVP-VA S630 (j), PVP K25 (h), C15 (c), K29/32 (d), K90D (e), cross-linked PVP(s) XL (i) and XL10 (f) approached each other and assumed values of ≤ 0.05. This meant that at negligible moisture levels, the microwave dielectric losses of these materials were similar to each other and that of lactose, acetylsalicylic acid and paracetamol. Hence, their dielectric loss versus moisture content profiles as depicted in Fig. 10 were likely to share similar points of origin.

Further support to the argument is provided by Fig. 11. It shows the relationship between the moisture contents and microwave-induced heating capabilities of the different materials at their respective densities during testing. In spite of the differences in physical properties of the materials, frequency and mode of dielectric assessment, the relationship that emerged resembled that of Fig. 10. In general, materials with higher moisture contents exhibited improved microwave-induced heating capabilities. Anhydrous dicalcium phosphate and starch showed slight deviations from the trend and exhibited moderately higher heating capabilities than predicted based on their moisture contents. Accordingly, materials apart from anhydrous dicalcium phosphate and starch may likewise be classified into two groups with different M_c values. The M_c values of PVP-VA S630, PVP K25, C15, K29/32 and sodium alginate fell within the range of 3-4 %w/w. The corresponding values for cross-linked PVP XL, XL10 and PVP K90D were in a higher range of 7-8 %w/w.

A.3.1. Critical Moisture Contents of Materials as Determined using Thermo-Gravimetric Analysis

As the assignment of M_c values to the different materials remained largely subjective at this juncture, the M_c of each material was verified by thermo-gravimetric analyses. Using this method, M_c was defined as the moisture content of the material that marked the end of the constant rate phase and start of the decreasing rate phase of drying (Van Scoik et al., 1991; Heng et al., 2004). The drying profiles (moisture content versus drying time) of the materials were first plotted following which the rate of moisture loss with time was derived by differentiation. For each material, the

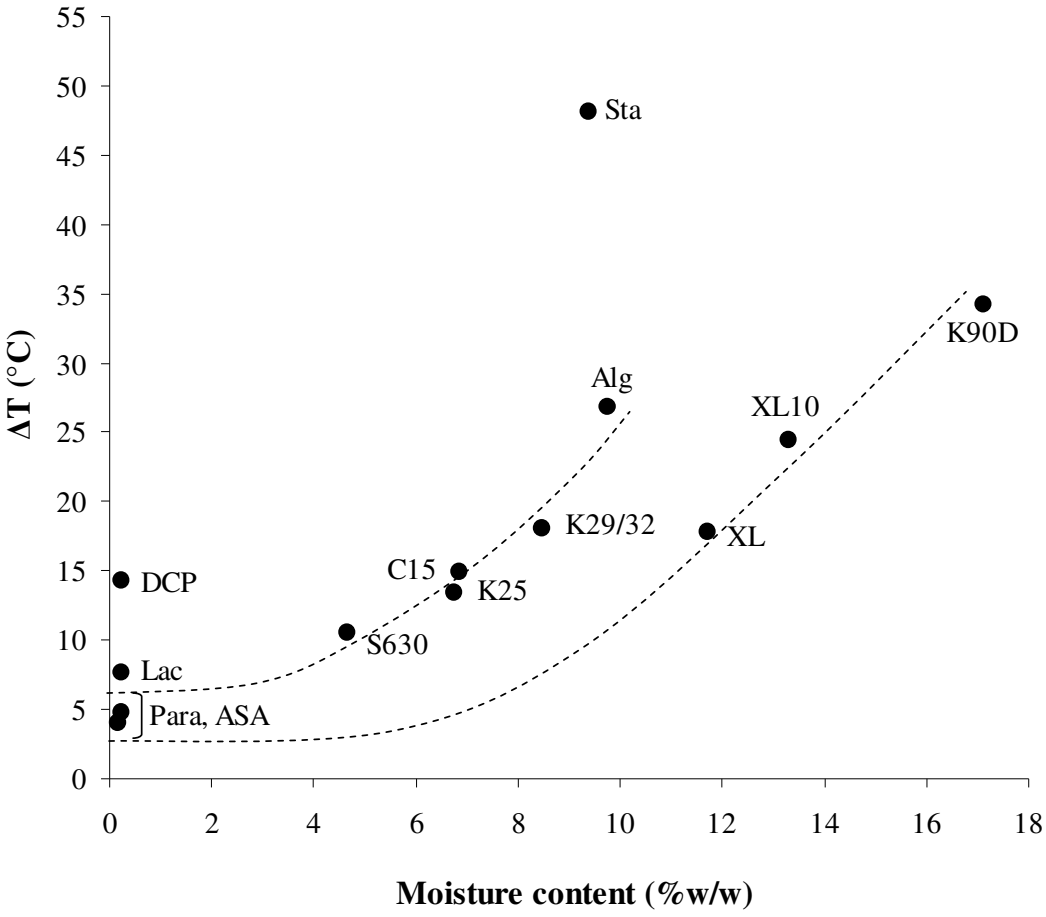

Fig. 11. Relationship between the moisture contents and microwave-induced heating capabilities (ΔT) of the materials at their respective densities during testing. Lac: lactose, DCP: anhydrous dicalcium phosphate, Sta: starch, Alg: sodium alginate, C15: PVP C15, K25: PVP K25, K29/32: PVP K29/32, K90D: PVP K90D, S630: PVP-VA S630, XL: cross-linked PVP XL, XL10: cross-linked PVP XL10, Para: paracetamol and ASA: acetylsalicylic acid.

drying time at which the rate of moisture loss began to decrease was determined. The moisture content of the material at this particular drying time point was then determined from its respective drying profile and defined as its M_c.

The specific M_c values of the materials are summarized in Fig. 12. As expected, two distinct groups of materials could be identified, classified based on their different ranges of M_c. PVP-VA S630, PVP K25, C15, K29/32 and sodium alginate possessed lower M_c values ranging from 2.1-3.5 %w/w. The M_c values of cross-linked PVP XL, XL10 and PVP K90D were in a higher range of 5.3-6.7 %w/w. Generally, the trends observed from the dielectric measurements, heating experiments and thermo-gravimetric analyses corroborated with each other apart from some minor discrepancies. It appeared that the M_c values estimated from the dielectric measurements (Fig. 10) were slightly higher than those derived from the heating experiments (Fig. 11) and thermo-gravimetric analyses (Fig. 12). These disparities stemmed from the differences in physical properties of the material samples. Since water molecules partake in inter-particulate bonding during compaction, compacted forms of materials such as those used in the dielectric measurements would be expected to contain higher levels of bound moisture and exhibit higher M_c values as compared to their corresponding bulk forms employed in both the heating experiments and thermo-gravimetric analyses. Due to similarities in physical properties of the material samples, the M_c estimates from the heating experiments were closer to those determined from thermo-gravimetric analyses.

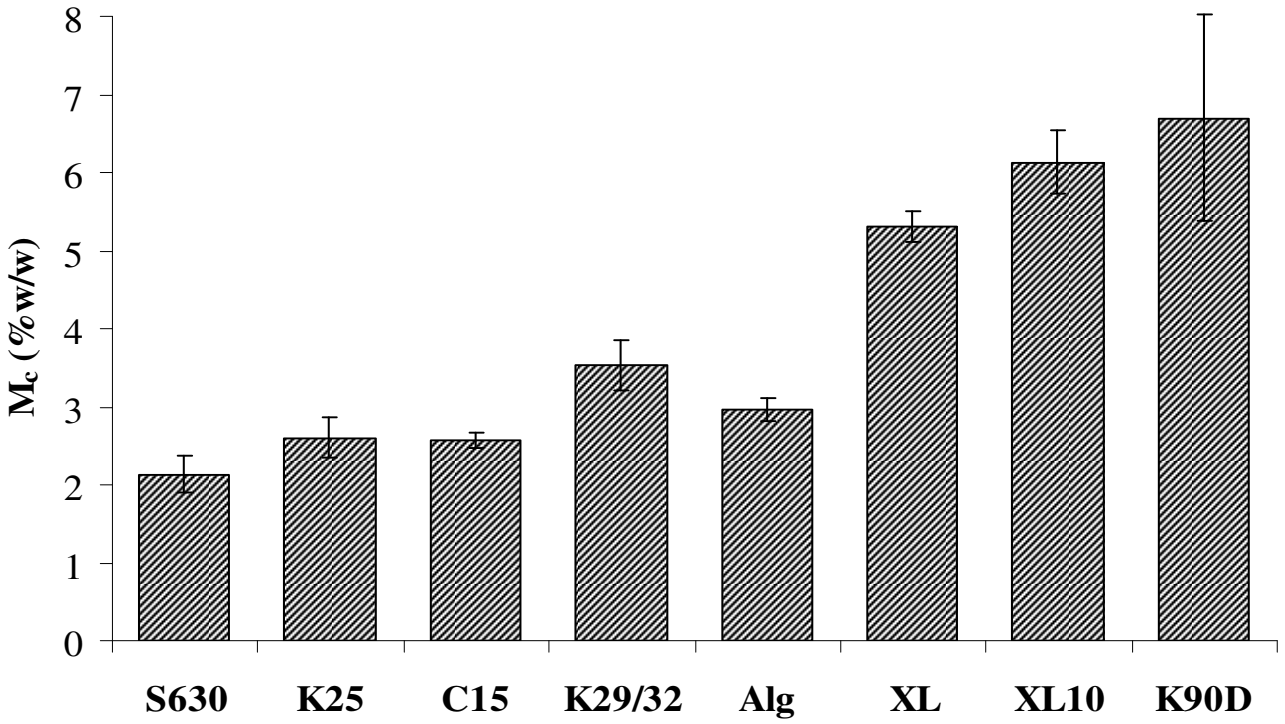

Fig. 12. Critical moisture contents (M_c) of selected materials as determined by thermo-gravimetric analysis. S630: PVP-VA S630, K25: PVP K25, C15: PVP C15, K29/32: PVP K29/32, Alg: sodium alginate, XL: cross-linked PVP XL, XL10: cross-linked PVP XL10 and K90D: PVP K90D.

The disparities in bound moisture concentrations in different physical forms of an identical material may have affected the sensitivity of the dielectric responses to moisture content. In the dielectric studies where moisture in the materials became bound to a greater extent due to compaction, a lower proportion of free moisture was available to interact with the applied microwave fields. This led to a rapid tapering of material dielectric responses at higher moisture contents as seen in Fig. 10. On the other hand, for the corresponding materials tested in their bulk forms in the heating experiments, a comparatively lower concentration of bound moisture translated to increased availability of free moisture which interacted far more readily with microwaves, leading to an almost proportionate increase in dielectric response with moisture content upon saturation (Fig. 11).

From the results obtained thus far, it appeared that between material density and moisture content, the latter contributed more significantly to the variation exhibited in the microwave dielectric losses of lactose, sodium alginate, paracetamol, acetylsalicylic acid, the PVP binders and disintegrants. Specifically, it was the way moisture apportioned into bound and unbound forms in these materials that was responsible for such differences. In their dry states, these materials were likely to possess similar dielectric responses at microwave frequencies.

On the other hand, it may be inferred that regardless of density or moisture content, the innate molecular properties of anhydrous dicalcium phosphate and starch were conducive for interacting with and absorbing microwave energy. Literature abounds with examples of microwave-starch interactions. Less information however, is available as yet on the microwave susceptibility of anhydrous dicalcium phosphate.

Anhydrous dicalcium phosphate comprises permanent dipoles bound in a crystalline lattice. From the results, it appeared that a large part of its dielectric susceptibility arose from its polarizable nature as exemplified by its high dielectric constant (Fig. 5i). As molecular orientations were unlikely due to its structural rigidity, the higher loss of anhydrous dicalcium phosphate stemmed from the electronic and ionic polarization of dipoles. Electronic polarization occurred when electron clouds surrounding the nucleus were displaced with respect to the positive center under the influence of the applied field. Alternatively, the positive and negative ions might have been displaced from their equilibrium positions by the applied field (ionic polarization) which resulted in changes to their effective dipole moments. These mechanisms are known to dominate the dielectric permittivity of solids within the frequency range of 1 MHz-1 GHz (Frederikse, 2008).

A.4. Use of Density-Independent Function for Moisture-Sensing Applications

As a preliminary step necessary in guiding further use of density-independent functions for moisture-sensing using microwave techniques, the effectiveness and applicability of a single frequency density-independent function $\sqrt{\varepsilon''}/\left(\sqrt[3]{\varepsilon'}-1\right)$ as described by Powell et al. (1988) was evaluated for all materials tested in this study. Compared to another commonly used single frequency expression $\varepsilon''/(\varepsilon'-1)$ defined by Meyer and Schilz (1980), this equation was selected on the basis that it provided better results in terms of density independence when applied to all materials tested.

For all materials, the magnitudes of $\sqrt{\varepsilon''}/\left(\sqrt[3]{\varepsilon'}-1\right)$ were computed at both microwave frequencies and plotted against density (Fig. 13). In contrast to Figs. 7 and 8, it could

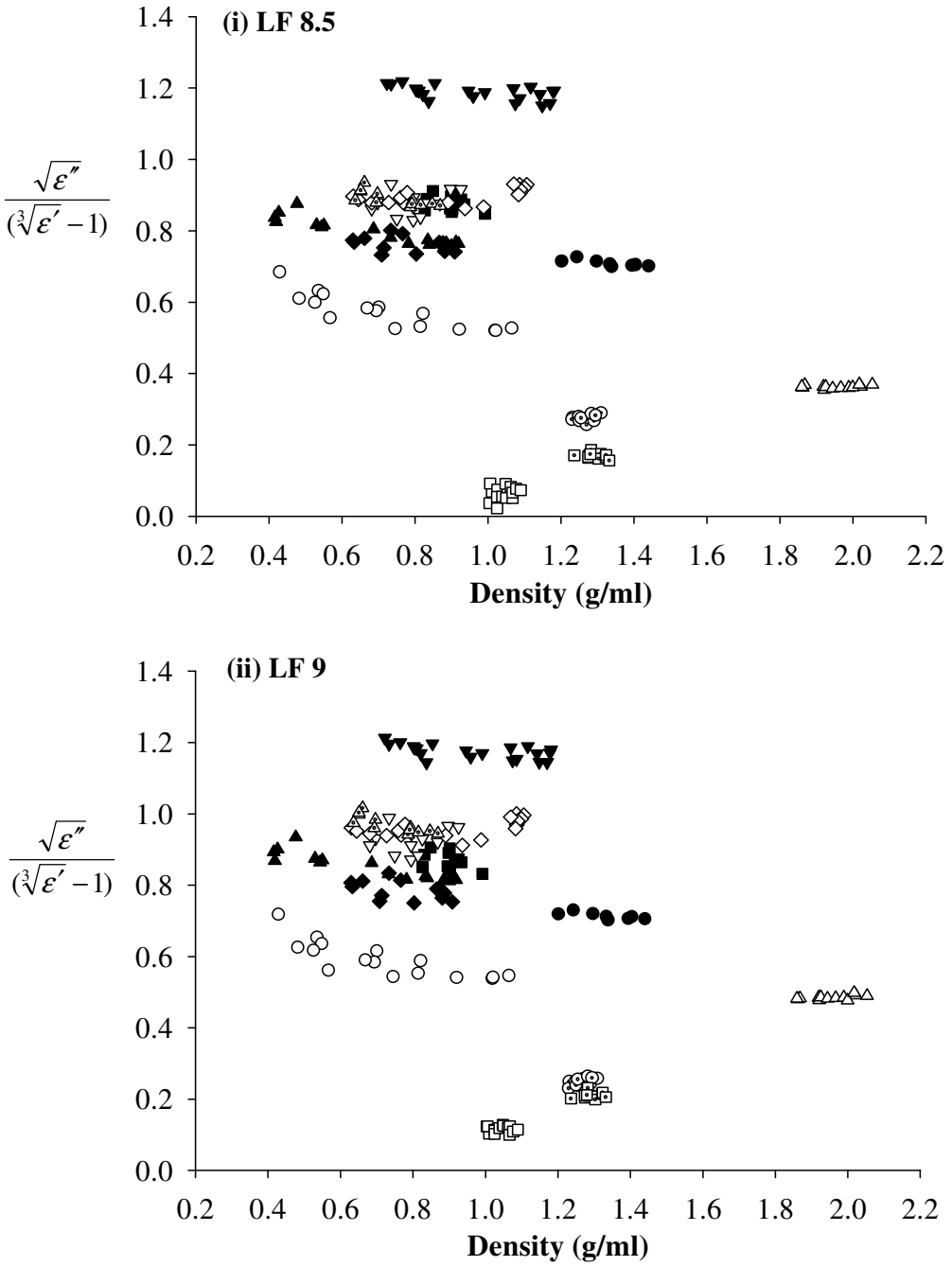

Fig. 13. Density-independent character of the function $\sqrt{\varepsilon''}/(\sqrt[3]{\varepsilon'}-1)$ as applied to (⊙) lactose, (Δ) anhydrous dicalcium phosphate, (▼) starch, (●) sodium alginate, (■) PVP C15, (♦) PVP K25, (▽) PVP K29/32, (◊) PVP K90D, (○) PVP-VA S630, (▲) cross-linked PVP XL, (◬) cross-linked PVP XL10, (□) paracetamol and (⊡) acetylsalicylic acid at both LF (i) 8.5 and (ii) 9.

be observed that the plotted points were mostly parallel to the density axis at both microwave frequencies, indicating that the chosen function possessed density-independent character. Slightly better results were obtained for materials such as starch, anhydrous dicalcium phosphate, sodium alginate and PVP K90D.

Being a widely popular excipient capable of performing multi-functional roles in pharmaceutical dosage forms, starch was selected to test the sensitivity of $\sqrt{\varepsilon''}/\left(\sqrt[3]{\varepsilon'}-1\right)$ to moisture variation. The drying curve, obtained by drying starch in a convection oven at 90 °C, is shown in Fig. 14. The initial moisture content of starch was calculated based on the weight loss of the completely dried and cooled starch samples as described earlier in section 3.2.2.2.

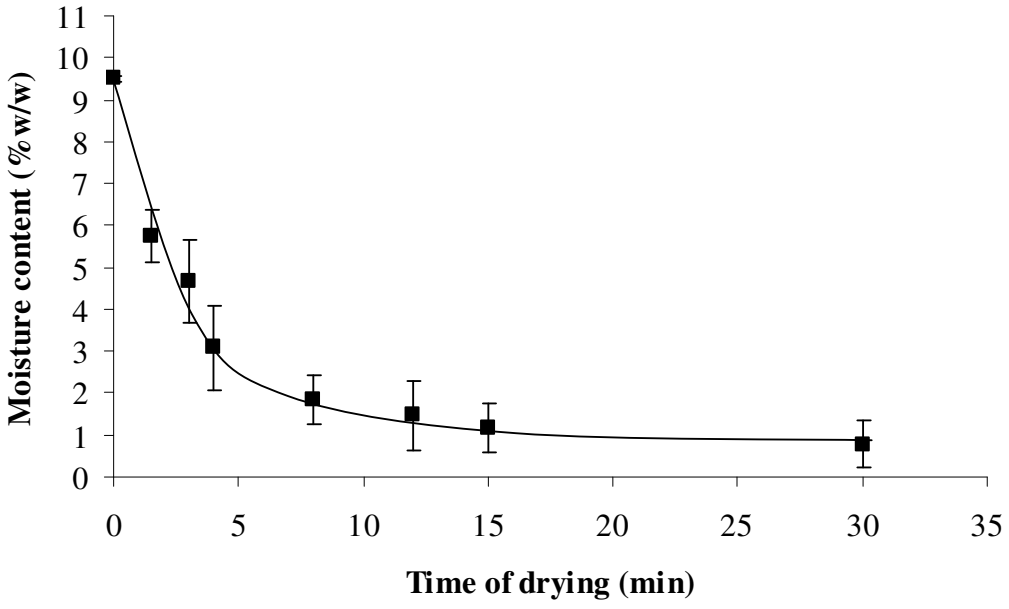

Fig. 14. Drying curve obtained by drying starch at 90 °C in a convection oven.

From Fig. 14, the M_c of starch was defined as the moisture content at which the rate of moisture loss from starch began to decrease. The initial moisture content and M_c of starch were found to be 9.51 %w/w and approximately 3 %w/w, respectively. These were consistent with the data obtained from thermo-gravimetric analysis (moisture content of starch = 9.40 %w/w, Table 1; M_c = 3.1 %w/w).

Physical characterization of the compacts prepared from starch sampled at the various drying time points revealed that their average densities spanned 0.9-1.2 g/ml. These values were within the density range where density independence of $\sqrt{\varepsilon''}/\left(\sqrt[3]{\varepsilon'}-1\right)$ was achieved for starch (Fig. 13). For each starch sample obtained at a specific drying time point, the average value of $\sqrt{\varepsilon''}/\left(\sqrt[3]{\varepsilon'}-1\right)$ was calculated and plotted with respect to moisture content at both microwave frequencies. This is shown in Fig. 15.

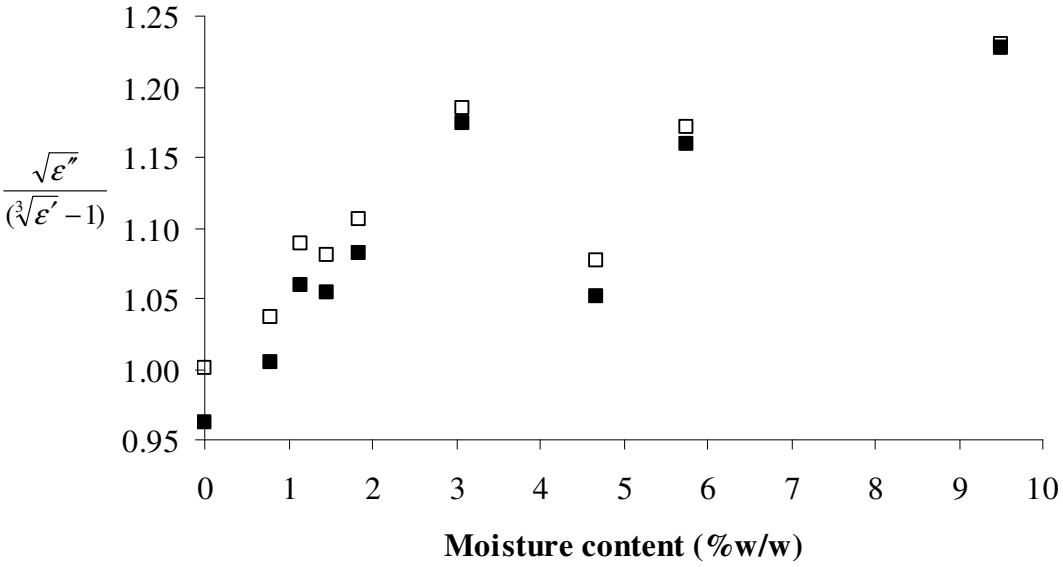

Fig. 15. Sensitivity of the density-independent function $\sqrt{\varepsilon''}/(\sqrt[3]{\varepsilon'}-1)$ to moisture variation of starch at LF (□) 8.5 and (■) 9.

At the outset, the relationship between $\sqrt{\varepsilon''}/\left(\sqrt[3]{\varepsilon'}-1\right)$ and moisture content seemed non-linear. On closer examination however, it appeared that the association between these variables differed depending on the moisture content of starch. Below the M_c of starch (3.1 %w/w), a strong linear relationship could be observed between $\sqrt{\varepsilon''}/\left(\sqrt[3]{\varepsilon'}-1\right)$ and moisture content with R^2 values of 0.973 and 0.978 at LF 8.5 and 9, respectively. When the moisture content of starch exceeded its M_c, a different relationship predominated which could not be accurately defined at this point of study. From these investigations, it appeared that the relevance of the selected density-independent function for moisture-sensing was confined within certain limits of material moisture content as dictated by the state of binding and resultant mobility of the associated water molecules.

Part B. Effect of Formulation Variables on Microwave-Assisted Drying and Drug Stability

Studies on microwave-assisted drying as seen in the literature to date have focused primarily on the technical aspects of the process. This part of the study examined microwave-assisted drying from a formulation or product-oriented perspective. Following the determination of dielectric properties in part A, a typical tablet formulation comprising lactose as the diluent, acetylsalicylic acid as the model drug, PVP-VA S630 and cross-linked PVP XL10 as the binder and disintegrant, respectively, was granulated and dried *in situ* using microwaves in a 25 L single pot high shear processor. Since the formulation constituents, particularly lactose, are dielectrically inert in their dry states, the efficiency of microwave-assisted drying was dependent on the microwave-induced heating capabilities of the water molecules entrapped in the granules and their subsequent movement through the granular structure. Investigation of microwave-assisted drying was thus based on the moisture contents and structural properties of granules.

The powder load, size of lactose particles and amount of granulating liquid employed for granulation were varied to prepare wet granules of different physical sizes, moisture contents and porosities (Table 2). Microwave-assisted drying was evaluated from a macroscopic and microscopic viewpoint. At the macroscopic level, the overall drying profiles of the different granule loads were first identified, following which their drying rates were derived for comparisons amongst granules of different physical sizes, moisture contents and porosities at the microscopic level. The effect of microwave-assisted drying on the stability of acetylsalicylic acid was also evaluated.

B.1. Influence of Powder Load on Microwave-Assisted Drying of Granules

The drying profiles of lactose 200M and 450M granules prepared using different powder loads and amounts of granulating liquid are shown in Figs. 16 and 17. Regardless of the size of lactose particles and amount of granulating liquid, the drying rate varied with time for granules prepared from smaller powder loads of 2.5 and 4 kg, increasing in the initial phases to a maximum, then falling towards the end of the drying process. Non-linear regression analysis revealed an excellent fit ($R^2 \geq 0.997$) of the experimental curves to a 3-parameter sigmoidal function, $y = a/\{1+ e^{-[(x-xo)/b]}\}$. As powder load increased to 6.5 and 7.5 kg, moisture removal tended towards a constant rate as reflected by the increasing linearity of the drying profiles. R^2 values ranging from 0.991–1.000 were obtained from linear regression analyses.

The volumes of granules, together with various parameters characterizing their drying performances, are shown in Table 4. The maximum drying rate, R_m (g/min), and rate constant, k (g/min), were derived from the drying profiles of granules prepared from the smaller (2.5 and 4 kg) and larger powder loads (6.5 and 7.5 kg), respectively. $T_{50\%}$ (min) referred to the time required for the removal of 50 % of the initial moisture content of granules.

$T_{50\%}$ was found to correlate significantly ($p < 0.01$) with the volume of granules, indicating that the drying profiles of granules were related to the changing dimensions of the granulation bed as powder load was varied. This could be explained based on the concepts of penetration depth. As mentioned in the introduction (section 1.3.6), microwaves are attenuated as it traverses an absorbing material load. As the load of wet granules increased, the effects of microwave penetration depth on drying became

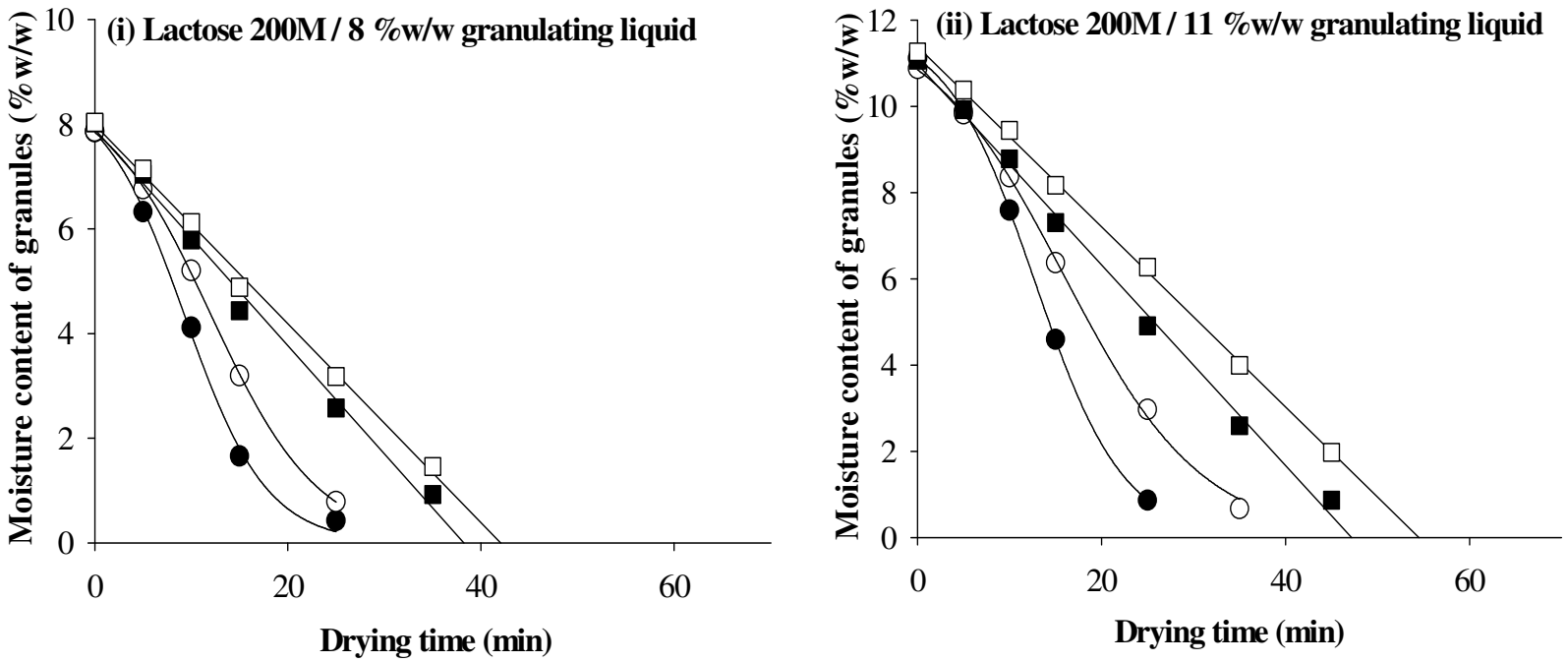

Fig. 16. Drying profiles of lactose 200M granules prepared using (i) 8 %w/w and (ii) 11 %w/w granulating liquid from powder loads of (●) 2.5 kg, (○) 4 kg, (■) 6.5 kg and (□) 7.5 kg. Symbols: experimental data, —: regression line/curve (Goodness of fit: $0.991 > R^2 > 1.000$).

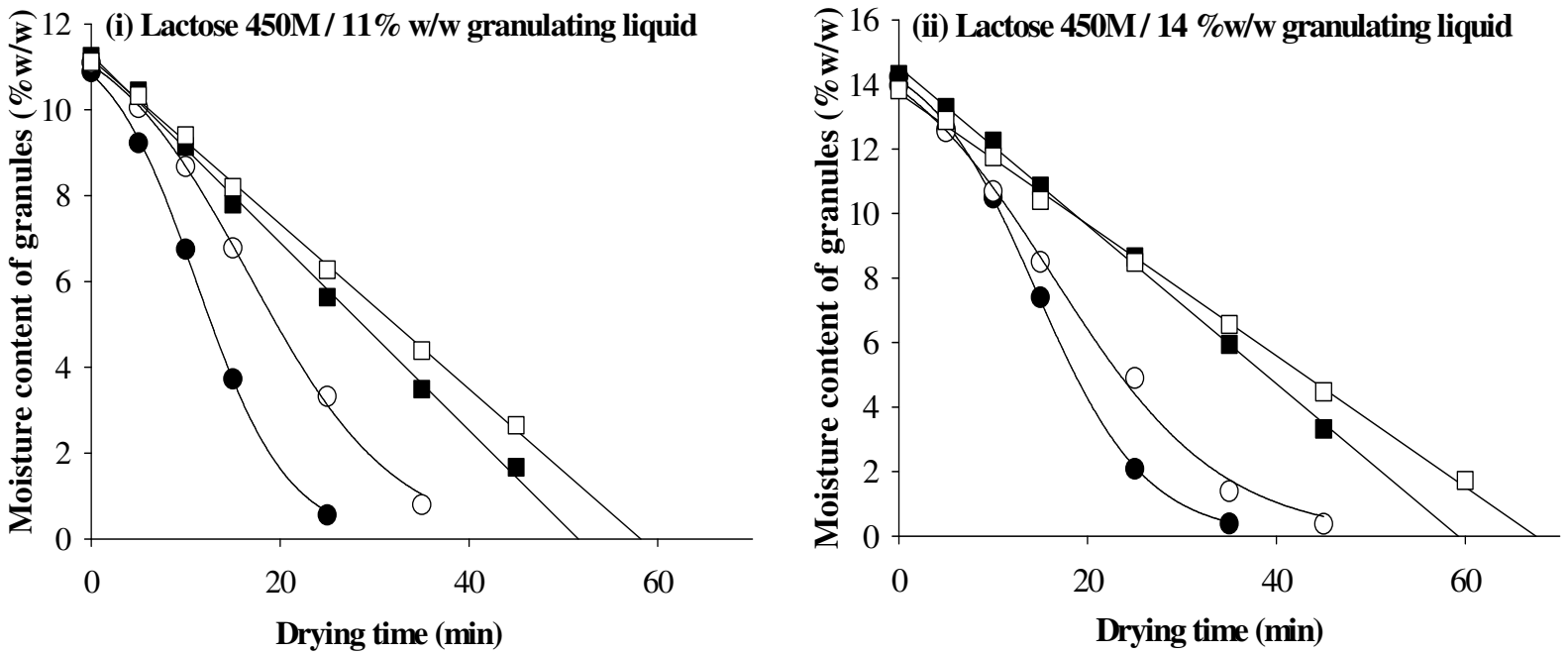

Fig. 17. Drying profiles of lactose 450M granules prepared using (i) 11 %w/w and (ii) 14 %w/w granulating liquid from powder loads of (●) 2.5 kg, (○) 4 kg, (■) 6.5 kg and (□) 7.5 kg. Symbols: experimental data, —: regression line/curve (Goodness of fit: $0.991 > R^2 > 1.000$).

Table 4. Various parameters characterizing the drying performance of all granules dried with and without microwave assistance as well as the volume of granules in the mixer bowl during drying.

Lactose / Amount of granulating liquid	**Powder load (kg)**	**Volume of granules (ml)**	**$T_{50\%}$ (min)**	**R_m (g/min)**	**k (g/min)**
200M / 8 %w/w	2.5	3799.4	10.15	12.92	-
	4	6092.9	13.15	15.68	-
	6.5	9622.5	19.12	-	13.42
	7.5	11223.3	21.02	-	14.25
200M / 11 %w/w	2.5	3203.5	13.37	15.48	-
	4	5558.6	17.54	16.17	-
	6.5	9201.6	23.62	-	15.12
	7.5	11081.0	27.25	-	15.67
450M / 11 %w/w	2.5	3547.4	13.04	15.73	-
	4	5784.5	18.30	16.04	-
	6.5	9687.0	25.86	-	14.20
	7.5	11061.9	29.12	-	14.41
450M / 14 %w/w	2.5	3385.2	15.39	16.50	-
	4	5614.0	18.81	18.11	-
	6.5	9502.9	29.64	-	15.93
	7.5	10897.2	33.79	-	15.26
Control granules					
200M / 11 %w/w	7.5	11127.6	43.21	-	9.37
450 / 11 %w/w	7.5	11350.7	41.42	-	9.66

$T_{50\%}$ refers to the time required for the removal of 50 % of the initial moisture content of granules.
R_m refers to the maximum drying rate of granules prepared from 2.5 and 4 kg powder loads.
k refers to the drying rate constant of granules prepared from 6.5 and 7 kg powder loads.

more pronounced. For granules prepared from larger powder loads of 6.5 and 7.5 kg, the depth of the granulation bed exceeded the wavelength of microwaves (12.2 cm). This implied that for these larger batches of wet granules, heating and moisture evaporation was largely restricted to the upper layers of the granulation bed. The efficiency of moisture removal was dependent on the diffusion of moisture and vapor from the wetter regions deeper within the bed to replenish what was lost on the upper surfaces. The maintenance of a constant diffusion gradient at the liquid-gas interface resulted in a predominantly linear drying profile and constant rate of drying. For wet granules prepared from smaller powder loads of 2.5 and 4 kg, microwaves traversed the granulation bed more completely. This led to a more rapid and efficient way of drying as exemplified by the sigmoidal drying profiles.

With regards to the rate of drying, it could be observed that drying progressed at a slower rate from granules prepared from larger powder loads, as evident from the increase in $T_{50\%}$ with powder load (Table 4). Larger granule loads contain higher quantities of moisture and the energy supplied under the prescribed conditions was inadequate for moisture to be removed at a rate comparable to the smaller loads.

For both lactose 200M and 450M granules, an increase in powder load from 2.5 to 7.5 kg resulted in an approximately 2 times increase in $T_{50\%}$. It was interesting to note that irrespective of the amount of granulating liquid used, the extent of increase in $T_{50\%}$ was marginally lower for lactose 200M granules. This suggested that lactose 200M granules possessed specific physical properties which were more favorable for drying such that the impact of increasing powder load on the efficiency of moisture removal was diminished. This would be further discussed in the following sections.

B.2. Influence of Lactose Particle Size and Amount of Granulating Liquid on Microwave-Assisted Drying of Granules

The mean sizes of the wet and resultant dried lactose granules, as represented by their mean equivalent circle diameters and mass median diameters (D_{50}), respectively, are shown in Fig. 18 and Table 5. From the mean equivalent circle diameters (Fig. 18) and D_{50} (Table 5) of the granules, it could be observed that when identical amounts of granulating liquid (11 %w/w) and powder loads were employed for granulation, lactose 200M granules were generally larger in size than corresponding lactose 450M granules. Lactose 200M granules also exhibited higher drying rates for the majority of the powder loads (4, 6.5 and 7.5 kg) as evidenced by their shorter $T_{50\%}$, higher R_m and k values.

These results were surprising because higher drying rates were expected from the finer lactose 450M granules due to the availability of a larger exposed surface area for moisture diffusion. This assumption was supported by data obtained from the control granules which clearly showed that when drying was performed without microwave assistance, the finer lactose 450M granules possessed comparatively shorter $T_{50\%}$ (41.42 min) and higher k (9.66 g/min) values than corresponding lactose 200M granules prepared using identical amounts of granulating liquid and powder loads (Table 4).

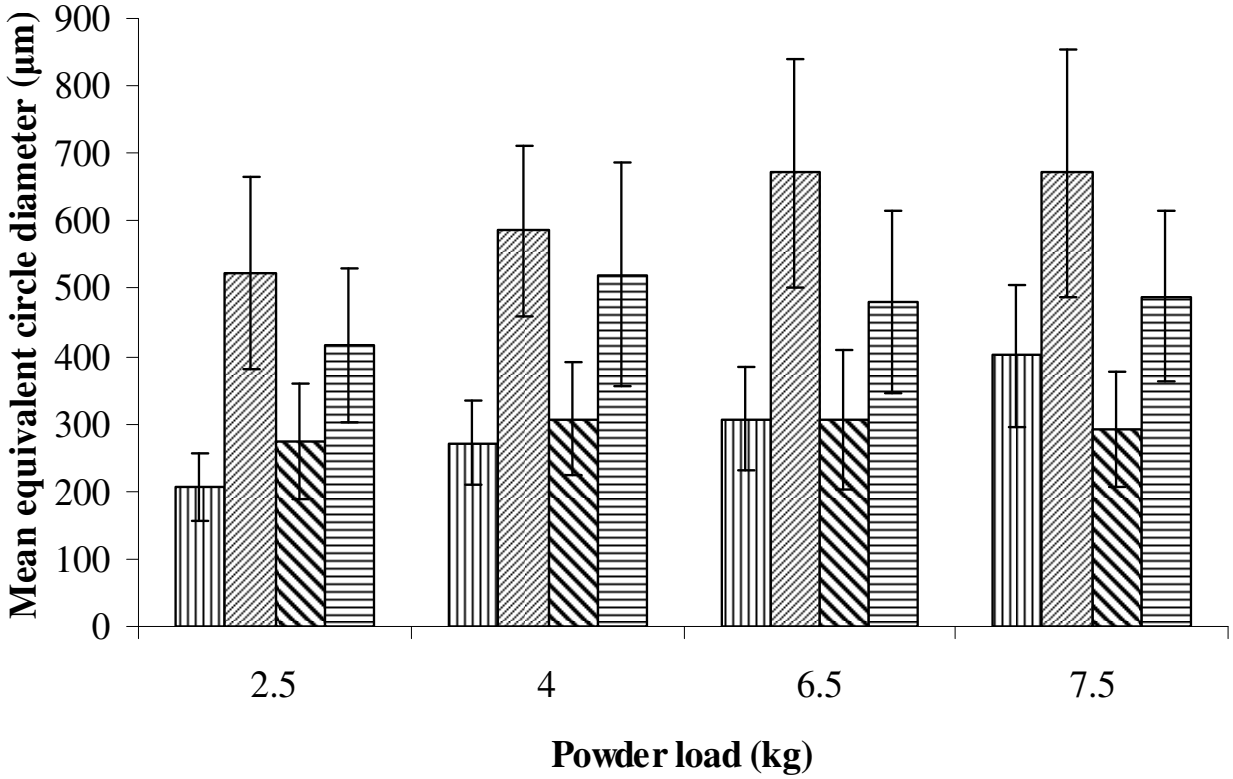

Fig. 18. Mean equivalent circle diameters of wet lactose 200M and 450M granules prepared using different powder loads and amounts of granulating liquid: (▥) 200M/8 %w/w, (▨) 200M/11 %w/w, (▧) 450M/11 %w/w and (▤) 450M/14 %w/w.

Table 5. Size analyses of all granules dried with and without microwave assistance.

Lactose / Amount of granulating liquid	Powder load (kg)	D_{50} (µm)	Modal size fraction (µm)	Lumps (%)
200M / 8 %w/w	2.5	226.3	250-355	2.8
	4	263.8	355-500	7.5
	6.5	327.5	355-500	12.5
	7.5	340.0	355-500	13.9
200M / 11 %w/w	2.5	533.0	500-710	2.7
	4	527.0	500-710	5.3
	6.5	336.0	710-1000	7.7
	7.5	360.0	710-1000	11.7
450M / 11 %w/w	2.5	305.0	250-355	5.8
	4	370.0	355-500	4.6
	6.5	327.5	355-500	12.0
	7.5	338.8	355-500	11.9
450M / 14 %w/w	2.5	611.3	500-710	7.7
	4	582.5	500-710	16.2
	6.5	530.0	500-710	17.0
	7.5	510.0	500-710	15.9
Control granules				
200M / 11 %w/w	7.5	428.8	710-1000	12.1
450M / 11 %w/w	7.5	366.7	355-500	12.6

D_{50} refers to the mass median diameter of granules.

Such discrepancies arose from the different heat generative mechanisms under the influence of microwaves and conventional heating. Due to the penetrative and volumetric heating nature of microwaves, drying under microwave-assisted conditions was not restricted to the surfaces of wet granules. As mentioned in the introduction (section 1.3.6), studies (Chamchong and Datta, 1999; Araszkiewicz et al., 2004; De la Hoz et al., 2005; Araszkiewicz et al., 2006) have shown that when microwaves were used for heating, heat was generated internally within the irradiated objects resulting in the establishment of thermal gradients 'inside out' and opposite from that encountered under conventional circumstances. Applied in the current context, higher temperatures might have been achieved within the interior of granules that resulted in the generation of pressure gradients for the outward movement of moisture and vapor from the granule cores. Under these circumstances, the structural properties of granules played a critical role in drying as they affected the migration of water from within the granules to their surfaces.

The mechanical strengths of granules supported the above argument. This is shown in Table 6 which summarized the crushing strengths and friability indices of lactose 200M and 450M granules prepared using 11 %w/w granulating liquid and different powder loads.

Table 6. Mechanical strengths of lactose 200M and 450M granules prepared using different powder loads and 11 %w/w granulating liquid.

Granule size (µm)	Test	Powder load / Type of granules							
		2.5 kg		4 kg		6.5 kg		7.5 kg	
		200M	450M	200M	450M	200M	450M	200M	450M
500	Crushing strength (mN)	3269	2922	3050	3275	2920	3236	3003	3136
710		5557	4915	5704	5527	5495	5757	5606	5670
1000		8360	6932	8409	7161	8340	8565	8799	9010
355-500	Friability index (%)	2.78	4.95	3.58	4.78	4.74	4.72	6.10	3.89

Regardless of size, lactose 200M granules generally possessed lower crushing strengths and higher friability indices than their lactose 450M counterparts at 6.5 and 7.5 kg powder loads. It could be inferred that these weaker lactose 200M granules were structurally more porous and this facilitated the migration of water and vapor from the granule cores resulting in overall higher drying rates (shorter $T_{50\%}$ and higher k) than lactose 450M granules. The reverse was observed at lower loads, in particular 2.5 kg, where all lactose 200M granules were mechanically stronger. Since mechanically stronger granules tend to be denser and less porous due to the greater number of inter-particulate contact points established between primary particles during granulation (Gokhale et al., 2005), a lower drying rate (longer $T_{50\%}$ and lower R_m) was observed for lactose 200M granules compared to lactose 450M granules prepared from 2.5 kg powder loads. These results clearly demonstrated the importance of the internal structural properties of granules in governing the efficiency of moisture removal under microwave-assisted conditions.

McLoughlin et al. (2003a) observed that the particle sizes of pharmaceutical materials exerted certain influences on their heat generative potential under the influence of microwaves. Larger particles were observed to heat better due to their improved heat entrapment and retention capabilities. Studies on the microwave heating of porous gypsum spheres have also shown that temperatures at the cores of spheres were higher than those at their surfaces. Higher core and surface temperatures were demonstrated for larger spheres as compared to smaller ones at identical liquid saturations (Araszkiewicz et al., 2004; Araszkiewicz et al., 2006). Based on these reported findings, it was possible that apart from their porous structures, the larger physical sizes of lactose 200M granules enabled greater internal heat entrapment, resulting in higher drying rates relative to corresponding lactose 450M granules.

The effects of granule size on drying could further be evaluated by comparing the drying rates of granules prepared using different amounts of granulating liquid. When the amounts of granulating liquid were increased from 8-11 %w/w and 11-14 %w/w for lactose 200M and 450M granules respectively, resultant granules were larger and these possessed higher R_m and k values (Table 4). For all batches of wet granules dried with microwave assistance, the relationships between the sizes of wet granules and their corresponding drying rates (R_m or k depending on powder load) are shown in Fig. 19. There were 2 distinct outliers at the lower loads where wet granules approximately 523 and 586 μm in size exhibited lower than expected R_m values. Incidentally, these corresponded to lactose 200M granules prepared from 2.5 and 4 kg powder loads using 11 %w/w of granulating liquid. As mentioned earlier, these

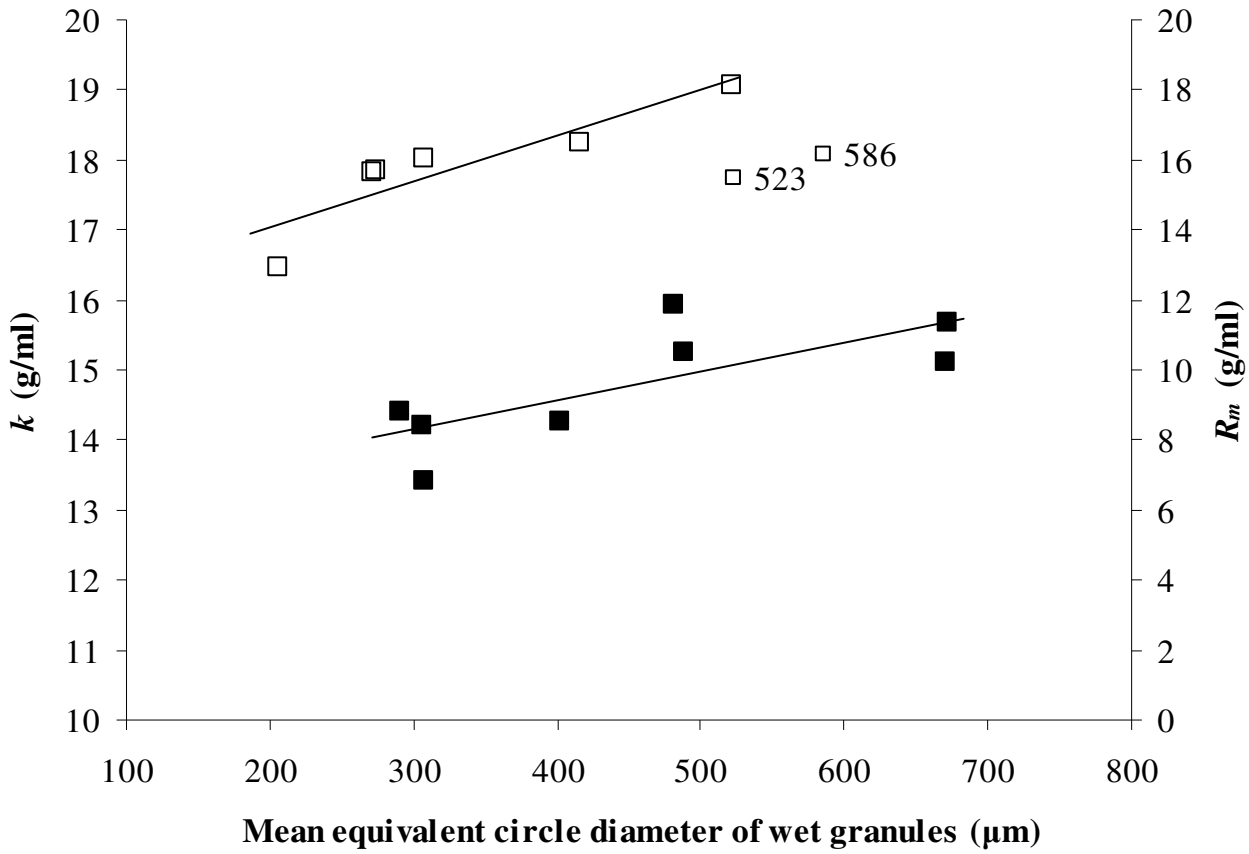

Fig. 19. Relationship between the sizes of wet lactose 200M and 450M granules and their corresponding (□) maximum drying rates, R_m, or (■) rate constants, k.

granules were found to be denser and structurally less porous than their lactose 450M counterparts (Table 6). Hence, despite their larger sizes which translated to improved heat retention capabilities, the movement of water and vapor within these lactose 200M granules were impeded due to their denser structures, resulting in a net decrease in their R_m values.

For the remaining wet lactose 200M and 450M granules, a positive correlation was observed between wet granule size and R_m (Pearson correlation coefficient, $R = 0.890$, $p < 0.05$) as well as k (Pearson correlation coefficient, $R = 0.744$, $p < 0.05$). These results reinforced the findings of the cited studies that larger particles heated better under microwave-assisted conditions and in the current context, dry at a faster rate than their smaller sized counterparts.

Apart from granule size, microwave-specific moisture-leveling effects could also account for the observed drying rates. Evaporation involves the escape of water molecules which have gained sufficient kinetic energy to overcome the surface tension forces holding them back at the liquid-gas interface. Under identical drying conditions, the rate of evaporation is governed primarily by the exposed surface area of wet granules and the difference in vapor pressure of water above the surfaces of granules and the surrounding environment. When conventional modes of heating are applied, it is unlikely that the rate of evaporation from granules would be enhanced when higher amounts of granulating liquid were used as the larger granules formed possess smaller exposed surface areas. When microwaves were used however, the higher moisture contents of granules increased their dielectric losses such that they became more susceptible to microwave-induced heating. The higher temperatures

attained by granules as a result increased the saturated vapor pressure of water above the surfaces of the granules with the consequence of an increased vapor pressure differential between them and the surrounding environment. The increased diffusion gradient enhanced the efficiency of vapor diffusion and moisture loss from granules prepared using higher amounts of granulating liquid.

B.3. Arc Detection as End Point of Drying

The absorption of microwaves by the wet granules was highly dependent on their moisture contents. Once their residual moisture contents had been reduced to a sufficiently low level, they ceased to absorb microwave energy resulting in a rise in electric field strength within the bowl. This culminated in an arcing phenomenon which automatically deactivated the magnetron, preventing further input of microwave energy. The times of arc detection and residual moisture contents of granules at those time points are presented in Table 7. The residual moisture contents of granules were determined from the drying profiles of granules shown earlier (Figs. 16 and 17).

Clearly, the increase in quantity of moisture brought about by granulating increasing powder loads delayed the time of arcing and resulted in a concomitant increase in the final residual moisture contents of granules. This was 0.1-0.5 %w/w for granules prepared from 2.5 and 4 kg powder loads and greater than 0.5 %w/w for those prepared from larger powder loads of 6.5 and 7.5 kg. From these observations, it

Table 7. Times of arc detection during microwave-assisted drying of granules and their corresponding residual moisture contents.

Lactose / Amount of granulating liquid	**Powder load (kg)**	**Time of arc detection (min)**	**Moisture content of granules at time of arc detection (%w/w)**
200M / 8 %w/w	2.5	17.0	0.249
	4	26.0	0.388
	6.5	–	–
	7.5	46.5	0.513
200M / 11 %w/w	2.5	23.5	0.439
	4	34.5	0.117
	6.5	47.7	0.677
	7.5	55.0	1.000
450M / 11 %w/w	2.5	25.5	0.268
	4	34.5	0.127
	6.5	51.5	0.925
	7.5	–	–
450M / 14 %w/w	2.5	26.5	0.263
	4	43.5	0.079
	6.5	55.5	1.650
	7.5	69.5	0.589

"–"means no arcs were detected.

could be inferred that powder load exerted an impact on the extent of drying experienced by the wet granules. Under a constant microwave power output, granules prepared from smaller powder loads were exposed to higher microwave intensities and this facilitated greater extents of drying with the consequence of lower residual moisture content in the end product. The energy supplied for the larger loads of granules (6.5 and 7.5 kg) was however, insufficient and this diminished the extent of drying.

From the size analysis data shown previously in Table 5, it could be observed that there was a tendency for the proportion of lumps to increase as powder load increased. As big lumps were inherently more difficult to dry uniformly, there was a possibility that nearing the end of the drying process when the majority of the granules had been adequately dried, residual moisture locked in the interior of these wet lumps resulted in the continuous absorption of microwave energy without the occurrence of any arcs. Indeed, these were observed in some batches of granules indicated by "–". These observations echoed the findings of Duschler et al. (1995) who had earlier reported that when localized accumulation and sticking of wet granules on the bowl wall occurred, a constant electric field strength persisted within the microwave cavity despite nearing the end point of drying due to the continuous and sustained absorption of microwave energy by the static wet masses. This disrupted the auto-regulation of the magnetron which inadvertently resulted in the dried granules being excessively exposed to microwave radiation. Such occurrences could pose significant risks to the stability of products particularly if they comprised dielectrically susceptible materials which interacted readily with microwaves even in the absence of water.

B.4. Influence of Microwave-Assisted Drying on Percent Degradation of Acetylsalicylic Acid

For all batches of granules prepared using the smallest and largest powder loads and dried with microwave assistance, the percent degradation of acetylsalicylic acid at various stages of processing are depicted in Fig. 20. Generally, drug degradation was minimal during granulation as could be inferred from the small differences in percent degradation of acetylsalicylic acid between the powders and wet granules. Depending on the formulation employed and dry powder load, microwave-assisted drying *per se* resulted in a 1.84 to 14.18 % degradation of acetylsalicylic acid. For lactose 200M and 450M granules dried without microwave assistance (control granules, Table 4), the % degradation of acetylsalicylic acid during the drying process itself were 12.78 and 12.45 %, respectively. These were higher than the corresponding values of granules (8.7-11.9 % of drug degraded during drying) prepared under identical conditions (7.5 kg dry powder load, 11 %w/w granulating liquid) but dried with microwave assistance.

For all granules dried with and without microwave assistance, a significant correlation (Pearson correlation coefficient, $R = 0.898$, $p < 0.01$) was detected between the percent degradation of acetylsalicylic acid during drying and the corresponding $T_{50\%}$ of granules (Fig. 21). Therefore, irrespective of the formulation, powder load and source of energy employed for drying, the drying time of granules was an over-riding factor influencing the stability of acetylsalicylic acid. There was minimal drug degradation during granulation as the duration of exposure of acetylsalicylic acid to moisture and heat was short as compared to the drying phase. Longer drying times

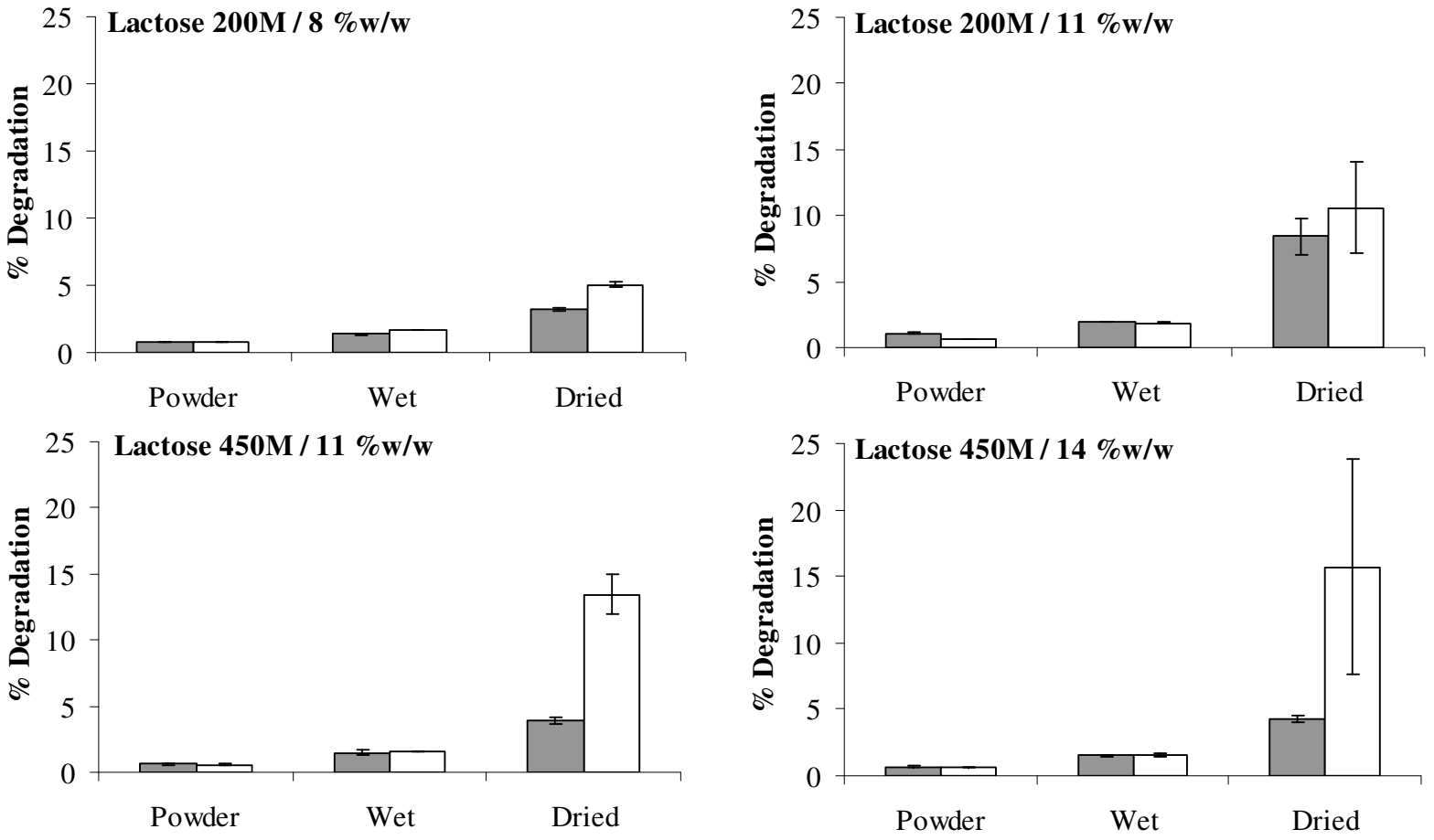

Fig. 20. Degradation of acetylsalicylic acid (%) at various stages of processing for granules prepared using powder loads of (▩) 2.5 kg and (□) 7.5 kg and dried with microwave assistance.

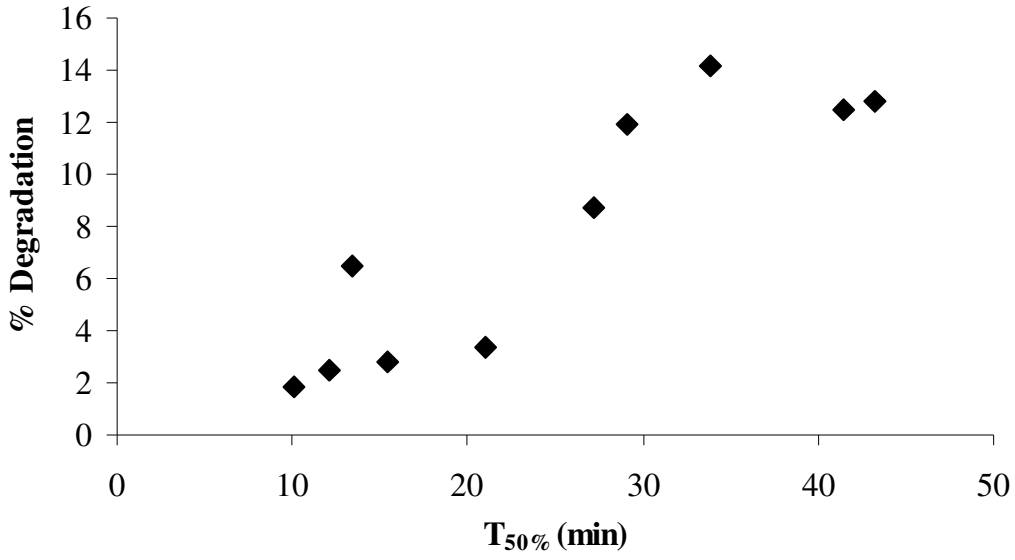

Fig. 21. Correlation between % degradation of acetylsalicylic acid and $T_{50\%}$ of all granules dried with and without microwave assistance.

resulted in greater extents of drug degradation due to prolonged exposure of drug to moisture and heat during the process.

From the results obtained, it could be concluded that supplementing existing drying methods with microwaves did not promote the degradation of acetylsalicylic acid as microwaves exerted negligible effects on the drug molecule. Instead, microwave-assisted drying preserved the stability of acetylsalicylic acid by accelerating the drying process. These results are in substantial agreement with those of Chee et al. (2005) who found that the over-riding factor influencing the extent of degradation of acetylsalicylic acid in lactose granules subjected to various drying methods such as fluidized-bed drying, hot air oven drying, dynamic as well as static modes of microwave-assisted drying was related to the efficiency at which moisture was removed in each of these processes rather than the specific usage of microwaves for drying.

Part C. A Study on Microwave-Induced Melt Granulation

The fundamental difference between the use of microwaves for drying and melt granulation lies in the choice of dielectric materials. Unlike drying where a myriad of pharmaceutical materials may be employed on condition that they are dielectrically inert, the selection criteria for materials used in melt granulation processes are more stringent. An important pre-requisite to fulfill is that the filler component of the formulation needs to possess a sufficiently high dielectric loss such that adequate heat is generated under the influence of microwaves for binder activation and agglomeration.

Based on the data obtained in part A, anhydrous dicalcium phosphate (DCP) was selected as the model dielectric material for the induction of melt granulation under the influence of microwaves. Powder admixtures comprising equivalent proportions by weight of lactose 200M and DCP were granulated with 20 %w/w of polyethylene glycol 3350 under the influence of microwave-induced heating in a 10 L single pot high shear processor. It was compared with conventional melt granulation in the same processor, performed by substituting microwaves with heat energy derived from the water-jacketed mixer bowl maintained at 60 °C.

The influences of the different heating strategies on the heat acquisition rates of the agglomerating powders were first assessed. This information was used to explain the effect of massing time (6-18 min) on agglomerate growth, as reflected by the resultant size distribution (mean granule size, % lumps, % fines, span and usable fraction of granules) and yield of granules in each process. During processing, the temporal evolution of mixer power consumption and product temperature provided real-time

information on agglomeration propensity. With the aid of multivariate data analyses, the process monitoring and control capabilities of the two processes were compared with particular reference to the use of product temperature and mixer power consumption, together with its derived parameters (energy and work done), for the depiction of agglomerate growth. In the subsequent discussions, microwave-induced and conventional melt granulation would be abbreviated as "MMG" and "CMG", respectively.

C.1. Mixer Power Consumption and Product Temperature Profiles during MMG and CMG

The typical mixer power consumption and product temperature profiles during MMG and CMG are shown in Fig. 22. Three distinct phases, characterized by the different states of powder during granulation, could be identified. In the initial stages of mixing when the temperature of the powder mass rose from 50-55 ºC, the mixer power consumption was low as minimal resistance was imposed on the impeller when rotating in the powder mixture. At 55 ºC, polyethylene glycol 3350 started to melt, moistening the powder mass and converting it into a cohesive mass. There were no statistical differences (one-way ANOVA, $p > 0.05$) in the melting flexure values amongst all the experiments carried out.

As heating continued with more binder particles converting to the molten state, the consistency of the moistened powder mass increased as indicated by the rising mixer power consumption. The power consumed peaked at approximately 57.5 ºC. This value was not found to differ significantly amongst all experiments conducted (one-

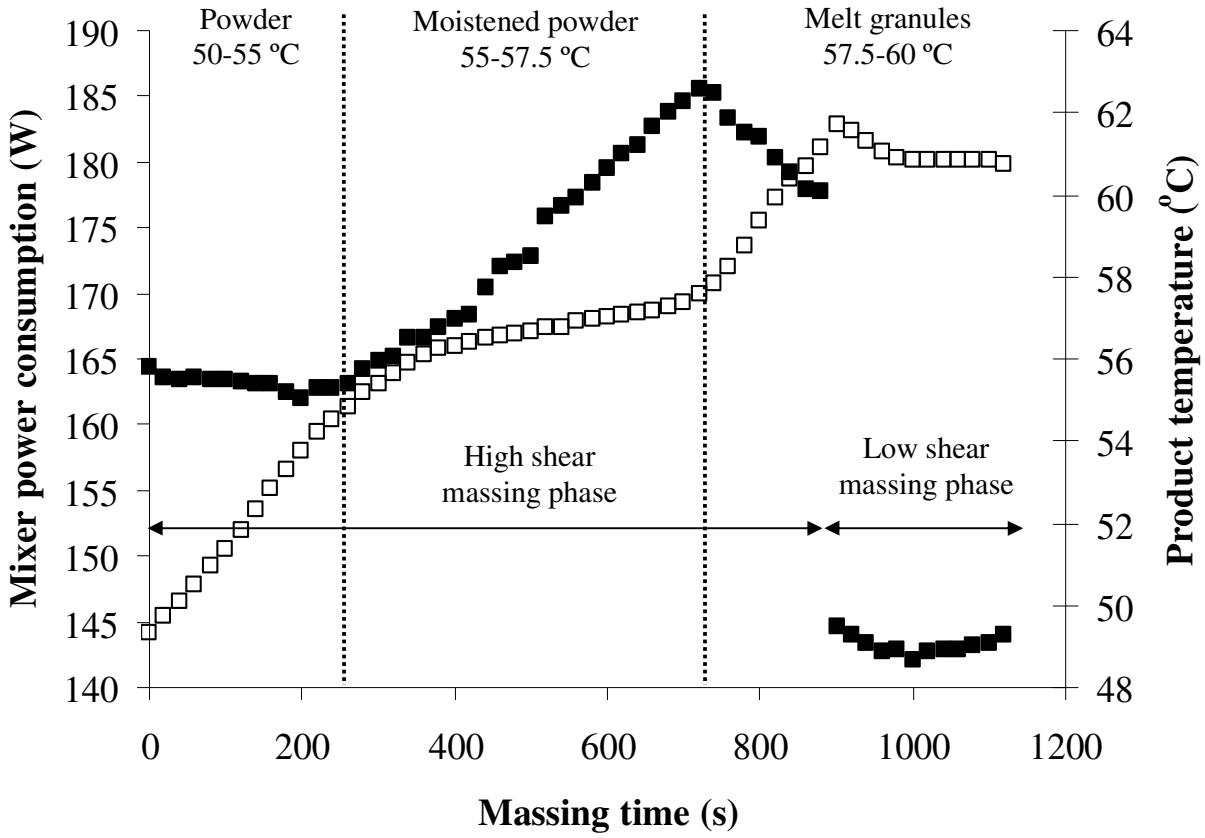

Fig. 22. Typical (■) mixer power consumption and (□) product temperature profiles during MMG and CMG.

way ANOVA, $p > 0.05$). Prolonged shearing resulted in the bulky wet masses breaking down into newly formed primary melt granules. This brought about a subsequent decrease in mixer power consumption (Heng et. al., 1999).

C.2. Heating Capabilities of Powder Masses at Various Stages of MMG and CMG

The heating capabilities of the powder masses were assessed based on the times required for them to attain specific temperature end points at various stages of MMG and CMG. This is presented in Fig. 23. Contrary to expectations, the heating capabilities of the powder masses were not improved when microwaves were employed for granulation. This could be inferred from the significantly longer times required (t-test, $p < 0.05$), particularly for the irradiated powders and moistened powder masses, to heat up to a similar extent as those subjected to conventional heating.

A possible reason that could have undermined the microwave-induced heating capabilities of the powders in MMG was that the content of DCP employed in the filler was insufficient. This was based on subsequent heating experiments which examined the significance of DCP content on the microwave-induced heating capabilities of lactose-DCP powder admixtures under process conditions identical to those employed during MMG. The results are presented in Fig. 24. "0 % DCP" referred to a powder admixture comprising only lactose 200M and 20 %w/w polyethylene glycol 3350. As the content of DCP in the admixture increased from 0-50 %, no significant differences were detected in the times required for the different

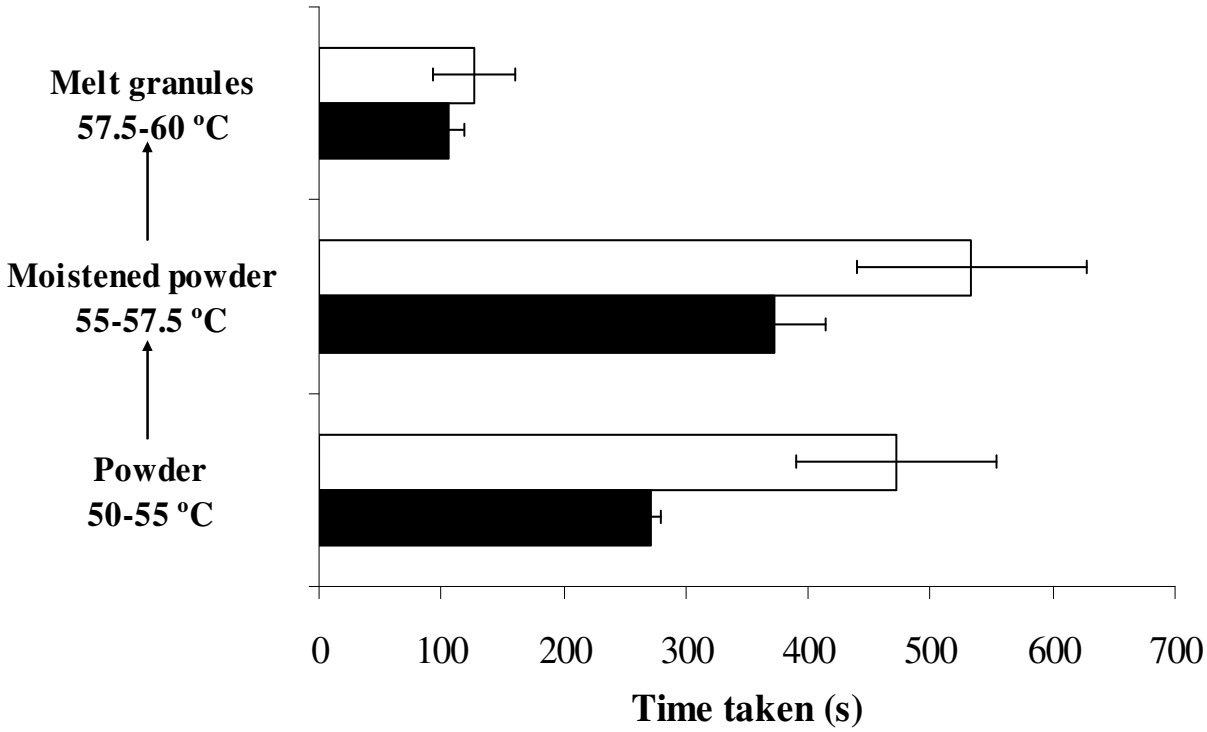

Fig. 23. Time required for the attainment of specific temperature end points by the different states of powder during (□) MMG and (■) CMG.

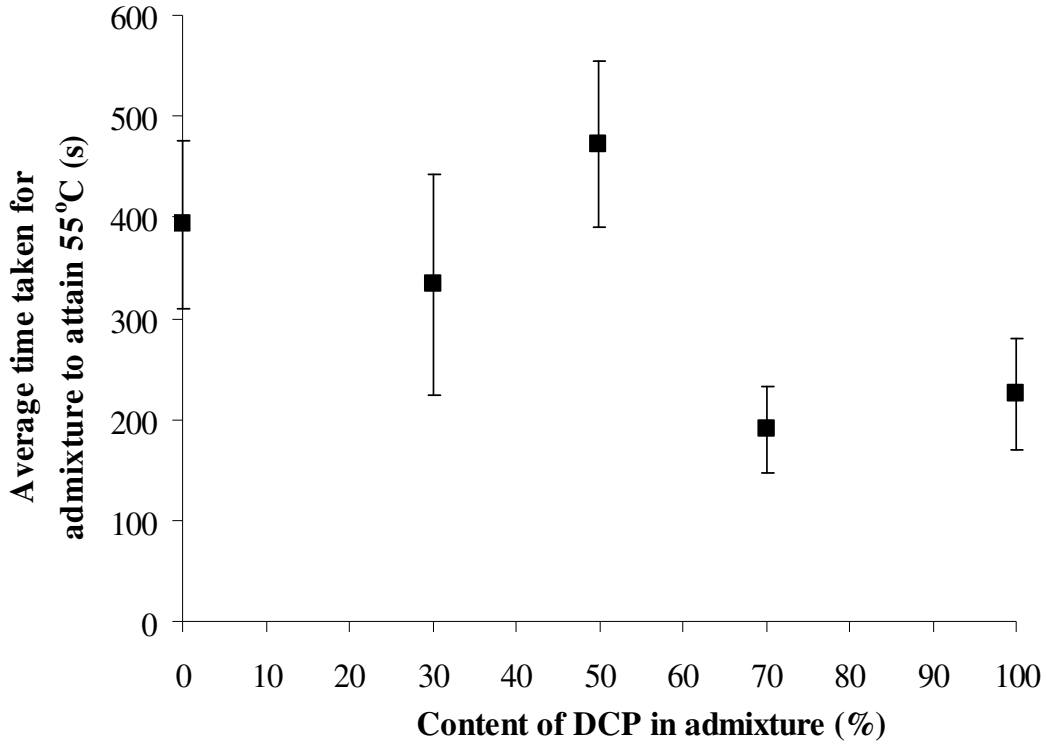

Fig. 24. Effect of DCP content on the microwave-induced heating capabilities of the powder masses under processing conditions identical to those employed during MMG.

powder admixtures to attain 55 ºC (One-way ANOVA, $p < 0.05$). This implied that their heating rates under the influence of microwaves were similar. Interestingly however, as the content of DCP increased further from 50-70 %, there was a subsequent drop in the time required for heating (t-test, $p < 0.01$), which indicated an increased heating rate of the powder admixtures. As the content of DCP increased beyond 70 %, no further improvements in heating rates of the powder admixtures were observed (t-test, $p > 0.05$).

These results could be explained by the dielectric mixture theory (section 1.3.5) which describes the overall dielectric response of a multi-component mixture as being skewed towards that of the component that occupies the largest volumetric fraction. To reiterate, the contribution of each component of a mixture to its overall dielectric property was proportional to its fractional volume in the mixture (Nelson, 1992a-b; Nelson and Datta, 2001). When the content of DCP fell within the range of 0-50 %, the fractional volume of lactose 200M in the powder admixture surpassed that of DCP due to the higher bulk density of the latter (Table 1). Consequently, the heating responses of the irradiated powder admixtures were skewed towards that of lactose with an intrinsically poor dielectric response. When the content of DCP was increased from 50-70 %, the situation became reversed with the fractional volume of DCP surpassing that of lactose 200M. This resulted in an improvement in the heating capabilities of the powder admixtures. Evidently, the content of DCP in the powder admixtures was critical to their microwave-induced heating capabilities and higher DCP contents (> 50 %) should be employed in the formulation in order to fully maximize the benefits of microwave-induced heating.

C.3. Agglomerate Growth in MMG and CMG

The yield and size distribution of melt granules produced in MMG and CMG are presented in Table 8. The proportions of fines were generally low and the proportions of usable granules ranged from 18-97 % depending on the processing conditions employed. The different ranges of massing times explored in MMG and CMG were related to the different agglomerate growth propensities in the two processes as mentioned earlier in section 3.2.5.2. This is clearly illustrated in Fig. 25 which shows the effect of massing time on the size (D_{50}) of melt granules. Although increased massing time enhanced agglomerate growth propensity, the rate of growth differed between the two processes. Under identical durations of massing (10-18 min), melt granules produced in MMG were smaller than those in CMG and this was indicative of a higher rate of growth in the latter process.

The disparity in heating capabilities of the powder masses in MMG and CMG (Fig. 23) was likely to have contributed to the differing agglomerate growth patterns. As mentioned earlier, the heat generative capabilities of the powder masses under the influence of microwaves was undermined by the dielectrically inert nature of the formulation. This delayed the rate and extent of binder activation which impeded agglomerate growth in MMG. On the other hand, the greater efficiencies of heating experienced by the powder masses in CMG resulted in the attainment of higher product temperatures which prompted further lowering of the viscosity of molten binder. The accompanying volume expansion enhanced the liquid saturations, surface plasticities and deformabilities of the newly formed melt granules. Binary coalescence of these granules prompted further growth and the formation of comparatively larger melt granules in CMG (Schaefer and Mathiesen, 1996).

Table 8. Yield and size distribution of melt granules produced in MMG and CMG.

Process	Massing time (min)	Yield[a] (%)	Lumps[a] (%)	Fines[a] (%)	D_{50} (µm)	Span[a]	Usable[a] (%)
MMG	10	97.73 (0.85)	0.64 (0.49)	0.86 (1.12)	473.8	0.96 (0.22)	97.10 (0.44)
	14	96.99 (1.37)	2.38 (1.60)	0.50 (0.53)	668.8	0.85 (0.17)	94.69 (2.33)
	16	78.15 (8.85)	32.67 (8.35)	0.05 (0.05)	1666.7	0.97 (0.05)	52.13 (0.56)
	18	87.21 (13.08)	18.17 (23.70)	0.53 (0.62)	1115.8	0.88 (0.12)	72.91 (27.08)
CMG	6	96.76 (0.33)	0.72 (0.12)	0.58 (0.08)	450.0	1.01 (0.01)	96.06 (0.38)
	8	94.94 (2.06)	1.58 (0.99)	0.28 (0.08)	619.2	0.94 (0.01)	93.43 (1.21)
	10	95.41 (1.36)	6.14 (4.20)	0.25 (0.20)	770.0	1.03 (0.04)	89.59 (5.14)
	12	87.73 (4.74)	28.63 (11.93)	0.20 (0.07)	1436.7	1.01 (0.06)	62.82 (12.35)
	14	54.48 (16.94)	57.43 (13.87)	0.38 (0.10)	966.7	1.80 (0.25)	21.93 (4.74)
	16	79.59 (8.02)	68.77 (7.39)	0.00 (0.00)	1960.0	0.69 (0.10)	24.47 (3.12)
	18	49.13 (23.44)	61.22 (7.53)	2.52 (2.25)	1442.5	1.18 (0.42)	18.30 (7.86)

[a] Standard deviations are indicated in parentheses.
D_{50} refers to the mass median diameter of melt granules.

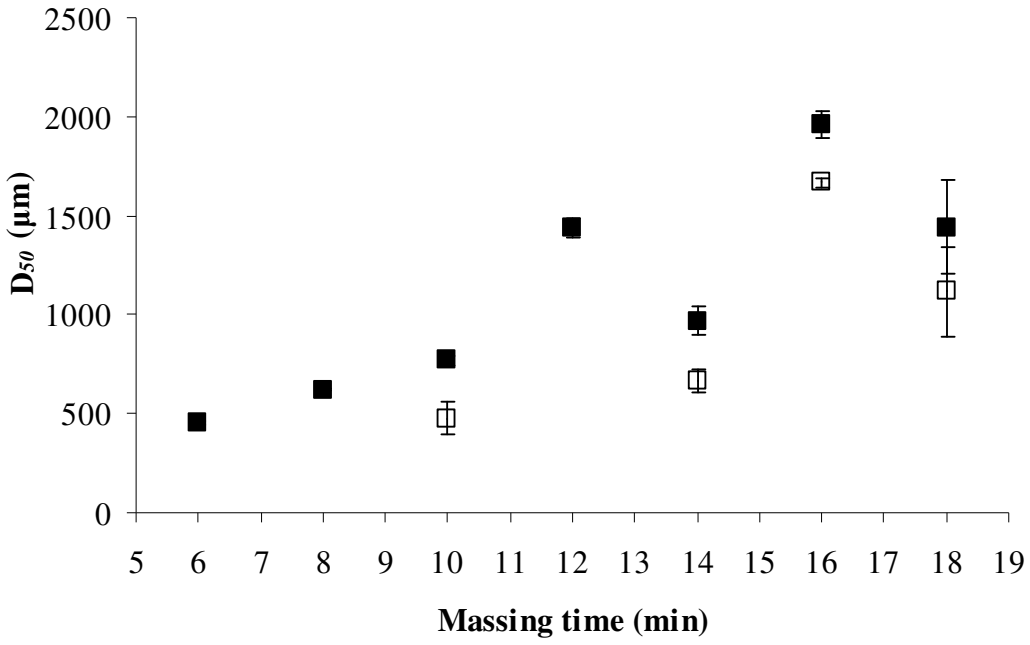

Fig. 25. Influence of massing time on agglomerate growth in (□) MMG and (■) CMG.

However, the high energy input associated with prolonged massing in CMG resulted in overgrowth, as evident from lump formation particularly as massing time increased beyond 14 min. This lowered the yield and fraction of usable granules (Table 8). Evidently, the range of massing times optimal for controlled agglomeration differed between the two processes. Due to the enhanced heating capabilities of the powder masses, optimal granule yields with desirable physical properties may be achieved within comparatively shorter process times in CMG as compared to MMG. Henceforth, massing times of 6-12 min and 10-18 min were defined as the optimum for CMG and MMG, respectively. Under these processing conditions, there were significantly less mass adhesion (> 78 % yield) and overgrowth (< 33 % lumps), resulting in a sizeable proportion (> 52 %) of usable granules.

C.4. Significance of Mixer Power Consumption in Depiction of Agglomerate Growth during MMG and CMG

It had been established that mixer power consumption signals were insufficiently sensitive to the rheological properties of melt granules as their surface deformabilities were too low relative to those produced in wet granulation (Schaefer et al., 1992a-b; Wong et al., 2005a). Moreover, as mixer power was also influenced by bearing wear and other changes in efficiency of the equipment drive system (Kristensen and Schaefer, 1987; Cliff, 1990; Covari et al., 1992; Horsthuis et al., 1993), a significant proportion of the power signal was not directly related to the productive work of granulation (Mort, 2005). This further diminished its sensitivity to the agglomeration process *per se*. Studies which have successfully correlated mixer power consumption and melt agglomerate growth required the use of large scale high shear mixers

(Schaefer at al., 1993b). For those involving laboratory scale mixers, excessively high impeller speeds were essential (Schaefer et al., 1993a; Schaefer, 1996).

The process control and monitoring capabilities of MMG and CMG were evaluated by applying multivariate data analyses to elicit the relationships between the process parameters obtained online (product temperature, mixer power consumption and its derived parameters) and agglomerate growth in the two processes. The inter-variable relationships amongst the specific parameters of product temperature and mixer power consumption as well as those related to agglomerate growth (mean granule size, yield and % lumps) in MMG and CMG are depicted in the loading plots as shown in Figs. 26 and 27, respectively.

A loading plot is interpreted based on the spatial distribution of the variables with respect to each other and the principal component axes. Variables situated close together in a loading plot co-vary positively, while those situated on opposing ends are negatively correlated to each other. Variables which overlap or are indistinguishable from each other are strongly and positively correlated. Variables orthogonal (perpendicular) to each other, on the other hand, are independent. "X-expl: 90 %, 8 %" (Fig. 26) meant that the first two principal components, PC1 and PC2, accounted for 98 % of the total variance in the data obtained from MMG whereas "X-expl: 70 %, 12 %" (Fig. 27) implied that both these principal components accounted for 82 % of the total variance in the data set obtained from CMG. These values meant that the majority of the variations and trends underlying the processes of MMG and CMG, respectively, could be explained using the first two principal components. This eliminated the need to analyze higher order components (Esbensen, 2001).

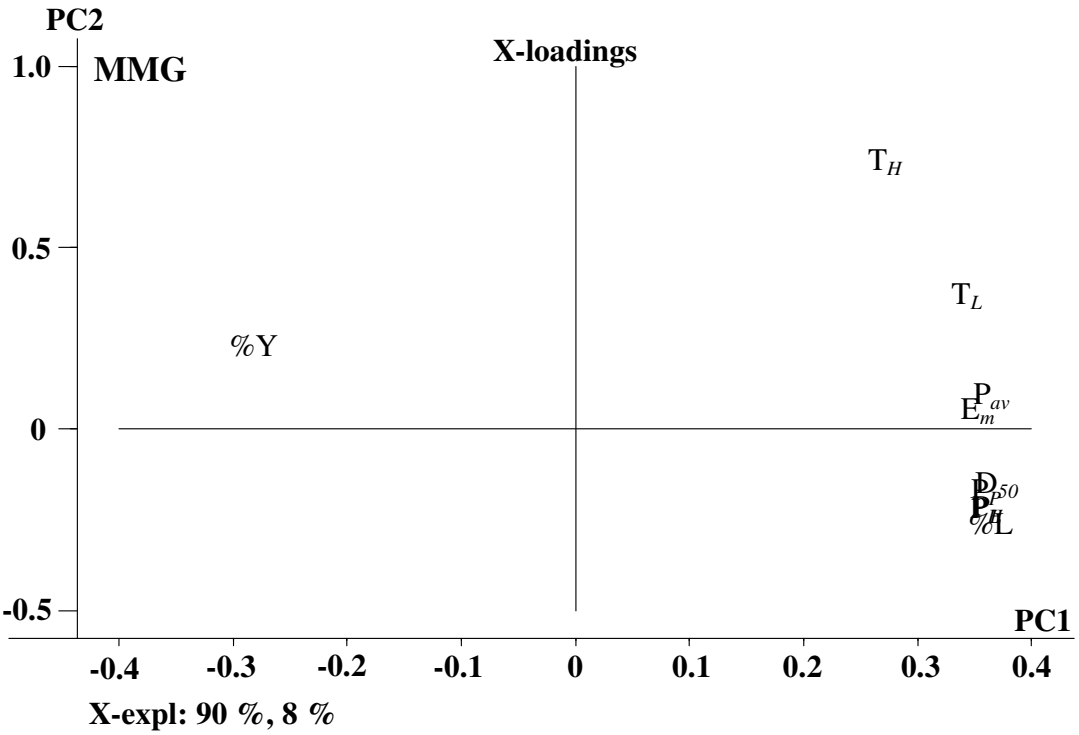

Fig. 26. Loading plot showing the relationships between agglomerate growth in MMG and various parameters relating to the mixer power consumption and product temperature evolved during processing. D_{50}: mass median diameter of melt granules (μm), %L: proportion of lumps (%), %Y: yield (%), P_P: peak mixer power consumption during high shear massing (W), P_H: mixer power consumption at the end of the high shear massing phase (W), P_L: mixer power consumption at the end of the low shear massing phase (W), T_H: product temperature at the end of the high shear massing phase (°C), T_L: product temperature at the end of the low shear massing phase (°C), E_m: post-melt specific energy consumption (Jkg^{-1}), P_{av}: average post-melt specific mixer power consumption (Wkg^{-1}).

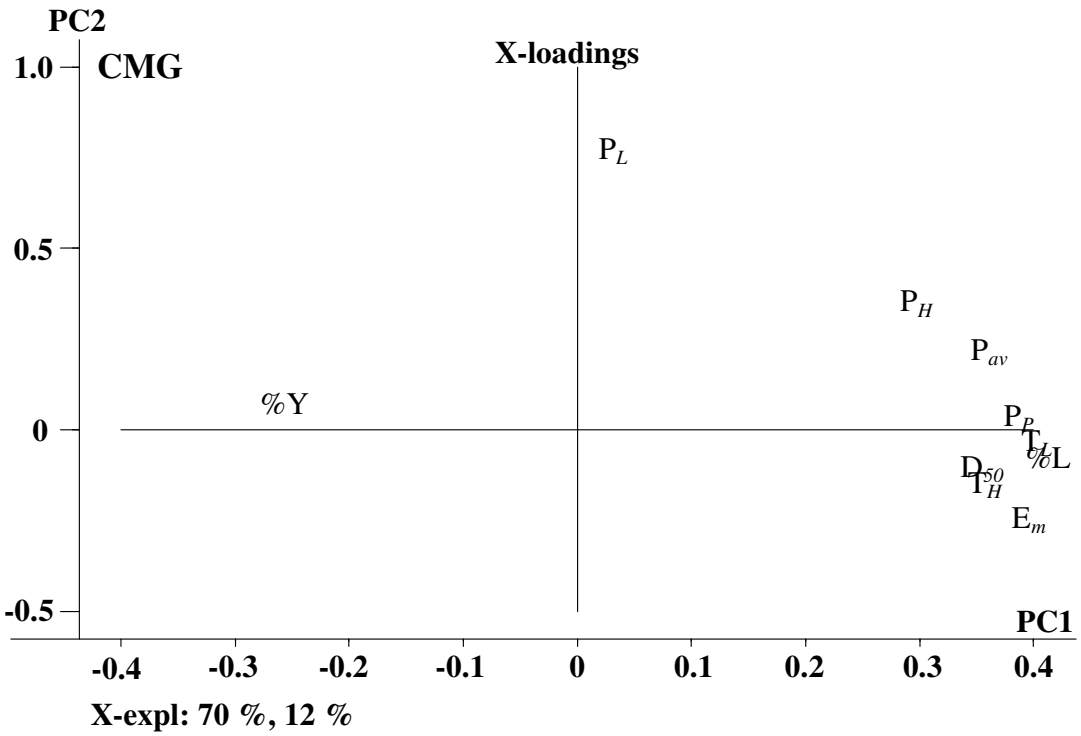

Fig. 27. Loading plot showing the relationships between agglomerate growth in CMG and various parameters relating to the mixer power consumption and product temperature evolved during processing. D_{50}: mass median diameter of melt granules (μm), %L: proportion of lumps (%), %Y: yield (%), P_P: peak mixer power consumption during high shear massing (W), P_H: mixer power consumption at the end of the high shear massing phase (W), P_L: mixer power consumption at the end of the low shear massing phase (W), T_H: product temperature at the end of the high shear massing phase (°C), T_L: product temperature at the end of the low shear massing phase (°C), E_m: post-melt specific energy consumption (Jkg^{-1}), P_{av}: average post-melt specific mixer power consumption (Wkg^{-1}).

It could be observed in Fig. 26 that the D_{50} of melt granules in MMG was closely related to P_P (Pearson correlation coefficient, $R = 0.989$, $p < 0.05$), P_H (Pearson correlation coefficient, $R = 0.992$, $p < 0.01$) and P_L (Pearson correlation coefficient, $R = 0.998$, $p < 0.01$). This suggested that the changing consistencies of the powder masses during MMG were indicative of agglomerate growth propensity. These findings were encouraging for they highlighted the potential of MMG as a promising alternative to CMG with the added advantage of improved process control capability. On the contrary, in spite of the wider range of massing times (6-18 min) investigated for CMG, the mixer power consumption parameters were more dissociated from the D_{50} of melt granules (Fig. 27). This suggested that agglomerate growth could not be reliably predicted by the evolved mixer power consumption signals, reinforcing the current status that these were poor agglomeration markers in CMG. The uncontrolled agglomerate growth that occurred at longer massing times in CMG was primarily responsible for the poor predictive ability of mixer power consumption. From the low yields of granules obtained at massing times of 14, 16 and 18 min in CMG (Table 8), it could be inferred that excessive growth and lump formation had resulted in the build-up and accumulation of product on the bowl wall and impeller. This created a load imbalance on the impeller which imparted greater resistance to its rotation. This led to variable mixer power consumption signals and its diminished sensitivity to the changing states of powder during granulation (Faure et al., 2001). On the contrary, agglomerate growth was more controlled and less erratic in MMG as the product temperatures attained were lower. This lessened the likelihood of product adhesion or build-up. Mixer power consumption signals were thus more consistent and reflective of granule size.

MMG and CMG differed primarily in their modes of heat application and specifically within the current context, the utilization of the water-jacketed mixer bowl during processing. The energy required for binder activation in CMG was derived largely from the mixer bowl maintained at 60 ºC. The temperature of the mixer bowl in MMG was however regulated in accordance to that of the irradiated powder masses as its primary function was to serve as an insulator preventing heat loss from the powders. The influence of mixer bowl temperature on the baseline mixer power consumption is shown in Fig. 28.

Clearly, mixer bowl temperature had a direct influence on the baseline mixer power consumption (Pearson correlation coefficient, $R = 0.796$, $p < 0.01$). Both the magnitude and variability of the baseline mixer power consumption increased with bowl temperature. From these observations, it could be inferred that different baseline conditions prevailed in MMG and CMG. In MMG, the discriminatory nature of microwaves resulted in a targeted, albeit slow rate of heating of the powder masses. Accordingly, the rise in temperature of the mixer bowl was slower and more gradual. In comparison, the mixer bowl temperature rose quickly to 60 ºC and was subsequently maintained at this set point throughout CMG. Due to sustained heating and higher mixer bowl temperatures in CMG, the baseline mixer power consumption was more pronounced and erratic. This could in part, have reduced the signal to noise ratio, thereby resulting in a poorer sensitivity of mixer power consumption to agglomerate growth in CMG. Hence, the relationship between the size of melt granules and mixer power consumption was indistinct in CMG. On the other hand, the baseline mixer power consumption was comparatively lower in magnitude and variability due to a cooler bowl in MMG. A higher signal to noise ratio and improved

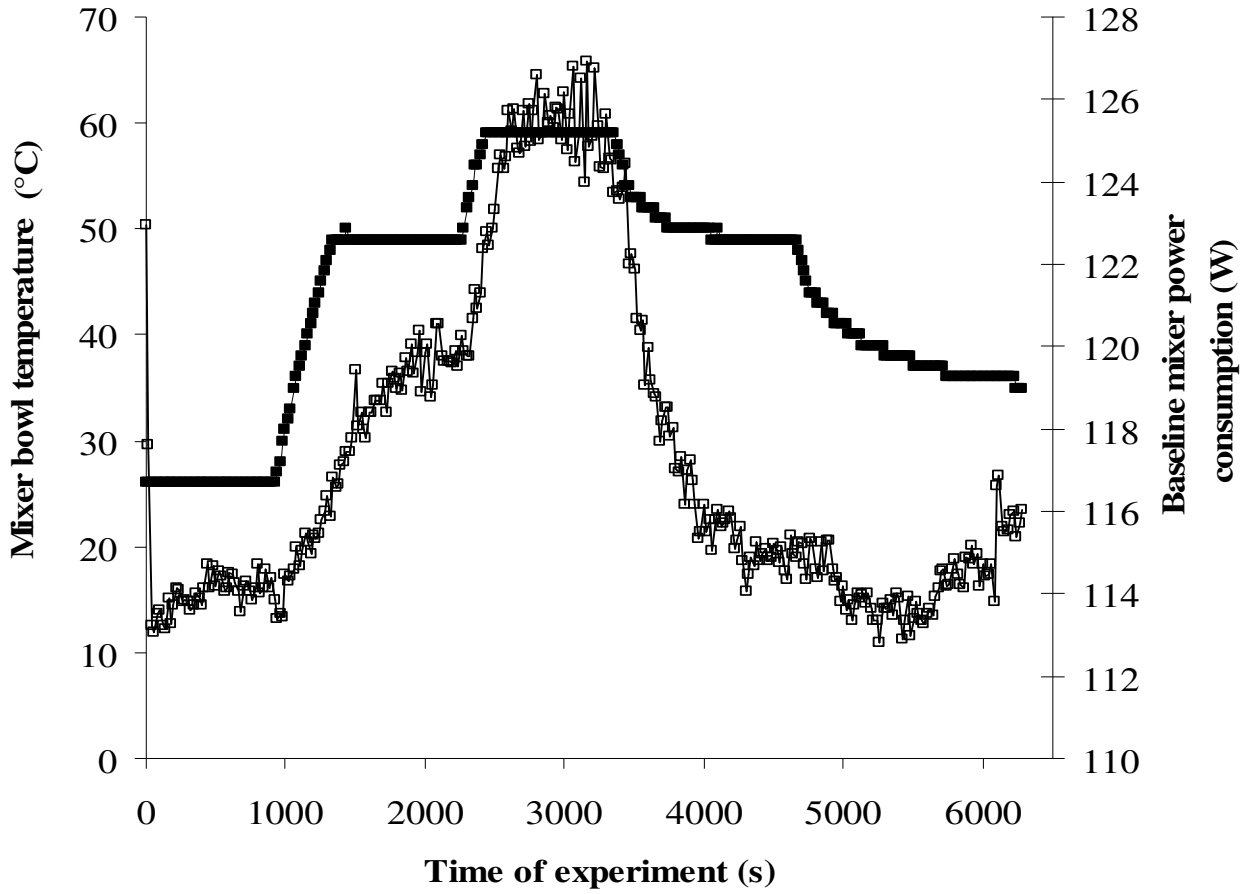

Fig. 28. Influence of (■) mixer bowl temperature on the (□) baseline mixer power consumption of the processor.

signal reproducibility contributed towards the strong association between mixer power consumption and agglomerate growth in MMG.

With regards to the energy invested and work done during the melt granulation processes, it could be inferred from Fig. 26 that agglomerate growth in MMG was closely associated to P_{av} (Pearson correlation coefficient, $R = 0.968$, $p < 0.05$) which was expected in light of the data obtained thus far. Agglomeration propensity in CMG (Fig. 27) was related to E_m (Pearson correlation coefficient, $R = 0.869$, $p < 0.05$). This was surprising since E_m and mixer power consumption were inter-related. A likely reason could be that since E_m was computed by taking into account the combined effects of mixer power, granulation time and powder mass (section 3.2.5.3), it was more robust, with lesser contributions from background noises and other external interferences. Consequently, E_m was a more suitable marker of agglomerate growth in CMG as compared to single point determinations of mixer power consumption as discussed earlier. These observations are in agreement with the findings of Heng et al. (1999).

C.5. Significance of Product Temperature in Depiction of Agglomerate Growth during MMG and CMG

Unlike mixer power consumption, product temperature was less suitable for process monitoring in MMG as the size (D_{50}) and temperature variables (T_H and T_L) were observed to be further apart (Fig. 26). In MMG, effective heating of the powders relied firstly on the selective coupling of microwaves with DCP followed by the transfer of energy from the heated DCP particles to the remaining powder mass by thermal conduction. The efficiency of thermal conduction was however, compromised

due to the low content of DCP employed and this reduced the efficiency at which heat could be generated volumetrically within the irradiated powders during massing. This led to differential heating of the powder masses and the occurrence of hot and cool spots that affected the regularity of product temperature measurements. Problems related to the non-homogeneous distribution of heat in materials exposed to microwaves have been extensively documented (Araszkiewicz et al., 2004; Araszkiewicz et al., 2006; Kelen et al., 2006a-b; McMinn et al., 2006).

In addition, the high impeller speeds employed during processing had potential to cause partial fluidization of the powder masses in the mixer bowl. Hence, the product temperature recorded represented that of a binary mixture comprising the powder and surrounding air. As air possesses a low dielectric constant and loss (Schiffmann, 1995), microwave irradiation of materials in air typically results in significant heating of the material *per se*, leaving the surrounding air largely unaffected (George and Burnett, 1991; Dolande and Datta, 1993). Thus, the air in the mixer bowl remained cool in MMG. This further exacerbated the temperature non-homogeneity within the bowl and its contents, resulting in erratic and irreproducible product temperature measurements. As such, the agglomeration process in MMG could not be reliably predicted based on the evolved product temperature.

The situation was slightly different in CMG. Due to the indiscriminate nature of conventional heat energy, the temperature of the surrounding air within the bowl increased in tandem with the bowl itself. Unlike MMG, the air in CMG served as a medium facilitating energy transfer between the heated mixer bowl and its contents thereby promoting the agglomeration process. Hence, with enhanced heating

capabilities and a decreased temperature differential between the powder masses and surrounding air, product temperatures measured in CMG were higher, more consistent and representative of the thermal environment under which agglomerate growth occurred. Therefore, both T_H (Pearson correlation coefficient, $R = 0.792$, $p < 0.05$) and T_L (Pearson correlation coefficient, $R = 0.877$, $p < 0.01$) were found to be closely associated with the D_{50} of melt granules in CMG (Fig. 27).

Supporting evidence is depicted in Fig. 29 which shows the inter-batch variations in product temperatures, T_H and T_L, recorded when massing was carried out for the different durations in MMG and CMG. Generally, both T_H and T_L exhibited higher degrees of variability, as shown by their higher relative standard deviations, in MMG as compared to CMG. This indicated that the heating abilities of the powders under the influence of microwaves were more inconsistent from batch to batch. It was also noteworthy that the inter-batch variations in product temperature were related to the duration of massing in MMG. When massing times were longer, greater inter-batch consistencies were observed in the measured product temperatures (decrease in relative standard deviations) as more time was available for heat distribution and thermal equilibration between the powder masses and their surrounding environment.

From the data obtained thus far, it could be concluded that although the heat generative capabilities of the powder masses in MMG were poorer in comparison to those in CMG as a result of a deficit of DCP in the formulation, the prospects of mixer power consumption and its derived parameters as agglomerate growth indicators of melt agglomeration were renewed under such circumstances. It was

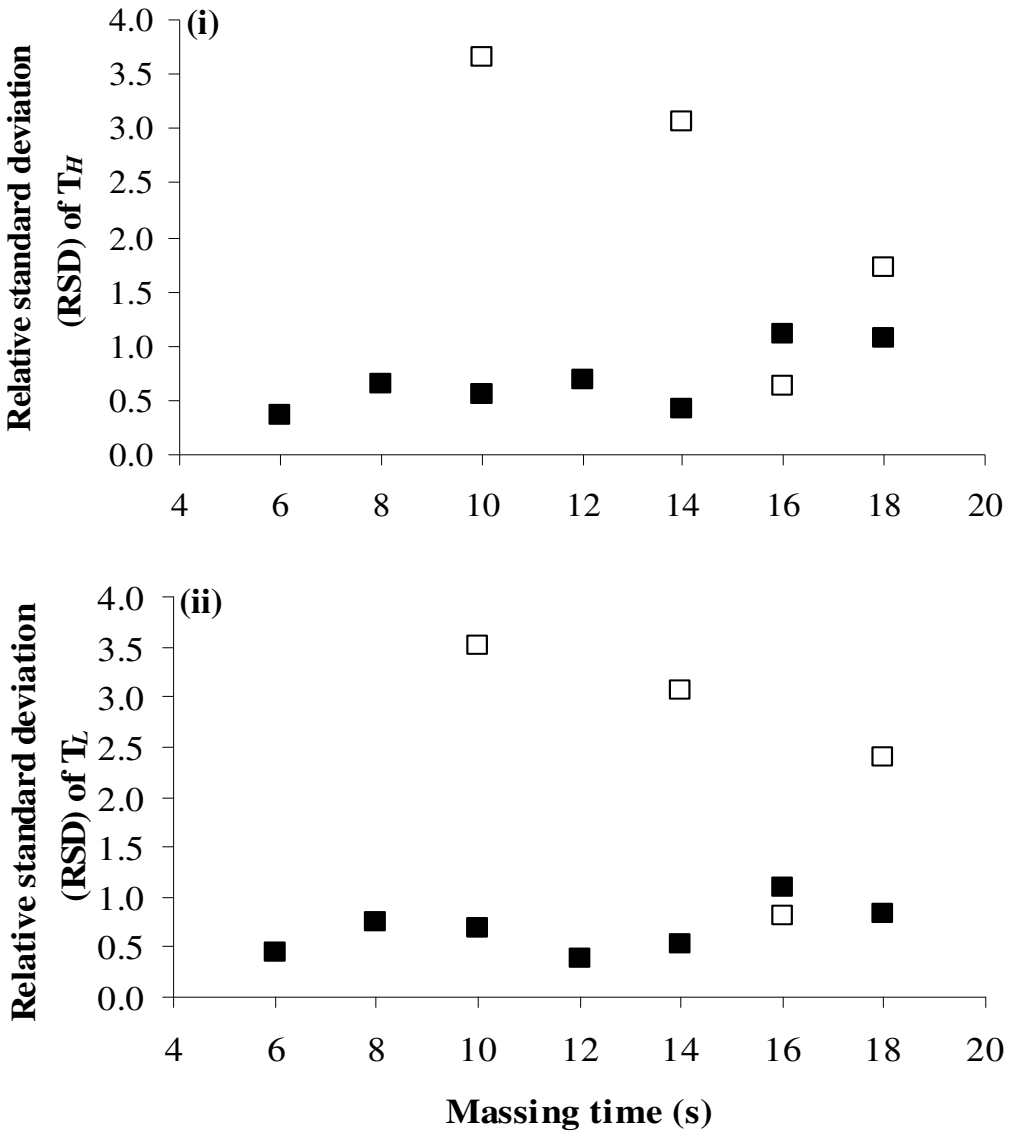

Fig. 29. Relative standard deviation (RSD) of (i) T_H and (ii) T_L providing an indication of the inter-batch variations in product temperature measurements when massing was carried out for different durations in (□) MMG and (■) CMG.

envisaged that if the quantity of DCP in the formulation was increased, product temperature measurements would figure more prominently and possibly surpass the importance of mixer power consumption as indicators of agglomeration in MMG. From Fig. 24, it could be inferred that if the content of DCP was increased to 70 %, the time required for the powder admixture to attain 55 ºC would be marginally shorter than that required for the current formulation under the influence of conventional heating (Fig. 23). This meant that the heating rates of powder admixtures comprising 70 % DCP would be faster on microwave exposure and product temperature may, under these circumstances, prove useful for monitoring agglomerate growth in MMG. These findings reiterated the impact the choice of dielectric materials exerted on the control and monitoring aspects of a microwave-assisted process. In the current context, the technique of process control may be adapted and customized in accordance to user preferences by fine-tuning the dielectric properties of the starting materials. Hence, the use of microwaves for melt granulation confers tremendous process flexibility, setting it apart from traditional melt granulation techniques.

C.6. Relationships Amongst Percent Lumps, Yield and Size of Melt Granules

The relationships amongst the percent lumps and yield as well as sizes of melt granules produced in MMG and CMG are illustrated in Figs. 30(i) and (ii), respectively. It could be observed that as agglomeration proceeded in both MMG and CMG (increased D_{50}), the tendency for lump formation increased. The proportion of lumps was also inversely related to percent yield which varied from 49-98 % depending on the mode of heating employed. Higher yields (78-98 %) were generally

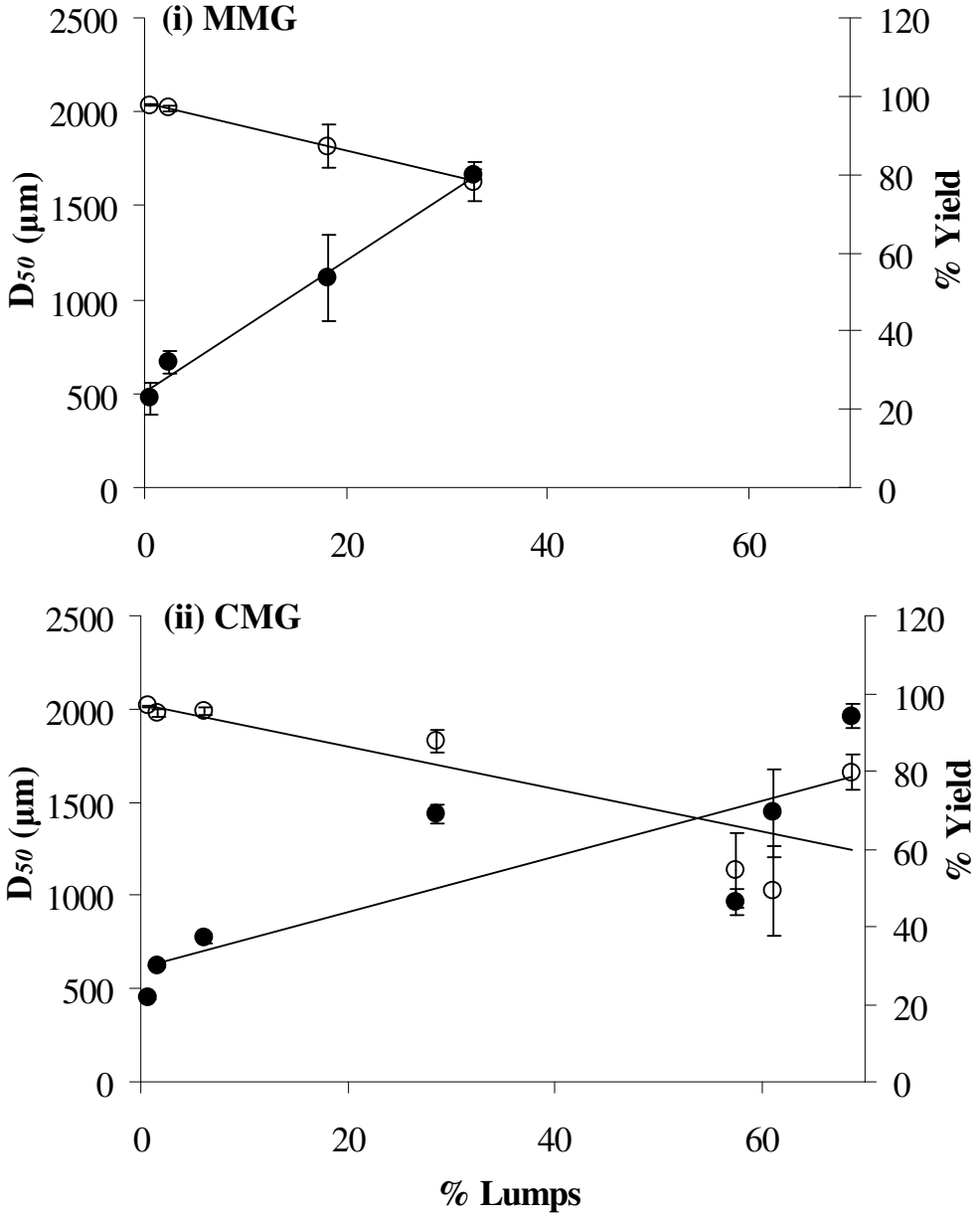

Fig. 30. Relationship amongst % lumps, (●) D_{50} of melt granules and (○) % yield in (i) MMG and (ii) CMG.

observed for MMG as compared to CMG at identical massing times. This was attributed to the uncontrolled agglomerate growth coupled with pronounced mass adhesion at longer massing times of 14, 16 and 18 min in CMG.

From these outcome variables, it may be concluded that MMG exhibited a greater level of process control and predictability than CMG as higher correlation coefficients were obtained between percent lumps and D_{50} (Pearson correlation coefficient, R = 0.994, $p < 0.05$) as well as percent yield (Pearson correlation coefficient, R = -1.000, $p < 0.01$). The corresponding correlation coefficients for CMG were lower. Granted that this might have arisen due to the uncontrolled and erratic growth patterns at longer massing times (14, 16 and 18 min), the analyses of the inter-variable relationships amongst D_{50}, percent lumps and yield in CMG were confined to shorter massing times of 6-12 min. Under these conditions, the correlation coefficients obtained between percent lumps and D_{50} (Pearson correlation coefficient, R = 0.988, $p < 0.05$) as well as percent yield (Pearson correlation coefficient, R = 0.980, $p < 0.05$) were marginally improved but still lower than those obtained in MMG. These results were consistent with earlier observations made in the loading plots (Figs. 26 and 27). It was demonstrated that a significant proportion (98 %) of the variation latent in the process of MMG could be explained by multivariate data analysis and thus provided useful information necessary for a more complete understanding of the process. This is in contrast to that of CMG where only 82 % of the data could be explained with the remaining 18 % unaccounted for, presumed to represent the 'noise' intrinsic to the process. The results of this study clearly established the potential of MMG as a promising alternative to traditional techniques of melt granulation with the added advantages of flexible and improved process monitoring and predictive capabilities.

Part D. Evaluation of Physicochemical Properties and Compaction Behavior of Melt Granules Produced in MMG and CMG

Melt granulation facilitates the study of agglomeration as the solidified binder material remains as a constituent in the end product (Wong et al., 2005a). Retaining the focus on melt granulation, this part of the study takes a step further by examining and comparing the qualities of products (granules and compacts) derived from MMG and CMG. The different heating strategies employed in the 2 melt granulation techniques would, at the outset, affect the distribution of molten binder material throughout the agglomerating powder masses. This would in turn, influence the physicochemical properties of resultant melt granules.

The binder distribution patterns, flow properties, porosities and moisture contents of melt granules produced under optimal conditions in MMG (10-18 min) and CMG (6-12 min) were first examined. The compaction behavior of melt granules were then evaluated based on the porosities and mechanical strengths of the compacts formed when the melt granules were compacted under a fixed pressure of 102 MPa. Multivariate data analyses were employed to study the influences of the various physicochemical properties of melt granules on their compaction behavior. The compressibility of selected batches of melt granules were also evaluated using the Heckel equation.

D.1. Binder Distribution of Melt Granules

Binder content was defined as the proportion by weight (%w/w) of polyethylene glycol 3350 in the melt granules. For product batches produced under optimal conditions in CMG (6-10 min) and MMG (10-18 min), the binder contents of the

different size fractions of granules are shown in Figs. 31 and 32, respectively. Each data point in the bar chart represented the binder content of a particular size fraction of melt granules produced at a specific massing time and the corresponding error bar reflected the inter-batch variation in the binder content of granules of that particular size. The intra-batch variation in the binder content of melt granules was inferred from the disparities in binder contents amongst the different size fractions of melt granules that constituted a representative sample of granules manufactured under a specific process condition. It was derived from the standard deviation of the binder content values of the different size fractions of granules present.

Theoretically, polyethylene glycol 3350 constituted a proportion of 16.7 % by weight of melt granules. At all massing times, it could be observed in both CMG and MMG that the binder contents of the different granule fractions closely approximated the theoretical value of 16.7 %w/w and decreased slightly as granule size fell below 355 μm. At the outset, it could be observed that the intra-batch variations in the binder contents of melt granules were lower in CMG (Fig. 31) as compared to MMG (Fig. 32). Although a specific fraction of granules (180-250 μm) prepared at a massing time of 10 min in CMG possessed an unexpectedly high amount of binder, relatively consistent binder content values were achieved across all remaining size classes of melt granules regardless of massing time. The small error bars further indicated that the inter-batch variations in binder contents of granules were minimal. These results

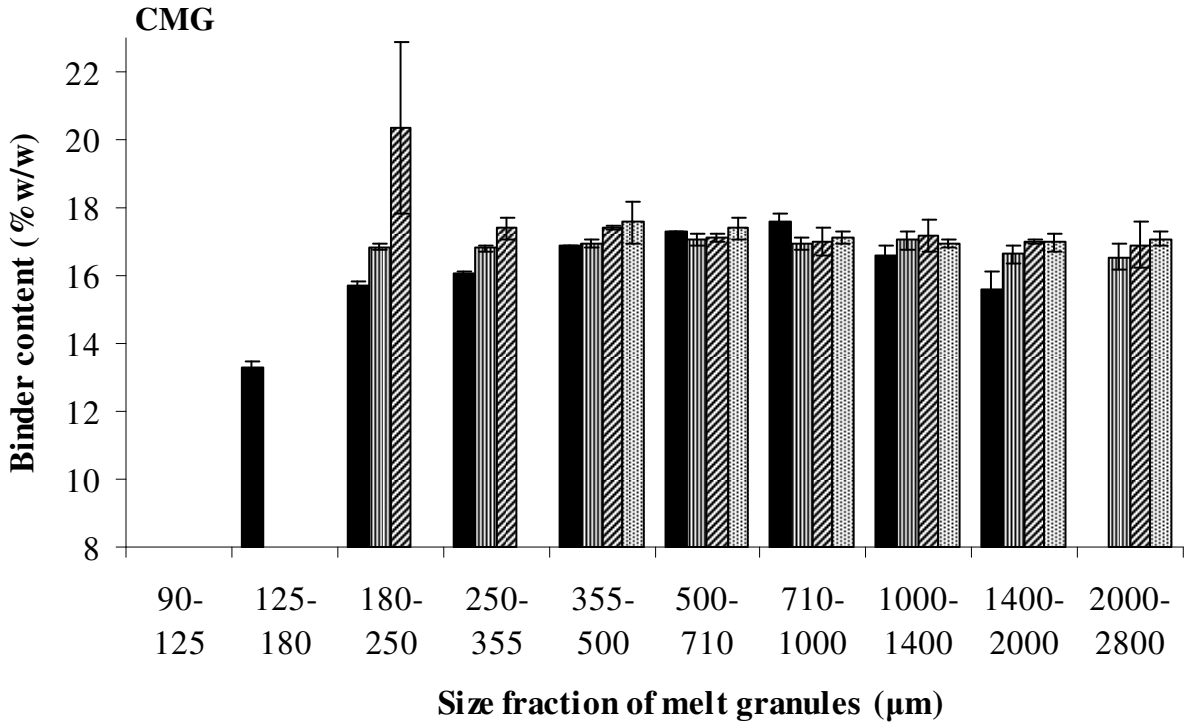

Fig. 31. Binder contents of the different size fractions of melt granules produced in CMG at massing times of (■) 6, (▥) 8, (▨) 10 and (▩) 12 min.

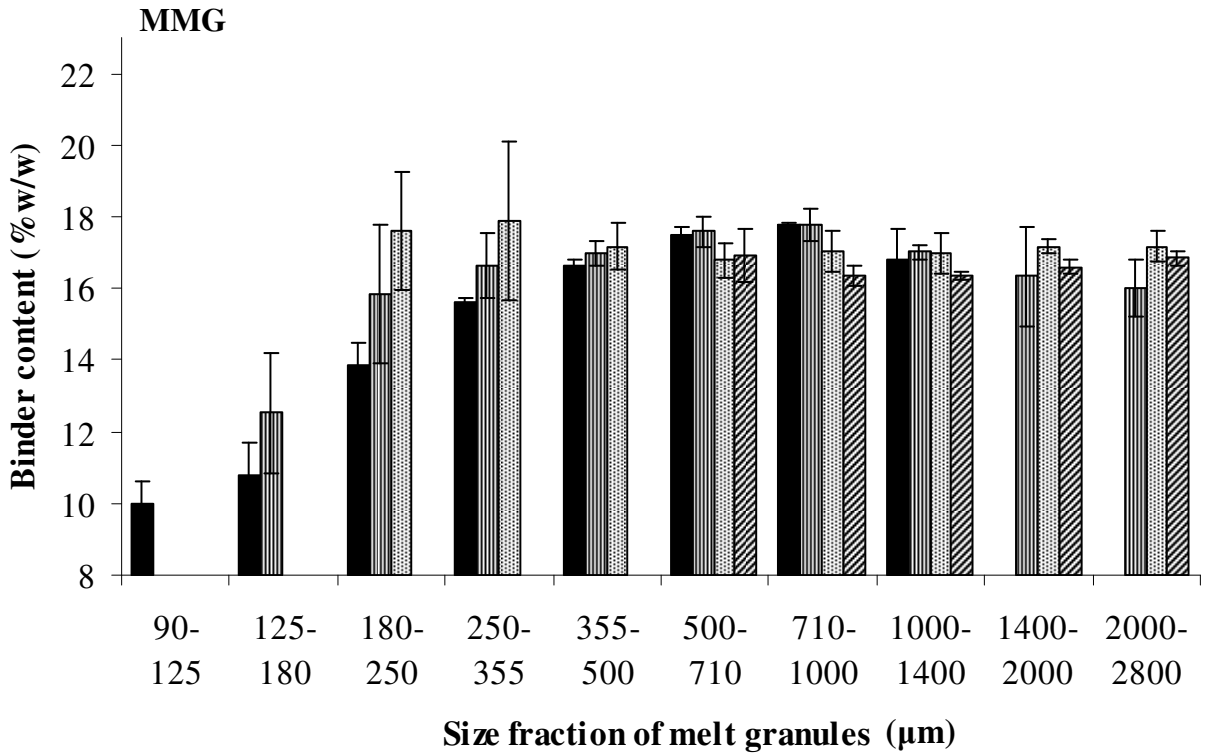

Fig. 32. Binder contents of the different size fractions of melt granules produced in MMG at massing times of (■) 10, (▥) 14, (▨) 16 and (▩) 18 min.

provided evidence of a robust and reproducible melt granulation process under the influence of conventional heating.

The situation was slightly different in MMG (Fig. 32). In spite of the longer durations of massing (10-18 min), the binder was distributed less homogeneously within each product batch as could be inferred from the greater disparities in binder contents amongst the different size fractions of granules. On closer examination, greater intra-batch variations in the binder contents of melt granules could be observed at shorter massing times of 10 and 14 min where binder content fell as low as 10.0 and 12.5 %w/w for melt granules less than 180 μm in size. Greater intra-batch consistencies in the binder contents of melt granules were achieved only when massing time was increased to 16 and 18 min. In addition, it was evident from the larger error bars that greater inter-batch variations in the binder contents of melt granules were observed for MMG as compared to CMG. This implied that the batch to batch reproducibility in binder distribution was relatively poorer in MMG.

These findings were believed to be a direct consequence of heat being dissipated non-uniformly within the powder masses under the influence of microwaves. As shown earlier in Figs. 29(i) and (ii), greater inter-batch variations in product temperature measurements (higher RSD of T_H and T_L) were observed in MMG as compared to CMG, believed to have arisen from the vastly different dielectric losses and thus microwave-induced heating capabilities of the powder mixtures and surrounding air. This provided supporting evidence that the poorer batch to batch reproducibility in binder distribution was attributed to heating irregularities of the air-powder mixtures when microwaves were employed. Coupled with the poor heat acquisition rates of the

agglomerating powders, the molten binder remained viscous and spread less readily and uniformly during MMG. Consequently, the effective distribution of binder became reliant on the effects of mixing and shearing which served not only to further reduce the size of the molten binder droplets to aid dispersion, but also to provide a supplementary source of frictional heat to assist binder activation.

Indeed, massing time was found to be critical to the intra-batch homogeneity of binder content in MMG where a negative correlation was detected between massing time and the intra-batch variations in binder contents of the melt granules (Pearson correlation coefficient, $R = -0.965$, $p < 0.05$). This indicated that as massing duration increased, the molten binder material became more uniformly dispersed within the powder masses, leading to an improvement in content homogeneity. No corresponding correlations were detected in CMG. It could be inferred from these results that the different heating strategies employed in MMG and CMG influenced the distribution of molten binder during granulation. Its implications on the physicochemical properties and compaction behavior of resultant melt granules would be discussed in the subsequent sections.

D.2. Moisture Contents of Melt Granules

From Karl Fischer analyses, the moisture contents of all melt granules ranged from 2.23-2.50 %w/w. This was marginally lower than the moisture content of the starting powder mixture which was found to be 2.61 %w/w based on an identical method of analysis. Given the conditions of reduced pressure (80 mbar) and elevated temperatures (55-60 °C) under which melt granulation was performed in the high shear mixer, evaporative moisture losses were expected. The relationships between

the sizes and moisture contents of melt granules produced in MMG and CMG are shown in Fig. 33.

For both MMG and CMG, moisture content increased with granule size and this was likely to be attributed to the gradual reduction in surface area available for moisture loss as agglomeration proceeded. The size and moisture contents of melt granules in MMG were strongly correlated (Pearson correlation coefficient, $R = 0.996$, $p < 0.01$). For CMG however, the trend was non-linear. Therefore, the decrease in rate of moisture loss with increased granule size appeared more marked in CMG, indicating that moisture was removed less readily from melt granules prepared in the latter process as compared to corresponding granules of similar size in MMG.

In view of the greater heating efficiencies and higher product temperatures attained in CMG, these findings were surprising as the thermal environment afforded in CMG was more favorable for evaporative moisture losses from the melt granules. The different agglomeration propensities in MMG and CMG could account for the observed moisture variation. In CMG, agglomerate growth proceeded more spontaneously due to the enhanced heating capabilities of the powder masses under the influence of the heated mixer bowl. The higher rate of growth and rapid transformation of smaller to larger granules resulted in greater moisture entrapment which contributed to the higher residual moisture contents in the resultant granules. To compensate for the heating inefficiencies of the powder masses in MMG, longer massing durations of 10-18 min were required for growth induction and production of granules that were of comparable size to those in CMG. Granule formation proceeded at a more gradual pace and the transformation of smaller to larger granules occurred

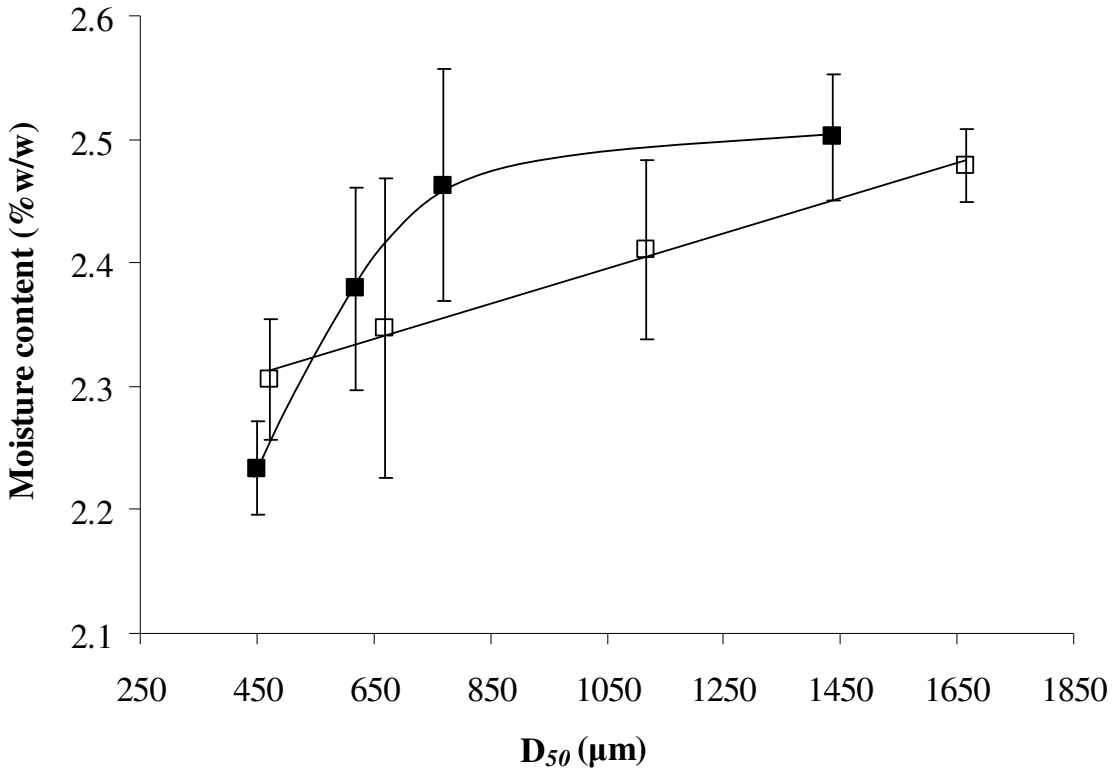

Fig. 33. Relationship between the size and moisture content of melt granules in (□) MMG and (■) CMG.

with less haste in MMG. Hence, more time was available for moisture loss during the agglomeration process. This, coupled with the constant input of mechanical energy from the high speed impeller for prolonged durations provided greater leeway and opportunities for evaporative moisture losses leading to a lower residual moisture content of melt granules produced in MMG.

D.3. Influences of Physicochemical Properties of Melt Granules on Compaction Behavior

The flow properties (bulk and tapped densities, Hausner ratios as well as compressibility indices) and porosities of melt granules produced in MMG and CMG are presented in Table 9. Their compaction behavior, as reflected by the mechanical strengths and porosities of compacts formed under a compaction pressure of 102 MPa, are similarly shown. Generally, all melt granules produced possessed excellent flow and their porosities ranged from 49-54 %. The mechanical strengths and porosities of resultant compacts ranged from 110-142 N and 4.8-6.1 %, respectively.

Multivariate data analyses were employed to assess the influences of the various physicochemical properties of melt granules on their compaction behavior. In addition to their flow properties and porosities as shown in Table 9, the physicochemical properties of melt granules also encompassed their size and size distribution (mass median diameters, spans and proportion of fines as listed in Table 8), binder as well as moisture contents (parts D.1 and D.2). As an un-sieved sample of melt granules was compacted each time, the binder content of melt granules was computed from the summation of the weighted contributions of the binder contents of the different size fractions of granules that constituted a representative sample of each product batch.

Table 9. Flow properties and porosities of melt granules produced in MMG and CMG as well as the porosities and mechanical strengths of corresponding compacts prepared under a compaction pressure of 102 MPa.

Process	Massing time (min)	BD[a] (g/ml)	TD[a] (g/ml)	HR[a]	CI[a] (%)	Єgr [a] (%)	Єcom[a] (%)	MECH[a] (N)
MMG	10	0.800 (0.073)	0.869 (0.032)	1.09 (0.06)	8.08 (5.04)	53.13 (1.72)	6.10 (0.44)	110.2 (3.0)
	14	0.867 (0.048)	0.912 (0.039)	1.05 (0.01)	5.00 (1.29)	50.81 (2.02)	4.84 (0.26)	115.0 (4.2)
	16	0.918 (0.015)	0.943 (0.018)	1.03 (0.01)	2.67 (0.76)	48.77 (1.23)	4.38 (0.33)	124.4 (4.5)
	18	0.865 (0.047)	0.909 (0.026)	1.05 (0.03)	4.92 (2.62)	50.67 (1.30)	4.64 (0.30)	129.8 (4.1)
CMG	6	0.807 (0.008)	0.858 (0.005)	1.06 (0.02)	6.00 (1.32)	53.82 (0.36)	5.72 (0.22)	121.6 (12.7)
	8	0.826 (0.028)	0.869 (0.012)	1.05 (0.02)	5.00 (2.00)	53.05 (0.69)	5.50 (0.19)	132.0 (3.9)
	10	0.852 (0.036)	0.893 (0.021)	1.05 (0.02)	4.67 (2.02)	51.85 (1.35)	5.38 (0.20)	139.8 (7.4)
	12	0.901 (0.026)	0.935 (0.037)	1.04 (0.01)	3.67 (1.04)	49.55 (1.98)	5.33 (0.18)	141.8 (8.8)

[a] Standard deviations are indicated in the parentheses.
BD: Bulk density of melt granules.
TD: Tapped density of melt granules.
HR: Hausner ratio of melt granules.
CI: Compressibility index of melt granules.
Єgr: Porosity of melt granules.
Єcom: Porosity of compact prepared under a compaction pressure of 102 MPa.
MECH: Mechanical strength of compact prepared under a compaction pressure of 102 MPa.

The results obtained from replicated production batches were then averaged. The inter-variable relationships amongst the physicochemical properties of melt granules, mechanical strengths and porosities of the corresponding compacts formed under a compaction pressure of 102 MPa are depicted in the loading plots in Figs. 34 (CMG) and 35 (MMG).

The loading plots were interpreted based on the spatial distribution of the variables with respect to each other and the principal component axes. To reiterate, variables situated close together in a loading plot co-vary positively, while those situated on opposing ends are negatively correlated to each other. Variables which overlap or are indistinguishable from each other are strongly and positively correlated. Variables orthogonal (perpendicular) to each other, on the other hand, are independent (Esbensen, 2001). Both the first and second principal components (PC1 and PC2) accounted for a total of 93 % and 95 % of the variance in the data obtained in CMG and MMG, respectively.

At the outset, it was clear from both loading plots that the size distribution of melt granules produced in the two processes exerted minimal influences on their compaction behavior. This could be gauged from the orthogonal relationship of "Span" with respect to the porosities (Єcom) and mechanical strengths (MECH) of compacts observed in both Figs. 34 and 35. Fundamentally, particle densification constitutes an important preliminary step towards agglomerate growth in high shear granulation. This was reflected in the loading plot for CMG (Fig. 34) where the opposing locations of "D50" with respect to both "Fines" and "Єgr" indicated that agglomerate growth (increased D50) was accompanied by reductions in the

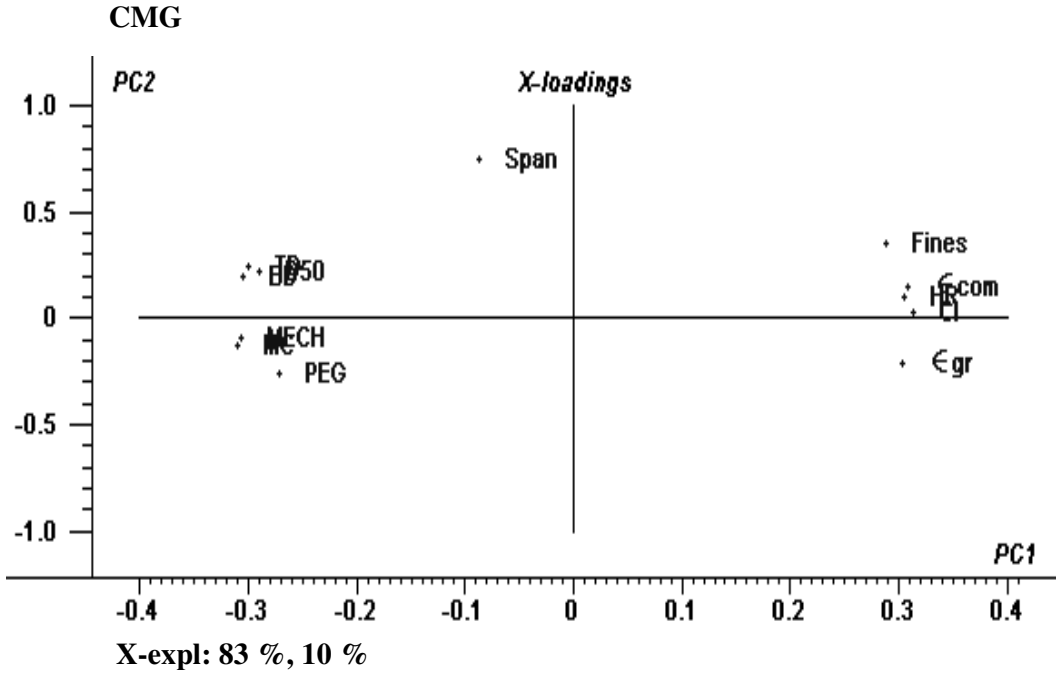

Fig. 34. Loading plot depicting the inter-variable relationships amongst the physicochemical properties of melt granules produced in CMG as well as the porosities and mechanical strengths of corresponding compacts. Abbreviated parameters are: D50: mass median diameter of melt granules (µm), BD: bulk density of melt granules (g/ml), TD: tapped density of melt granules (g/ml), HR: Hausner ratio of melt granules, CI: compressibility index of melt granules (%), Єgr: porosity of melt granules (%), PEG: binder content of melt granules (%w/w), MC: moisture content of melt granules (%w/w), Єcom: porosity of compact (%) prepared under a compaction pressure of 102 MPa, MECH: mechanical strength of compact (N) prepared under a compaction pressure of 102 MPa. The span and proportion of fines (%) are not abbreviated.

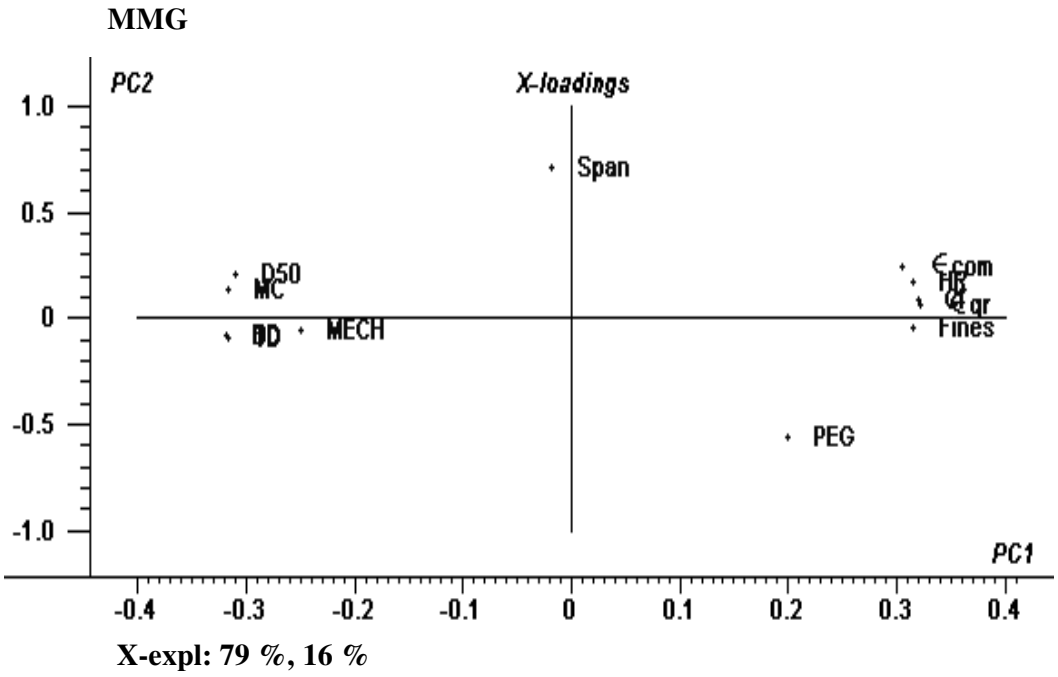

Fig. 35. Loading plot depicting the inter-variable relationships amongst the physicochemical properties of melt granules produced in MMG as well as the porosities and mechanical strengths of corresponding compacts. Abbreviated parameters are: D50: mass median diameter of melt granules (μm), BD: bulk density of melt granules (g/ml), TD: tapped density of melt granules (g/ml), HR: Hausner ratio of melt granules, CI: compressibility index of melt granules (%), Єgr: porosity of melt granules (%), PEG: binder content of melt granules (%w/w), MC: moisture content of melt granules (%w/w), Єcom: porosity of compact (%) prepared under a compaction pressure of 102 MPa, MECH: mechanical strength of compact (N) prepared under a compaction pressure of 102 MPa. The span and proportion of fines (%) are not abbreviated.

proportion of fine particles and granule porosity (Pearson correlation between D50 and Єgr, R = -0.988, $p < 0.05$). Granule porosity in turn, correlated significantly with their compressibility indices (Pearson correlation between Єgr and CI, R = 0.963, $p < 0.05$) and this indicated that larger and denser granules possessed improved flow and packing properties. When a denser granular bed was achieved in the die cavity, the inter-granular void spaces were minimized and this increased the specific surface area available for inter-granular attraction and bonding during compaction. Denser compacts with reduced porosities were thus formed. As the porosities of compacts decreased, their mechanical strengths increased. This could be inferred from the opposing locations of "MECH" and "Єcom" in the loading plot (Pearson correlation between Єcom and MECH, R = -0.998, $p < 0.01$).

The binder and moisture contents of melt granules produced in CMG also figured prominently in their compaction behavior. From the physical locations of "PEG" and "MC" with respect to "Єcom" and "MECH", it appeared that melt granules containing higher binder and moisture contents formed compacts of lower porosities and increased mechanical strengths (Pearson correlation between MECH and PEG, R = 0.953, $p < 0.05$; MECH and MC, R = 0.998, $p < 0.01$). Such observations were to be expected. Solid polyethylene glycols, being plastic and deformable in nature (Lin and Cham, 1995; Larhrib et al., 1997), have been widely exploited for modulating the tabletting behavior of aggregates (Nicklasson and Alderborn, 1999) as well as providing cushioning protection to drug-coated pellets during compaction (Bechard and Leroux, 1992; Torrado and Augsburger, 1994; Beckert et al., 1996). This was achieved through the ability of the material to deform, absorb and dissipate the applied stresses effectively during compaction, thereby enhancing the compressibility

of the aggregates and pellets. In addition, it has been reported that the compressibility of granules manufactured in a high shear mixer was more sensitive to their residual moisture contents after drying than to changes in processing conditions such as wet massing time and impeller speed (Farag Badawy et al., 2000). In the light of these findings, both the binder and moisture contents of melt granules were expected to play significant roles in their compressibility. Melt granules containing higher binder and moisture contents were likely to be more deformable and amenable to compression. At any particular compaction pressure, these melt granules deformed more readily. This facilitated the development of larger surface areas for inter-granular contact and bond formation which were responsible for the mechanical integrity of the formed compact. Thus, by way of their enhanced compressibility and deformability, melt granules containing higher binder and moisture contents formed less porous compacts of increased mechanical resilience.

Similar relationships were observed for MMG (Fig. 35). Granule growth brought about a reduction in the proportion of fines and granule porosity. Denser granules possessed better flow (Pearson correlation between ϵ_{gr} and HR, $R = 0.986$, $p < 0.05$; ϵ_{gr} and CI, $R = 0.999$, $p < 0.01$) and improved packing properties which in turn yielded compacts with reduced porosities (Pearson correlation between ϵ_{com} and HR, $R = 0.982$, $p < 0.05$; ϵ_{com} and CI, $R = 0.956$, $p < 0.05$). Accordingly, compacts of lower porosities possessed higher mechanical strengths and vice versa. With regards to the influence of the moisture contents of melt granules, a trend similar to that in CMG was observed where granules containing higher moisture contents formed mechanically stronger compacts with decreased porosities. However, a slight difference was observed in MMG pertaining to the contribution of the binder contents

of melt granules. It appeared from the distant location of “PEG” with respect to “Ɛcom” and “MECH” that the binder contents of melt granules in MMG exerted minimal bearing on their compaction behavior.

This anomaly was believed to be attributed to the non-homogeneities in binder distribution during MMG. By pooling the data sets obtained from MMG and CMG, Fig. 36 shows the relationship between the binder contents of all batches of melt granules produced and the mechanical strengths of corresponding compacts prepared under a compaction pressure of 102 MPa. Apart from two distinct outliers (marked with *), a reasonable correlation (Pearson correlation coefficient, $R = 0.870$, $p < 0.05$) was detected between the two variables for the remaining granule batches where an increase in the binder contents of melt granules led to a corresponding increase in the mechanical strengths of the resultant compacts. The ambiguity pertaining to the effect of binder content on the compaction behavior of melt granules in MMG may be addressed by the outliers which incidentally, represented the binder contents and compaction behavior of melt granules produced in MMG at massing times of 10 (MMG10) and 14 min (MMG14). Based on the binder contents of these granules, the corresponding compacts possessed unexpectedly low mechanical strengths. Those derived from the same process but at longer massing times of 16 and 18 min conformed to the general trend exhibited by the batches of melt granules and compacts derived from CMG.

From these results, it may be inferred that in MMG, the effect of the binder contents of melt granules on their compaction behavior was masked by the deviation from the

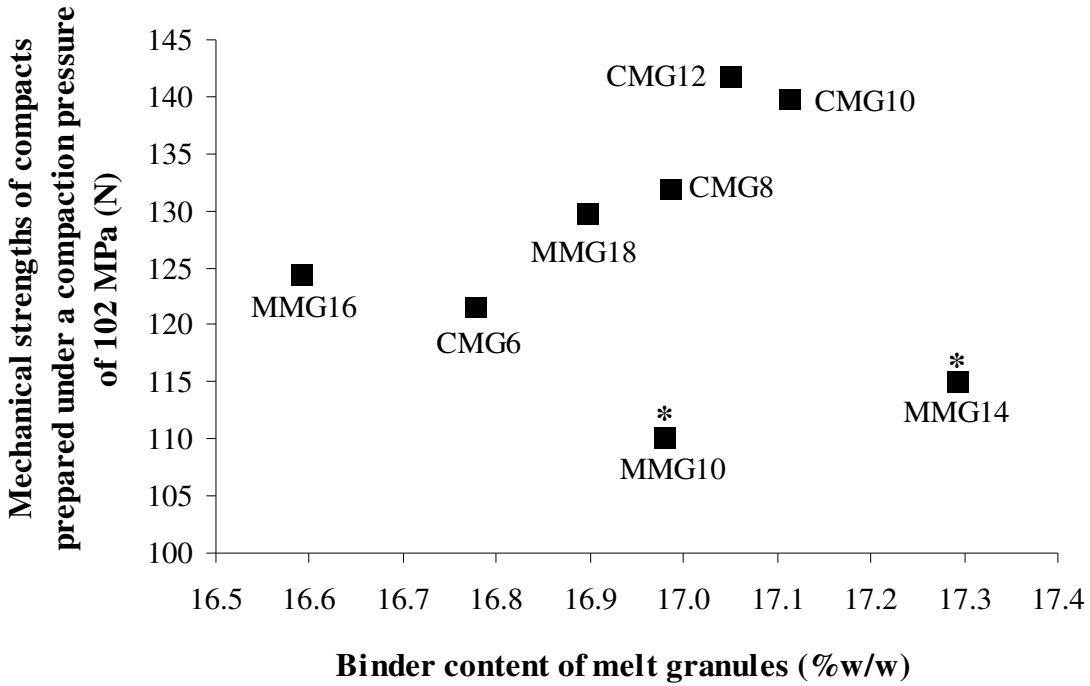

Fig. 36. Effect of the binder contents of melt granules produced at different massing times in CMG and MMG on the mechanical strengths of corresponding compacts prepared under a compaction pressure of 102 MPa. "*" refers to the outliers.

expected trend, of the melt granules produced under specific massing times of 10 and 14 min. A likely explanation for this non-conformity stemmed from issues related to content homogeneity. As discussed earlier in part D.1, greater intra- and inter-batch variations in binder contents of melt granules were observed in MMG as compared to the conventional process due to the inherent difficulties encountered in heat production and transfer. Specifically, melt granules produced at shorter massing times of 10 and 14 min in MMG exhibited greater levels of binder heterogeneity. Under such circumstances, each compact prepared from granules produced at these particular massing times may not have contained the calculated amount of binder material. This was because it was difficult to ensure that the small quantity of melt granules sampled for each compaction cycle (~ 0.5 g) comprised the different size fractions of melt granules in their correct proportions, and if disparities existed amongst the binder contents of the different size fractions of granules, the binder contents of the different granule samples compacted would be variable, inconsistent and not contain a representative amount of binder material as calculated. Thus, for the granule batches produced at 10 and 14 min in MMG, their binder contents as calculated based on the weighted contributions of the different size fractions of melt granules present might not have provided a true reflection of the actual content of binder material in each formed compact. These specific MMG experiments masked the effect of the binder contents of melt granules on their compaction behavior which would have otherwise surfaced in the loading plot in Fig. 35.

D.4. Compressibility of Melt Granules

The data presented in Fig. 36 provided the first signs of evidence that the disparities in compaction behavior of melt granules produced in MMG and CMG were attributed in

part, to the differences in their binder contents. To gain further insight and to quantify these effects, the compressibility of selected batches of melt granules produced from the two processes were studied by subjecting the melt granules to compaction pressures ranging from 13-304 MPa.

As aforesaid, melt granules prepared at shorter massing times in MMG were plagued by higher levels of binder heterogeneity. Hence, those produced at the longest massing time i.e. 18 min (MMG18) were chosen to circumvent this problem and ensure greater validity of the results. Moreover, melt granules from MMG18 exhibited the closest conformity to the general trend in Fig. 36. For CMG, melt granules produced at massing times of 6 and 10 min were selected (CMG6 and CMG10 respectively). The rationale for these choices was that the binder contents of melt granules manufactured under these 3 specific conditions (MMG18, CMG6 and CMG10) spanned a wider range and encompassed the higher, lower and intermediate ranges of binder contents amongst all the batches of melt granules eligible for assessment.

The Heckel plots of these melt granules are presented in Fig. 37. From the steep linear portions of the profiles at the initial stages of compaction (13-63 MPa), it was evident that the melt granules underwent extensive volume reduction early in the process. Beyond 100 MPa, volume reduction of the granule bed became almost negligible. It is well known that both lactose and DCP are brittle materials which undergo fragmentation during compaction (Garr and Rubinstein, 1992; Ilkka and Paronen, 1993; Juppo, 1996; Larhrib and Wells, 1998). Interestingly, however, the compaction profiles of the melt granules conformed to the type C variant of the Heckel plot which

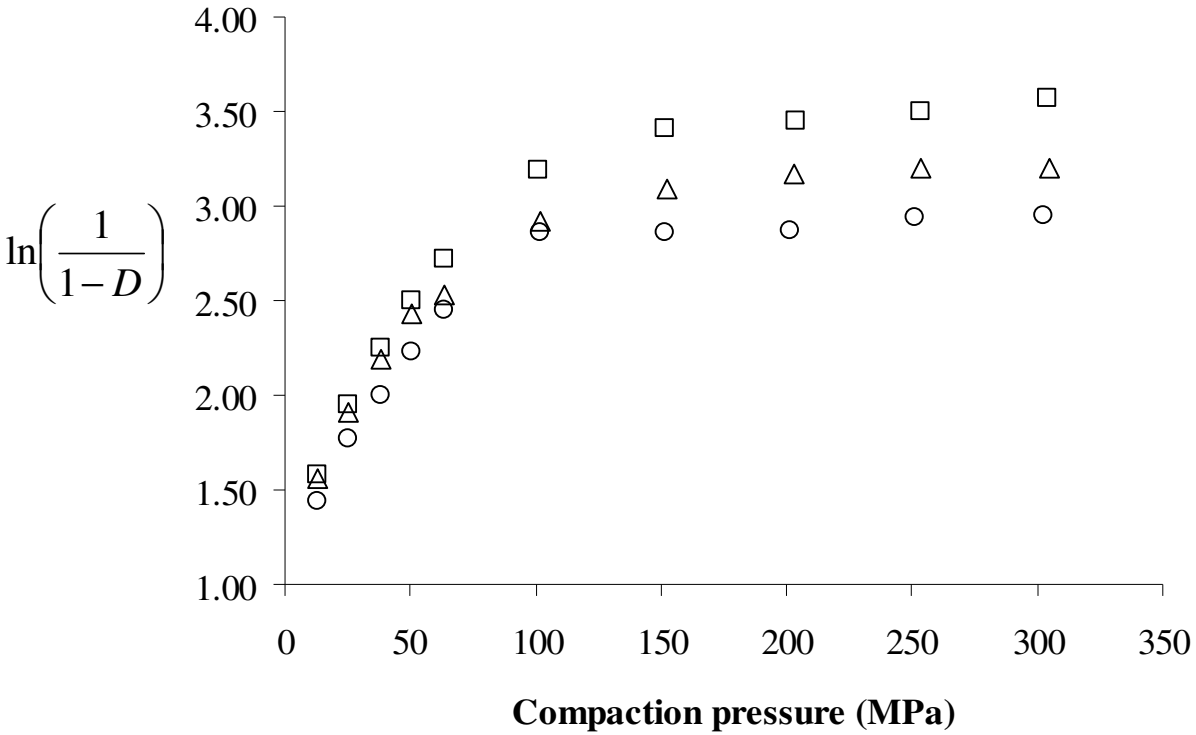

Fig. 37. Heckel plots of selected batches of melt granules produced in CMG at massing times of (○) 6 and (Δ) 10 min as well as MMG at a massing time of (□) 18 min.

indicated that they consolidated by plastic flow (Paronen and Ilkka, 1995).

Clearly, the presence of a soft, waxy and plastically-deforming material such as polyethylene glycol 3350 in the lactose and DCP-based granules caused significant modifications to their volume reduction behavior and changed it from one that was primarily fragmenting to another dominated by plastic deformation. This phenomenon has been reported in studies that involved the compaction of powder mixtures comprising both fragmenting and plastically-deforming materials. In these systems, it was found that plastic flow exerted more pronounced effects on volume reduction than fragmentation (Ilkka and Paronen, 1993). It has also been reported that when polyethylene glycol was employed as a binding agent in granules, incorporated both in solution (polyethylene glycol 6000) and molten form (polyethylene glycols 6000 and 20000) in wet and melt granulation, respectively, the deformation tendencies of resultant granules were enhanced significantly (Nicklasson and Alderborn, 1999; Kidokoro et al., 2002). These observations were likely to be attributed to the low yield pressures of polyethylene glycols (Larhrib and Wells, 1998) which render them highly susceptible to deformation even at low compaction pressures. Compaction studies of pure polyethylene glycol 10000 (Larhrib and Wells, 1997a-b) revealed that the majority of volume reduction of the powder bed occurred at low pressures ($\leq$ 82 MPa). A predominantly linear profile was observed during the initial stages of compaction following which changes in powder volume, if any, were minimal or negligible as compaction pressures increased. This information is consistent with the pronounced volume reduction of melt granules observed at pressures below 100 MPa.

Further evidence that supported the predominance of plastic deformation rather than fragmentation as the main mechanism of volume reduction of the melt granules pertained to the effects of the porosities of granules on their compaction behavior. In compaction studies of agglomerates comprising materials which are brittle and fragmenting in nature, agglomerates of higher porosities typically exhibited increased fragmentation propensities and formed compacts which were mechanically stronger and less porous. This was attributed to the increased surface areas available for inter-particulate bonding as a result of particle fragmentation (Wikberg and Alderborn, 1991, 1992a-b, 1993). Interestingly however, a trend reversal was observed in the current study where granules of lower porosities formed compacts of increased mechanical strengths instead. As depicted earlier in Figs. 34 and 35, this was mediated through the improved packing properties of the denser granules in the die cavity. These findings provided a clear indication that up to a compaction pressure of 102 MPa, granule fragmentation was not the predominant mechanism responsible for the volume reduction and compaction behavior of melt granules. The critical underlying factors were the amount and availability of binding material in the melt granules which affected the extent to which they could deform and fill up existing inter-granular void spaces to facilitate bonding interactions amongst the granules in the die cavity.

Taking a step further, the yield pressures of melt granules were computed. Regression analyses were performed over the pressure ranges of 25-63 MPa for melt granules produced at 6 and 18 min in CMG (CMG6) and MMG (MMG18), respectively. A lower pressure range of 13-50 MPa was selected for melt granules produced at 10 min in CMG (CMG10). These ranges were employed as the experimental data points

possessed the highest goodness-of-fit (R^2) values. The linear equations together with the corresponding yield pressures of granules are summarized in Table 10.

Table 10. Equations governing the linear portions of the Heckel plots and corresponding yield pressures of selected batches of melt granules.

Type of melt granules	Equation	R^2	Yield pressure (MPa)
CMG6	y = 0.018x + 1.318	1.000	55.56
CMG10	y = 0.0228x + 1.300	0.993	43.86
MMG18	y = 0.0201x + 1.464	0.995	49.75

It had been reported that materials with yield pressures of less than 80 MPa deformed mainly by plastic flow and as the value increased beyond this limit, there was an increased likelihood of material fragmentation (Podczek and Revesz, 1993). The yield pressures of the melt granules ranged from 43.9-55.6 MPa which were significantly lower than 80 MPa and those of pure α-lactose monohydrate (~ 200 MPa) or DCP (~ 550 MPa) (Doldán et al., 1995; Busignies et al., 2004). This further attested to their plastic nature.

As mentioned earlier, the residual moisture present in the melt granules also enhanced their tendencies to deform plastically. As both the binder and moisture contents of melt granules were expressed in an identical manner (%w/w), they were summed up to provide a measure of the total fraction by weight of melt granules that were composed of these two components. Their effects on the yield pressures of the 3 selected batches of melt granules are quantified in Fig. 38.

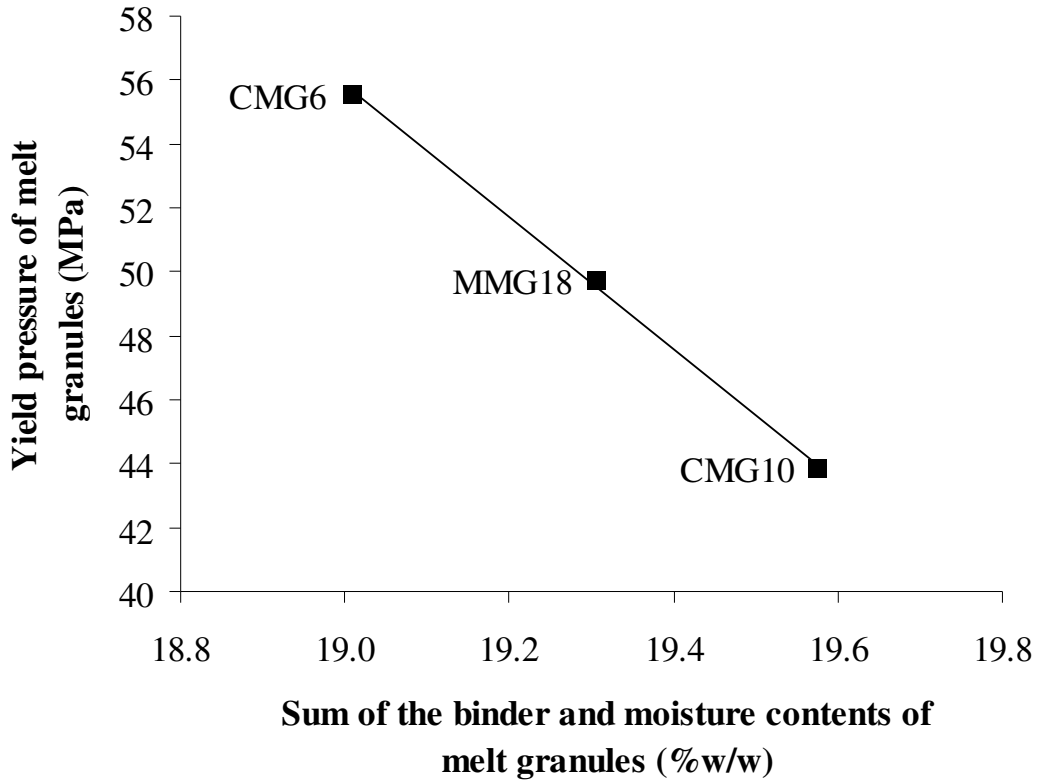

Fig. 38. The influences of the binder and moisture contents of melt granules on their yield pressures.

Clearly, the influences of the binder and moisture contents of melt granules on their compressibility were mediated through their combined effects on the yield pressures of granules. A linear relationship was obtained (R^2 = 0.999) where melt granules which possessed the highest combined binder and moisture content i.e. CMG10 exhibited the lowest yield pressure and vice versa. Being most deformable upon compaction, melt granules produced in CMG10 formed compacts of highest mechanical strength (139.8 N), followed by those produced from MMG18 (129.8 N) and CMG6 (121.6 N) in decreasing order.

5. CONCLUSION

The microwave dielectric responses of several important pharmaceutical materials were determined at 300 MHz, 1 GHz and 2.45 GHz. At their respective bulk densities, the variation in dielectric responses of the materials was found to be attributed primarily to the disparities in their moisture contents. For each material, a linear relationship was established between its dielectric response and density from which material dielectric responses at different bulk densities may be determined by extrapolation.

The use of microwaves for drying acetylsalicylic acid-loaded lactose granulations in a single pot high shear processor was investigated from a formulation perspective. Macroscopically, the volume of the granulation bed affected the overall drying profiles of granules via its effects on the extent of microwave penetration into the product load. At the microscopic level, drying was dependent on the heating capabilities and movement of water molecules entrapped in the granular structure, with larger and more porous granules exhibiting higher drying rates. This is in contrast to conventional drying where the exposed surfaces of granules played a more important role in determining the efficiency of drying. The stability of acetylsalicylic acid was unaffected by microwaves.

The dielectric properties of the starting materials played a more significant role when microwaves were employed for melt granulation as compared to drying. This is because unlike microwave-assisted drying where water constituted the main target for heating, the feasibility of microwave-induced melt granulation relied on the heating capabilities of the starting dry powder mixture on microwave exposure. It was found

that the heating capabilities of the agglomerating powder masses under the influence of microwaves were reliant on the volume fraction of the dielectrically active component, anhydrous dicalcium phosphate, incorporated in the formulation. When used in a 1:1 ratio with lactose, anhydrous dicalcium phosphate did not bring about an improvement in the heating rates of the powder masses under the influence of microwaves as compared to the conventionally-heated ones. The low heat acquisition rates of the powders was further exacerbated by non-uniformities in microwave heating which affected process monitoring and efficiency as well as the physicochemical and compaction properties of resultant melt granules produced from microwave-induced melt granulation. The use of higher concentrations of anhydrous dicalcium phosphate could potentially mitigate these effects of microwave-induced heating.

In conclusion, the dielectric properties of a wide range of common pharmaceutical materials have been evaluated to address the current knowledge gap in the area. Additionally, the work done has contributed further to the understanding of the mechanism of microwave-assisted drying of pharmaceutical granules and unveiled further opportunities for future applications of microwaves in melt granulation. As exemplified in these specific drying and granulation studies, the dielectric properties of materials exert a significant impact on the control and outcomes of microwave-assisted processes. This sets it apart from processes fuelled by conventional energy sources where material properties assume a less critical role.

Apart from the significance of material dielectric properties, it was found that the unique mechanism of microwave-induced heating had contributed to differences in

the product qualities, efficiencies and control of processes fuelled by microwaves and conventional energy sources. In a nutshell, as long as a judicious choice of dielectric materials has been made at the outset, the use of microwaves as an alternative energy source for pharmaceutical manufacturing processes can improve process efficiencies and product qualities as well as confer greater flexibilities in the control and monitoring aspects of these operations.

6. REFERENCES

Adu, B., Otten, L., 1996. Modeling microwave heating characteristics of granular hygroscopic solids. J. Microwave Power EE., 31, 35-42.

Anuar, N.K., Wong, T.W., Deepak, K.G., Taib, M.N., 2007. Characterization of hydrocypropylmethylcellulose films using microwave non-destructive testing technique. J. Pharmaceut. Biomed., 43, 549-557.

Araszkiewicz, M., Koziol, A., Lupinska, A., Lupinski, M., 2006. Temperature distribution in a single sphere dried with microwaves and hot air. Dry Technol., 24, 1381-1386.

Araszkiewicz, M., Koziol, A., Lupinska, A., Lupinski, M., 2007. IR techniques for studies of microwave-assisted drying. Dry Technol., 25, 569-574.

Araszkiewicz, M., Koziol, A., Oskwarek, A., Lupinski, M., 2004. Microwave drying of porous materials. Dry Technol., 22, 2331-2341.

Arbós, P., Campanero, M.A., Arangoa, M.A., Renedo, M.J., Irache, J.M., 2003. Influence of surface characteristics of PVM/MA nanoparticles on their bioadhesive properties. J Control Release, 89, 19-30.

Arbós, P., Wirth, M., Arangoa, M.A., Gabor, F., Irache, J.M., 2002. Gantrez® AN as a new polymer for the preparation of ligand-nanoparticles conjugates. J. Control Release, 83, 321-330.

Aulton, M.E., 2007. Drying. In: Aulton, M.E. (Ed.), Pharmaceutics: the design and manufacture of medicines, 3rd Edn., Churchill Livingstone, New York, pp. 425-440.

Bataille, B., Ligarski, K., Jacob, M., Thomas, C., Duru. C., 1993. Study of the influence of spheronization and drying conditions on the physico-mechanical properties of neutral spheroids containing avicel PH101 and lactose. Drug Dev. Ind. Pharm., 19, 653-671.

Bechard, S.R., Leroux, J.C., 1992. Coated pelletized dosage form: effect of compaction on drug release. Drug Dev. Ind. Pharm., 18, 1927-1944.

Beckert, T.E., Lehman, K., Schmidt, P.C., 1996. Compression of enteric coated pellets to disintegrating tablets. Int. J. Pharm., 143, 13-23.

Berbert, P.A., Stenning, B.C., 1996. Analysis of density-independent equations for determination of moisture content of wheat in the radiofrequency range. J. Agr. Eng. Res., 65, 275-286.

Bergese, P., Colombo, I., Gervasoni, D., Depero, L.E., 2003. Microwave generated nanocomposites for making insoluble drugs soluble. Mat. Sci. Eng. C-Bio. S., 23, 791-795.

Berteli, M.N., Marsaioli, A.J., Rodier, E., 2007. Study of a microwave-assisted vacuum drying process applied to the granulated pharmaceutical drug hydrochlorothiazide. J. Microwave Power EE., 40, 241-250.

Betz, G., Bürgin, P.J., Leuenberger, H., 2004. Power consumption measurement and temperature recording during granulation. Int. J. Pharm., 272, 137-149.

Bodek, K.H., Bak, G.W., 1999. Ageing phenomena of chitosan and chitosan-diclofenac sodium systems detected by low frequency dielectric spectroscopy. Eur. J. Pharm. Biopharm., 48, 141-148.

Buckton, G., Dissado, L.A., Hill, R.M., Newton, J.M., 1987. The potential value of dielectric response measurements in the assessment of the wettability of powders. Int. J. Pharm., 38, 1-7.

Buschmüller, C., Wiedey, W., Döscher, C., Dressler, J., Breitkreutz, J., 2007. In-line monitoring of granule moisture in fluidized–bed dryers using microwave resonance technology. Eur. J. Pharm. Biopharm., 69, 380-387.

Busignies, V., Tchoreloff, P., Leclerc, B., Besnard, M., Couarraze, G., 2004. Compaction of crystallographic forms of pharmaceutical granular lactoses. I. Compressibility. Eur. J. Pharm. Sci., 58, 569-576.

Chamchong, M., Datta, A. K., 1999. Thawing of foods in a microwave oven: II Effect of load geometry and dielectric properties. J. Microwave Power EE, 34, 22-32.

Chatrath, M., Staniforth, J.N., 1990. The relative influence of dielectric and other drying techniques on the physico-mechanical properties of a pharmaceutical tablet excipient. Part I: compaction characteristics. Dry Technol., 8, 1089-1109.

Chee, S.N., Johansen, A.L., Gu, L., Karlsen, J., Heng, P.W.S., 2005. Microwave drying of granules containing a moisture sensitive drug: a promising alternative to fluid bed and hot air oven drying. Chem. Pharm. Bull., 53, 770-775.

Chen, G., Wang, W., Mujumdar, A.S., 2001. Theoretical study of microwave heating patterns on batch fluidized bed drying of porous material. Chem. Eng. Sci., 56, 6823-6835.

Chua, K.J., Mujumdar, A.S., Chou, S.K., 2003. Intermittent drying of bioproducts-an overview. Bioresource Technol., 90, 285-295.

Cliff, M.J., 1990. Granulation end point and automated process control of mixer granulators: part I. Pharm. Technol., 14, 112-132.

Cole, K.S., Cole, R.H., 1941. Dispersion and absorption in dielectrics. I. Alternating current characteristics. J. Chem. Phys., 9, 341-351.

Covari, V., Fry, W.C., Seibert, W.L., Augsburger, L., 1992. Instrumentation of a high shear mixer: evaluation and comparison of a new capacitive sensor, a watt meter and a strain gauge torque sensor for wet granulation monitoring. Pharm. Res., 9, 1524-1533.

Craig, D.Q.M., 1992. Applications of low frequency dielectric spectroscopy to the pharmaceutical sciences, Drug Dev. Ind. Pharm., 18, 1207-1223.

Craig, D.Q.M., 1995. Dielectric analysis of pharmaceutical systems, Taylor and Francis, London.

Craig, D.Q.M., Davies, C.F., Boyd, J.C., Hakes, L.B., 1991. Characterization of the variation between batches of fast-flo lactose using low frequency dielectric spectroscopy. J. Pharm. Pharmacol., 43, 444-445.

Craig, D.Q.M., Tamburic, S., 1997. Dielectric analysis of bioadhesive gel systems. Eur. J. Pharm. Biopharm., 44, 61-70.

Dávid, Á., Benkóczy, Z., Ács, Z., Greskovits, D., Dávid, Á.Z., 2000. The theoretical basis for scaling-up by the use of the method of microwave granulation, Drug Dev. Ind. Pharm., 26, 943-951.

De la Hoz, A., Díaz-Ortiz, Á., & Moreno, A., 2005. Microwaves in organic synthesis: Thermal and non-thermal microwave effects. Chem. Soc. Rev., 34, 164-178.

De Loor, G.P., 1968. Dielectric properties of heterogeneous mixtures containing water. J. Microwave Power, 3, 67-73.

Debye, P.J.W., 1929. Polar molecules, Chemical Catalogue Co., New York.

Doelling, M.K., Jones, D.M., Smith, R.A., Nash, R.A., 1992. The development of a microwave fluid-bed processor. I. Construction and qualification of a prototype laboratory unit. Pharm. Res, 9, 1487-1492.

Doelling, M.K., Nash, R.A., 1992. The development of a microwave fluid bed processor. II. Drying performance and physical characteristics of typical pharmaceutical granulations. Pharm. Res., 9, 1493-1501.

Dolande, J., Datta, A., 1993. Temperature profiles in microwave heating of solids: A systematic study. J. Microwave Power EE., 28, 58-67.

Doldán, C., Souto, C., Concheiro, A., Martínez-Pacheco, R., Gómez-Amoza, J.L., 1995. Dicalcium phosphate dihydrate and anhydrous dicalcium phosphate for direct compression: a comparative study. Int. J. Pharm., 124, 69-74.

Duschler, G., Carius, W., Bauer, K.H., 1995. Single step granulation method with microwaves: preliminary studies and pilot scale results. Drug Dev. Ind. Pharm., 21, 1599-1610.

Esbensen, K.H., 2001. Principal component analysis (PCA) - introduction. In: Esbensen, K.H., (Ed.), Multivariate data analysis in practice – an introduction to multivariate data analysis and experimental design, 5th Edn., Camo Software AS, Norway, pp. 19-74.

Eskilsson, C.S., Björklund, E., 2000. Analytical-scale microwave-assisted extraction. J. Chromatogr. A, 902, 227-250.

Farag Badawy, S.I., Menning, M.M., Gorko, M.A., Gilbert, D.L., 2000. Effect of process parameters on compressibility of granulation manufactured in a high-shear mixer. Int. J. Pharm., 198, 51-61.

Faure, A., York, P., Rowe, R.C., 2001. Process control and scale-up of pharmaceutical wet granulation processes: a review. Eur. J. Pharm. Biopharm., 52, 269-277.

Frederikse, H.P.R., 2008. Section 12 Polarizabilities of atoms and ions in solids. In: Lide, D.R., (Ed.), Handbook of chemistry and physics, CRC Press, Ohio, pp. 13-14.

Gabriel, C., Gabriel S., Grant, E.H., Halstead, B.S.J., Mingos, D.M.P., 1998. Dielectric parameters relevant to microwave dielectric heating. Chem. Soc. Rev., 27, 213-223.

García, A., Bueno, J.L., 1998. Improving energy efficiency in combined microwave-convective drying. Dry Technol., 16, 123-140.

Garr, J.S.M., Rubinstein, M.H., 1992. Consolidation and compaction characteristics of a three-component particulate system. Int. J. Pharm., 82, 71-77.

George, R.M., Burnett, S-A., 1991. General guidelines for microwaveable products, Food Control, 2, 35-43.

Giry, K., Genty, M., Viana, M., Wuthrich, P., Chulia, D., 2006. Multiphase versus single pot granulation process: influence of process and granulation parameters on granule properties. Drug Dev. Ind. Pharm., 32, 509-530.

Gladstone, J.H., Dale, T.P., 1863. Researches on the refraction, dispersion and sensitiveness of liquids. Phil. Trans., 153, 317-343.

Goggin, P.L., He, R., Craig, D.Q.M., Gregory, D.P., 1998. An investigation into the use of low frequency dielectric spectroscopy as a means of characterizing the structure of creams based on aqueous cream BP. J. Pharm. Sci., 87, 559-564.

Gokhale, R., Sun Y., Shukla, A.J., 2005. High-Shear Granulation. In: Parikh, D.M. (Ed.), Handbook of pharmaceutical granulation technology, 2nd Edn., Taylor and Francis Group, London, pp. 191-228.

Goyette, J., Chahine, R., Bose, T.K., 1990. Importance of the dielectric properties of materials for microwave heating. Dry Technol., 8, 1111-1121.

Gradinarsky, L., Brage, H., Lagerholm, B., Björn, I.N., Folestad, S., 2006. *In-situ* monitoring and control of moisture content in pharmaceutical powder processes using an open-ended coaxial probe. Meas. Sci. Technol., 17, 1847-1853.

Gunasekaran, S., 1999. Pulsed microwave-vacuum drying of food materials. Dry Technol., 17, 395-412.

Heckel, R.W., 1961. Density-pressure relationship in powder compaction. Trans. Metall. Soc., AIME, 221, 671-675.

Hedrick, J.L., Miller, R.D., Hawker, C.J., Carter, K.R., Volksen, W., Yoon, D.Y., Trollsås, M., 1998. Templating nanoporosity in thin-film dielectric insulators. Adv. Mater., 10, 1049-1053.

Hegedűs, Á., Pintye-Hódi, K., 2007. Comparison of the effects of different drying techniques on properties of granules and tablets made on a production scale. Int. J. Pharm., 330, 99-104.

Heng, P.W.S., Liew, C.V., Soh, J.L.P., 2004. Pre-formulation studies on moisture absorption in microcrystalline cellulose using differential thermo-gravimetric analysis. Chem. Pharm. Bull., 52, 384-390.

Heng, P.W.S., Wong, T.W., Shu, J.J., Wan, L.S.C. 1999. A new method for the control of size of pellets in the melt pelletization process with a high shear mixer. Chem. Pharm. Bull., 47, 633-638.

Hill, R.M., Beckford, E.S., Rowe, R.C., Jones, C.B., Dissado, L.A., 1990. The characterization of oil in water emulsions by means of a dielectric technique. J. Colloid Interf. Sci, 138, 521-533.

Hoang, T.H., Sharma, R., Susanto, D., Di Maso, M., Kwong, E., 2007. Microwave-assisted extraction of active pharmaceutical ingredient from solid dosage forms. J. Chromatogr. A, 1156, 149-153.

Horsthuis, G.J.B., Van Laarhoven, J.A.H., Van Rooij, R.C.B.M., Vromans, H., 1993. Studies on upscaling parameters of the Gral high shear granulation process. Int. J. Pharm., 92, 143-150.

İçier F., Baysal T., 2004. Dielectrical properties of food materials – 1: factors affecting and industrial uses. Crit. Rev. Food Sci., 44, 465-471.

Ilkka, J., Paronen, P., 1993. Prediction of the compression behavior of powder mixtures by the Heckel equation. Int. J. Pharm., 94, 181-187.

Jansen, W., Van der Wekken, B., 1991. Modelling of dielectrically assisted drying. J. Microwave Power EE., 26, 227-236.

Jia, X., 1993. Experimental and numerical study of microwave power distributions in a microwave heating applicator. J. Microwave Power EE., 28, 25-31.

Jones, P.L., Rowley, A.T., 1996. Dielectric drying. Dry Technol., 14, 1063-1098.

Juppo, A.M., 1996. Change in porosity parameters of lactose, glucose and mannitol granules caused by low compression force. Int. J. Pharm., 130, 149-157.

Kardum, J.P., Sander, A., Skansi, D., 2001. Comparison of convective, vacuum and microwave drying of chlorpropamide. Dry Technol., 19, 167-183.

Kelen, A., Pallai-Varsanyi, E., Ress, S., Nagy, T., Pintye-Hodi, K., 2006b. Practical method for choosing diluent that ensures the best temperature uniformity in the case of pharmaceutical microwave vacuum drying of a heat sensitive product. Eur. J. Pharm. Biopharm., 62, 101-109.

Kelen, A., Ress, S., Nagy, T., Pallai-Varsanyi, E., Pintye-Hodi, K., 2006a. "3D layered thermography" method to map the temperature distribution of a free flowing bulk in case of microwave drying. Int. J. Heat Mass Tran., 49, 1015-1021.

Kelen, A., Ress, S., Nagy, T., Pallai-Varsanyi, E., Pintye-Hodi, K., 2006c. Mapping of temperature distribution in pharmaceutical microwave vacuum drying. Powder Technol., 162, 133-137.

Kent, M., Meyer, W., 1982. A density-independent microwave moisture meter for heterogeneous foodstuffs. J. Food Eng., 1, 31-42.

Kerč, J., Srčič, S., Kofler, B., 1998. Alternative solvent-free preparation methods for felodipine surface solid dispersions. Drug Dev. Ind. Pharm., 24, 359-363.

Kibbe, A.H., Weller, P.J., 2005. Lactose. In: Rowe, R.C., Sheskey, P.J., Weller P.J. (Eds.), Handbook of pharmaceutical excipients, 4th Edn., Pharmaceutical Press, Chicago, pp. 323-332.

Kidokoro, M., Haramiishi, Y., Sagasaki, S., Shimizu, T., Yamamoto, Y., 2002. Application of fluidized hot-melt granulation (FHMG) for the preparation of granules for tableting; properties of granules and tablets prepared by FHMG. Drug Dev. Ind. Pharm., 28, 67-76.

Killeen, M.J., 1999. Comparison of granular and tablet properties for products produced by forced air and microwave/vacuum drying. Pharm. Eng., 19, 48-58.

Kinney, G.F., 1957. Engineering properties and applications of plastics. John Wiley and Sons Inc., New York.

Kockisch, S., Rees, G.D., Tsibouklis, J., Smart, J. D., 2005. Mucoadhesive, triclosan-loaded polymer microspheres for application to the oral cavity: preparation and controlled release characteristics. Eur. J. Pharm. Biopharm., 59, 207-216.

Kraszewski, A., Trabelsi, S., Nelson, S.O., 1998. Comparison of density-independent expressions for moisture content determination in wheat at microwave frequencies. J. Agr. Eng. Res., 71, 227-237.

Kraszewski, A.W., Nelson, S.O., 1992. Wheat moisture content and bulk density determination by microwave parameters measurement. Can. Agr. Eng., 34, 327-335.

Kristensen, H.G., Schaefer, T., 1987. A review of pharmaceutical wet granulation. Drug Dev. Ind. Pharm., 13, 803-872.

Ku, H.S., Siores, E., Taube, A., Ball, J.A.R., 2002. Productivity improvement through the use of industrial microwave technologies. Comput. Ind. Eng., 42, 280-290.

Kudra, T., 2004. Energy aspects in drying, Dry Technol., 22, 917-932.

Kudra, T., Raghavan, G.S.V., Akyel, C., Bosisio, R., Van De Foort, F.R., 1992. Electromagnetic properties of milk and its constituents at 2.45 GHz. J Microwave Power EE., 27, 199-204.

Kumar, V., Reus-Medina, M., Yang, D., 2002. Preparation, characterization and tabletting properties of a new cellulose-based pharmaceutical aid. Int. J. Pharm., 235, 129-140.

Labhasetwar, V.D., Dorle, A.K., 1988. A study on the dielectric constant of salicylic acid and aspirin compacts during aging. Int. J. Pharm., 47, 261-262.

Landau, L.D., Lifshitz, E.M., 1960. Electrodynamics of continuous media, Pergamon Press, Oxford.

Larhrib, H., Wells, J.I., 1997a. Compression of thermally treated polyethylene glycol 10000. Int. J. Pharm., 153, 51-58.

Larhrib, H., Wells, J.I., 1997b. Polyethylene glycol and dicalcium phosphate mixtures: effect of tableting pressure. Int. J. Pharm., 159, 75-83.

Larhrib, H., Wells, J.I., 1998. Compression speed on polyethylene glycol and dicalcium phosphate tableted mixtures. Int. J. Pharm., 160, 197-206.

Larhrib, H., Wells, J.I., Rubinstein, M.H., 1997. Compressing polyethylene glycols: the effect of compression pressure and speed. Int. J. Pharm., 147, 199-205.

Lewandowicz, G., Fornal, J., Walkowski, A., 1997. Effect of microwave radiation on potato and tapioca starches. Carbohyd. Polym., 34, 213-220.

Lewandowicz G, Jankowski T, Fornal J., 2000. Effect of microwave radiation on physico-chemical properties and structure of cereal starches. Carbohyd. Polym., 42, 193-199.

Lin, C., Cham, T., 1995. Compression behavior and tensile strength of heat-treated polyethylene glycols. Int. J. Pharm., 118, 169-179.

Looyenga, H., 1965. Dielectric constants of heterogeneous mixtures. Physica, 31, 401-406.

Luppi, B., Cerchiara, T., Bigucci, F., Di Pietra, A.M., Orienti, I., Zecchi, V., 2003. Crosslinked poly(methyl vinyl ether-co-maleic anhydride) as topical vehicles for hydrophilic and lipophilic drugs. Drug Deliv., 10, 239-244.

Malafaya, P.B., Elvira, C., Gallardo, A., San Román, J., Reis, R.L., 2001. Porous starch-based drug delivery systems processed by a microwave route. J. Biomat. Sci.-Polym. E., 12, 1227-1241.

Mandal, T.K., 1995. Evaluation of microwave drying for pharmaceutical granulations. Drug Dev. Ind. Pharm., 21, 1683-1688.

Mathes, K.N., 1988. Electrical properties. In: Kroschwitz, J.I. (Ed.), Electrical and electronic properties of polymers: a state-of-the-art compendium, John Wiley and Sons Inc., New York, pp. 101-181.

Matsuya, Y., Antonucci, J.M., Matsuya, S., Takagi, S., Chow, L.C., 1996. Polymeric calcium phosphate cements derived from poly(methyl vinyl ether-maleic acid). Dent. Mater., 12, 2-7.

McLoughlin, C.M, McMinn, W.A.M., Magee, T.R.A., 2003a. Physical and dielectric properties of pharmaceutical powders. Powder Technol., 134, 40-51.

McLoughlin, C.M., McMinn, W.A.M., Magee, T.R.A., 2003b. Microwave drying of multi-component powder systems. Dry Technol., 21, 293-309.

McMinn, W.A.M., McLoughlin, C.M., Magee, T.R.A., 2004. Temperature variations in powder beds during combined microwave-convective drying. Dry Technol., 22, 1897-1919.

McMinn, W.A.M., McLoughlin, C.M., Magee, T.R.A., 2006. Temperature characteristics of pharmaceutical powders during microwave drying. Dry Technol., 24, 571-580.

Metaxas, A.C., Meredith, R.J., 1983. Industrial microwave heating, Peter Peregrinus Ltd., London.

Meyer, W., Schilz, W., 1980. A microwave method for density-independent determination of the moisture content of solids. J. Phys. D. Appl. Phys., 13, 1823-1830.

Moneghini, M., Bellich, B., Baxa, P., Princivalle, F., 2008. Microwave generated solid dispersions containing ibuprofen. Int. J. Pharm., 361, 125-130.

Mort, P.R., 2005. Scale up of binder agglomeration processes. Powder Technol., 150, 86-103.

Nacsa, Á., Ambrus, R., Berkesi, O., Szabó-Révész, P., Aigner, Z., 2008. Water-soluble loratadine inclusion complex: Analytical control of the preparation by microwave irradiation. J. Pharmaceut. Biomed., 48, 1020-1023.

Nelson, S.O., 1983. Observations on the density dependence of the dielectric properties of particulate materials. J. Microwave Power, 18, 143-152.

Nelson, S.O, 1992a. Estimation of permittivities of solids from measurements on pulverized or granular materials. In: Priou, A. (Ed.), Dielectric properties of heterogeneous materials, Elsevier Science Publishing Co., New York, pp. 231-271.

Nelson, S.O., 1992b. Measurement and applications of dielectric properties of agricultural products. IEEE T. Instrum. Meas., 41, 116-122.

Nelson, S.O., 1994. Measurement of microwave dielectric properties of particulate materials. J. Food Eng. 21, 365-384.

Nelson, S.O., Datta, A.K., 2001. Dielectric properties of food materials and electric field interactions. In: Nelson, S.O., Datta, A.K. (Eds.), Handbook of microwave technology for food applications, Marcel Dekker, New York, pp. 69-114.

Newman, A.W., 1995. Micromeritics. In: Brittain, H.G., (Ed.), Physical characterization of pharmaceutical solids, Marcel Dekker, New York, pp. 253-280.

Nicklasson, F., Alderborn, G., 1999. Modulation of the tabletting behavior of microcrystalline cellulose pellets by the incorporation of polyethylene glycol. Eur. J. Pharm. Science, 9, 57-65.

Nieuwmeyer, F.J.S., Maarschalk, K., Vromans, H., 2007. Granule breakage during drying processes. Int. J. Pharm., 329, 81-87.

Nurjaya, S., Wong, T.W., 2005. Effects of microwave on drug release properties of matrices of pectin. Carbohyd. Polym., 62, 245-257.

Orfeuil, M., 1987. Electric process heating: technologies, equipments, applications, Battelle Press, Ohio.

Owens, T.S., Dansereau, R.J., Sakr, A., 2005. Development and evaluation of extended release bioadhesive sodium fluoride tablets. Int. J. Pharm., 288, 109-122.

Papadimitriou, S.A., Bikiaris, D., Avgoustakis, K., 2008. Microwave-induced enhancement of the dissolution rate of poorly water-soluble Tibolone from polyethylene glycol solid dispersions. J. Appl. Polym. Sci., 108, 1249-1258.

Parker, T.G., 1972. Dielectric properties of polymers II. In: Jenkins, A.D. (Ed.), Polymer science, a materials science handbook, North-Holland Publishing Company, Amsterdam, pp. 1297-1327.

Paronen, P., Ilkka, J., 1995. Porosity-pressure functions. In: Alderborn, G., Nystrom, C., (Eds.), Pharmaceutical powder compaction technology, Marcel Dekker, New York, pp. 55-75.

Péré, C., Rodier, E., Louisnard, O., 2001. Microwave vacuum drying of porous media: verification of a semi empirical formulation of the total absorbed power. Dry Technol., 19, 1005-1022.

Perkin, R.M., 1979. Prospects of drying with radio frequency and microwave electromagnetic fields. J. Separ. Process Tech., 1, 14-23.

Podczek, F., Revesz, O., 1993. Evaluation of the properties of microcrystalline and microfine cellulose powders. Int. J. Pharm., 91, 183-193.

Poska, R., 1991. Integrated mixing granulating and microwave drying: a development experience. Pharm. Eng. 11, 9-13.

Powell, S.D., McLendon, B.D., Nelson, S.O., Kraszewski, A., Allison, J.M., 1988. Use of a density independent function and microwave measurement system for grain moisture measurement. T. ASAE., 31, 1875-1880.

Prosetya, H., Datta, A., 1991. Batch microwave heating of liquids: an experimental study. J. Microwave Power EE., 26, 215-226.

Ratanadecho, P., Aoki, K., Akahori, M., 2001. A numerical and experimental study of microwave drying using a rectangular waveguide. Dry Technol., 19, 2209-2234.

Ratanadecho, P., Aoki, K., Akahori, M., 2002. Influence of irradiation time, particle sizes and initial moisture content during microwave drying of multi-layered capillary porous materials. J. Heat Transf., 124, 151-161.

Remmen, H.H.J., Ponne, C.T., Nijhuis, H.H., Bartels, P.V., Kerkhof, P.J.A.M., 1996. Microwave heating distributions in slabs, spheres and cylinders with relation to food processing. J. Food Sci., 61, 1105-1113.

Rowe, R.C., 1997. Variation in cetostearyl alcohol and lecithin from different sources: evaluation by dielectric analysis. J. Pharm. Pharmacol., 49, 592-593.

Ryynanen., S., 1995. The electromagnetic properties of food materials: a review of the basic principles. J. Food Eng., 26, 409-429.

Salman, H.H., Gamazo, C., Campanero, M.A., Irache, J.M., 2005. Salmonella-like bioadhesive nanoparticles. J. Control Release, 106, 1-13.

Sanga, E., Mujumdar, A.S., Raghavan, G.S.V., 2000. Microwave drying: principles and applications. In: Mujumdar, A.S., Suvachittanont, S. (Eds.), Developments in drying, Vol. 1, Kasetsart University Press, Bangkok, pp. 112-141.

Schaefer, T., 1996. Melt pelletization in a high shear mixer. X. Agglomeration of binary mixtures. Int. J. Pharm., 139, 149-159.

Schaefer, T., Holm, P., Kristensen, H.G., 1992a. Melt pelletization in a high shear mixer. II. Power consumption and granule growth. Acta Pharm. Nordica, 4, 141-148.

Schaefer, T., Holm, P., Kristensen, H.G., 1992b. Melt pelletization in a high shear mixer. III. Effects of lactose quality. Acta Pharm. Nordica, 4, 245-252.

Schaefer, T., Mathiesen, C., 1996. Melt pelletization in a high shear mixer. VII. Effects of product temperature. Int. J. Pharm., 134, 105-117.

Schaefer, T., Taagegaard, B., Thomsen, L.J., Kristensen, H.G., 1993a. Melt pelletization in a high shear mixer. IV. Effects of process variables in a laboratory scale mixer. Eur. J. Pharm. Sci., 1, 125-131.

Schaefer, T., Taagegaard, B., Thomsen, L.J., Kristensen, H.G., 1993b. Melt pelletization in a high shear mixer. V. Effects of apparatus variables. Eur. J. Pharm. Sci., 1, 133-141.

Schiffmann, R.F., 1986. Food product development for microwave processing. Food Technol., 40, 94-98.

Schiffmann, R.F., 1995. Microwave and dielectric drying. In: Mujumdar, A.S. (Ed.), Handbook of industrial drying, Marcel Dekker, New York, pp. 345-372.

Shrestha, B.L., Wood, H.C., Sokhansanj, S., 2005. Prediction of moisture content of alfalfa using density-independent functions of microwave dielectric properties. Meas. Sci. Technol., 16, 1179-1185.

Smith, G., Duffy, A.P., Shen, J., Olliff, C.J., 1995. Dielectric relaxation spectroscopy and some applications in the pharmaceutical sciences. J. Pharm. Sci., 84, 1029-1044.

Stahl, H., Van Vaerenbergh, G., 2005. Single-pot processing. In: Parikh, D.M. (Ed.), Handbook of pharmaceutical granulation technology, 2nd Edn., Taylor and Francis, London, pp. 311-331.

Stammer, A., Schlünder, E.U., 1993. Determination of local moisture profiles during microwave and convective drying. Chem. Eng. Process, 32, 339-344.

Szepes, A., Fiebig, A., Ulrich, J., Szabó-Révész, P., 2007. Structural study of α-lactose monohydrate subjected to microwave irradiation. J. Therm. Anal. Calorim., 89, 757-760.

Szepes, A., Hasznos-Nezdei, M., Kovács, J., Funke, Z., Ulrich, J., Szabó-Révész, P., 2005. Microwave processing of natural biopolymers-studies on the properties of different starches. Int. J. Pharm., 302, 166-171.

Szepes, A., Szabó-Révész, P., 2007. Water sorption behavior and swelling characteristics of starches subjected to dielectric heating. Pharm. Dev. Technol., 12, 555-561.

Taggard, P., 2004. Starch as an ingredient: manufacture and applications. In: Ann-Charlotte Eliasson, A. (Ed.), Starch in food, Woodhead Publishing Limited, England, pp. 363-392.

Torrado, J.J., Augsburger, L.L., 1994. Effect of different excipients on the tableting of coated particles. Int. J. Pharm., 106, 149-155.

Trabelsi, S., Nelson, S.O., 1998. Density independent functions for on-line microwave moisture meters: a general discussion. Meas. Sci. Technol., 9, 570-578.

Van Scoik, K.G., Zoglio, M.A., Carstensen, J.T., 1991. In: Swarbrick, J., Boylan, J.C., (Eds.), Encyclopedia of pharmaceutical technology, Vol. 4, Marcel Dekker, New York, pp. 485-515.

Vandelli, M.A., Romagnoli, M., Monti, A., Gozzi, M., Guerra, P., Rivasi, F., Forni, F., 2004. Microwave-treated gelatin microspheres as drug delivery system. J. Control Release, 96, 67-84.

Venkatesh, M.S., Raghavan, G.S.V., 2004. An overview of microwave processing and dielectric properties of agri-food materials. Biosyst. Eng., 88, 1-18.

Venkatesh, M.S., Raghavan, G.S.V., 2005. An overview of dielectric properties measuring techniques. Canadian Biosystems Engineering, 47, 7.15-7.30.

Vromans, H., 1994. Microwave drying of pharmaceutical excipients: comparison with conventional conductive drying. Eur. J. Pharm. Biopharm., 40, 333-336.

Wang, Z.H., Chen, G., 2000. Theoretical study of fluidized-bed drying with microwave heating. Ind. Eng. Chem. Res., 39, 775-782.

Wikberg, M., Alderborn, G., 1991. Compression characteristics of granulated materials. IV. The effect of granule porosity on the fragmentation propensity and the compactibility of some granulations. Int. J. Pharm., 69, 239-253.

Wikberg, M., Alderborn, G., 1992a. Compression characteristics of granulated materials. V. Mechanical properties of individual granules assessed by diametrical compression, in granulations with different volume reduction behavior. STP Pharm. Sci., 2, 313-319.

Wikberg, M., Alderborn, G., 1992b. Compression characteristics of granulated materials. VI. Pore size distribution, assessed by mercury penetration, of compacts of two lactose granulations with different fragmentation propensities. Int. J. Pharm., 84, 191-195.

Wikberg, M., Alderborn, G., 1993. Compression characteristics of granulated materials. VII. The effect of intragranular binder distribution on the compactibility of some lactose granulations. Pharm. Res., 10, 88-94.

Wong, T.W., 2008. Use of microwave in processing of drug delivery systems. Curr. Drug Deliv., 5, 77-84.

Wong, T.W., Chan, L.W., Kho, S.B., Heng, P.W.S., 2002. Design of controlled-release solid dosage forms of alginate and chitosan using microwave. J. Control Release, 84, 99-114.

Wong, T.W., Chan, L.W., Kho, S.B., Heng, P.W.S., 2005b. Aging and microwave effects on alginate/chitosan matrices. J. Control Release, 104, 461-475.

Wong, T.W., Cheong, W.S., Heng, P.W.S., 2005a. Melt granulation and pelletization. In: Parikh, D.M. (Ed.), Handbook of pharmaceutical granulation technology, 2nd Edn., Taylor and Francis, London, UK, pp. 385-406.

Wong, T.W., Deepak, K.G., Taib, M.N., Anuar, N.K., 2007a. Microwave non-destructive testing technique for characterization of HPMC-PEG 3000 films. Int. J. Pharm., 343, 122-130.

Wong, T.W., Wahab, S., Anthony, Y., 2007b. Effects of microwave on drug release property of poly(methyl vinyl ether-co-maleic acid) matrix. Drug Dev. Ind. Pharm., 33, 737-746.

Wong, T.W., Wahab, S., Anthony, Y., 2008. Drug release responses of zinc ion cross-linked poly(methyl vinyl ether-co-maleic acid) matrix towards microwaves. Int. J. Pharm., 357, 154-163.

Wong, T.W., Wan, L.S.C., Heng, P.W.S., 1999. Effects of physical properties of PEG 6000 on pellets produced by melt pelletization. Pharm. Dev. Technol., 4, 449-456.

Zhang, D., Mujumdar, A.S., 1992. Deformation and stress analysis of porous capillary bodies during intermittent volumetric thermal drying. Dry Technol., 10, 421-443.

7. LIST OF PUBLICATIONS

Journal Publications:

Loh, Z.H., Liew, C.V., Lee, C.C., Heng, P.W.S., 2008. Microwave-assisted drying of pharmaceutical granules and its impact on drug stability. Int. J. Pharm., 359, 53-62.

Liew, C.V., Loh, Z.H., Heng, P.W.S., Lee, C.C., 2008. A study on microwave-induced melt granulation in a single pot high shear processor. Pharm. Dev. Technol., 13, 401-411.

Heng, P.W.S., Loh, Z.H., Liew, C.V., Lee, C.C., 2009. Dielectric properties of pharmaceutical materials relevant to microwave processing – effects of field frequency, material density and moisture content. J. Pharm. Sci. *(accepted for publication).*

Loh, Z.H., Liew, C.V., Heng, P.W.S., Lee, C.C. Evaluation of the physicochemical properties and compaction behavior of melt granules produced in microwave-induced and conventional melt granulation *(manuscript in preparation).*

Conference Presentations:

Loh, Z.H., Liew, C.V., Lee, C.C., Heng, P.W.S. A screening study on dielectric properties of pharmaceutical materials relevant to microwave processing – effects of field frequency, material moisture content and density. Oral presentation in: ASEAN Scientific Conference in Pharmaceutical Technology, 1-3 June 2008, Penang, Malaysia.

Sia, B.Y., Loh, Z.H., Liew, C.V. Microwave-induced and conventional melt granulation: granule physical properties. Poster presentation in: 4th AAPS-NUS Student Chapter Symposium, 2 Apr 2008, Singapore.

Loh, Z.H., Liew, C.V., Heng, P.W.S., Lee, C.C. A study on microwave-induced melt granulation in a single pot high shear processor. Poster presentation in: Asian Association of Schools of Pharmacy (AASP) Conference, 25-28 Oct 2007, Manila, Phillipines.

Loh, Z.H., Liew, C.V., Lee, C.C., Heng, P.W.S., Microwave-induced high shear melt agglomeration with a focus on the intrinsic heating capabilities of materials under microwave exposure. Poster presentation in: Asian Pharmaceutics Graduate Congress – The Science of Product Design and Pharmaceutical Technology, 25-27 Sept 2006, Singapore.

Heng, P.W.S., Liew, C.V., Lee, C.C., Loh, Z.H. Use of a hybrid drying method for acetylsalicylic acid granules in a single pot processor. Poster presentation in: American Association of Pharmaceutical Scientists (AAPS) Annual Meeting, 6-10 Nov 2005, Nashville, Tennessee.

Loh, Z.H., Liew, C.V., Heng, P.W.S., Lee, C.C. Microwave-induced melt granulation – comparison with conventional melt granulation. Poster presentation in: 3rd AAPS-NUS Student Chapter Symposium, 5 Mar 2007, Singapore.